bioRxiv preprint doi: https://doi.org/10.1101/2020.02.29.969014; this version posted March 3, 2020. The copyright holder for this preprint (which was not certified by peer review) is the author/funder. All rights reserved. No reuse allowed without permission.

Integrated role of microRNA-30e-5p through targeting negative regulators of innate immune pathways during HBV infection and SLE

Richa Mishra[1], Sanjana Bhattacharya[1], Bhupendra S Rawat[2], Ashish Kumar[1], Akhilesh Kumar[1], Kavita Niraj[3], Ajit Chande[4], Puneet Gandhi[3], Dheeraj Khetan[5], Amita Aggarwal[6], Seiichi Sato[7], Prafullakumar Tailor[2], Akinori Takaoka[7], Himanshu Kumar[1,8*]

Affiliations: 1. Department of Biological Sciences, Laboratory of Immunology and Infectious Disease Biology, Indian Institute of Science Education and Research (IISER) Bhopal, Bhopal-462066, MP, India; 2. Laboratory of Innate Immunity, National Institute of Immunology (NII), New Delhi-110067, India; 3. Department of Research (Medical Biotechnology), Bhopal Memorial Hospital & Research Centre (BMHRC), Bhopal-462038, MP, India; 4. Department of Biological Sciences, Molecular Virology Laboratory, Indian Institute of Science Education and Research (IISER) Bhopal, Bhopal-462066, MP, India; 5. Department of Transfusion Medicine, Sanjay Gandhi Post Graduate Institute of Medical Sciences (SGPGIMS), Lucknow-226014, UP, India; 6. Department of Clinical Immunology and Rheumatology, Sanjay Gandhi Post Graduate Institute of Medical Sciences (SGPGIMS), Lucknow-226014, UP, India; 7. Division of Signaling in Cancer and Immunology, Institute for Genetic Medicine, Hokkaido University, Sapporo, Japan; 8. Laboratory of Host Defense, WPI Immunology, Frontier Research Centre, Osaka University, Osaka 5650871, Japan.

***Corresponding author:** H Kumar, Department of Biological Sciences, Laboratory of Immunology and Infectious Disease Biology, Indian Institute of Science Education and Research (IISER) Bhopal, AB-3, Room No. 220, Bhopal By-pass Road, Bhauri, Bhopal 462066, MP, India. Tel: +91 755 6691413; Fax: +91 755 669 2392; E-mail: hkumar@iiserb.ac.in

bioRxiv preprint doi: https://doi.org/10.1101/2020.02.29.969014; this version posted March 3, 2020. The copyright holder for this preprint (which was not certified by peer review) is the author/funder. All rights reserved. No reuse allowed without permission.

Abstract

Precise regulation of innate immunity is crucial for the development of appropriate host immunity against microbial infections and the maintenance of immune homeostasis. The microRNAs are small non-coding RNA, post-transcriptional regulator of multiple genes and act as a rheostat for protein expression. Here, we identified microRNA(miR)-30e-5p (miR-30e) induced by the hepatitis B virus (HBV) and other viruses that act as a master regulator for innate immune responses. Moreover, pegylated type I interferons treatment to HBV patients for viral reduction also reduces the miRNA. Additionally, we have also shown the immuno-pathological effects of miR-30e in systemic lupus erythematous (SLE) patients and SLE mouse model. Mechanistically, the miR-30e targets multiple negative regulators namely *TRIM38, TANK, ATG5, ATG12, BECN1, SOCS1, SOCS3* of innate immune signaling pathways and enhances innate immune responses. Furthermore, sequestering of endogenous miR-30e in PBMCs of SLE patients and SLE mouse model respectively by the introduction of antagomir and locked nucleic acid based inhibitor significantly reduces type I interferon and pro-inflammatory cytokines. Collectively, our study demonstrates the novel role of miR-30e in innate immunity and its prognostic and therapeutic potential in infectious and autoimmune diseases.

bioRxiv preprint doi: https://doi.org/10.1101/2020.02.29.969014; this version posted March 3, 2020. The copyright holder for this preprint (which was not certified by peer review) is the author/funder. All rights reserved. No reuse allowed without permission.

Introduction

The host innate immunity is an evolutionarily conserved defense system against microbial threats. These microbes express signature molecule known as pathogen-associated molecular patterns (PAMPs) which are sensed by host's effectively conserved sensors known as pattern-recognition receptors (PRRs) in various compartments of cells. The coordinated interactions among them, activate a complex cascade of signaling pathways resulting in the development of innate immune responses for the elimination of invading microbes, through production of pro-inflammatory cytokines, type I and III interferons (IFNs) and chemokines, recruitment of immune cells and trigger various types of cell death[1]. These PRRs also interact with some host endogenous molecules known as danger-associated molecular patterns (DAMPs) and initiate innate immune responses without microbial infection and may establish or trigger autoimmune diseases[2].

The micro RNA (miRNA) is a class of small non-coding RNA (18-22 nucleotide) that fine-tune protein expression through direct interaction with 3'UTR of the gene transcript[3]. miRNA interacts with target transcript through base pairing and initiates degradation or blocking of translation machinery via multiprotein complex known as RNA-induced silencing complex (RISC)[4]. It has been reported that a single miRNA has multiple mRNA targets and regulate cell signaling cascades and cellular responses during viral infections[5]. Several viruses evade immunity and establish infection by perturbing the host cellular miRNA expression or expressing viral(v)-miRNA upon infection[6]. In contrast, it has been reported that several host miRNAs restrict viral replication by targeting viral genome or those host genes which are essential for viral replication[7],[30]. In this study, we have identified miR-30e induced by DNA and RNA viruses such as Hepatitis B virus (HBV), Human

bioRxiv preprint doi: https://doi.org/10.1101/2020.02.29.969014; this version posted March 3, 2020. The copyright holder for this preprint (which was not certified by peer review) is the author/funder. All rights reserved. No reuse allowed without permission.

cytomegalovirus (HCMV), New Castle disease virus (NDV) and Sendai virus (SeV) in primary cells such as human PBMCs and various mammalian cell lines. Notably, higher miR-30e levels were also detected in the serum of therapy naive HBV patients. Introduction of miR-30e into the cells promote production of pro-inflammatory cytokines, type I/III IFNs and globally enhances the innate immunity and therefore reduces viral load. However, HBV patients treated with pegylated type I IFNs present reduced HBV infection in terms of viral load and disease pathology, and significant concomitant reduction in miRNA30e levels, illuminating the correlation of innate immune responses and miR-30e expression. We utilized bioinformatic tools and transcriptomic approaches to identify miR-30e targets negative regulators namely *TRIM38, TANK, ATG5, ATG12, BECN1, SOCS1* and *SOCS3* of PRRs-mediated signaling pathways such as TLR, RLR and DNA sensing innate immune signaling pathways[8, 9]. Additionally, we showed miR-30e and 3'UTR of negative regulator transcripts makes a complex with Argonaute 2 (Ago2) protein, a component of RNA induced silencing complex (RISC), reduces transcript levels and subsequently protein expression thereby enhances innate immune responses. In contrast, patients with Systemic Lupus Erythematosus (SLE), a disease characterized by Type I IFN signature had higher expression of miR-30e[10, 11]. Further, NZB/NZW F1 hybrid, an animal model of lupus[31] also showed increased expression of miR-30e. In connection, the introduction of miR-30e antagomir into PBMCs of SLE patients and lock nucleic acid (LNA) inhibitor for miR-30e through intra-orbital injection to the SLE mouse model significantly reduces type I IFNs and proinflammatory cytokines and moderately enhances the innate negative regulation. In conclusion, our study, proposes the novel role of miR-30e in innate immunity and its prognostic and therapeutic potential in HBV and SLE.

bioRxiv preprint doi: https://doi.org/10.1101/2020.02.29.969014; this version posted March 3, 2020. The copyright holder for this preprint (which was not certified by peer review) is the author/funder. All rights reserved. No reuse allowed without permission.

Results

miRNA-30e is induced upon viral infection and enhances innate antiviral responses to inhibit viral replication.

To investigate the miRNAs involved in regulation of innate immune response during viral infections, we performed unbiased data analyses on previously published reports and miRNA microarray GEO datasets as shown in schematic workflow (Fig. S1A). In particular, the miRNA reports in H5N1 or Epstein Barr virus were analyzed for upregulated miRNAs. These upregulated miRNAs were compared to our previous miRNA profiling dataset from NDV infection in HEK293T cells (GSE65694). Upon comparison with NDV infection we selected miR-30e-5p, miR-27a-3p and mir-181a/2-3p as the common miRNAs across miRNA profiles related to viral diseases (Fig. S1B). Our analysis identified miR-30e as a unique miRNA that was predicted to target various PRR-mediated signaling regulators during negative regulation of innate immune responses (Fig. S1C) and was upregulated in viral infections moreover its mature form was highly conserved among the wide range of species (Fig. S1D). Additionally, datasets for H1N1 infection in mice (GSE69944), H5N1 infection in human lung carcinoma cells (A549 cells, GSE96857) and HBV infected liver tissues of hepatitis patients (GSE21279) were also analyzed by GEO2R package for upregulated miRNAs and among all upregulated miRNAs, miR-30e upregulation is represented here (Fig. S1E). The expression of miR-30e was upregulated during viral infections or stimulation with PAMPs *in-vitro* in various cell-lines (Fig. S2A-F). At the transcriptional level, miR-30e promoter activity was moderately enhanced by NDV but was unaffected by *IFNβ* or *TNFα* stimulation which activated the *ISRE* and *NFκB* promoters respectively, suggesting that miR-30e expression might be induced by the viral infections

bioRxiv preprint doi: https://doi.org/10.1101/2020.02.29.969014; this version posted March 3, 2020. The copyright holder for this preprint (which was not certified by peer review) is the author/funder. All rights reserved. No reuse allowed without permission.

but not by the cytokines produced during infection (Fig. S2G-L). To understand the clinical relevance, induction of miR-30e was tested in the cohort of 51 non-treated HBV patients (demographic details mentioned in Table T1). To this end, the expression of miR-30e was evaluated from serum samples of therapy naive chronic hepatitis B (CHB) patients in comparison with healthy controls, and significantly elevated levels of miR-30e were detected in HBV patients (Fig. 1A). Similar results were obtained with HepG2 cell line treated with serum from HBV patients (HBV PS) for different time points, as shown (Fig. 1B), the induction of miR-30e enhanced significantly at 1*dpi*, 2*dpi* and 3*dpi* (days post infection) with maximum expression at 3*dpi*. Additionally, miR-30e mimic (miR-30e) inhibited HBV infection in HepG2 cells treated with serum from HBV patients or HepG2215 cells, stably expressing HBV replicon cells as compared to control miRNA (miR-NC1) treated cells as tested by HBV-specific RNA and DNA (Fig. 1C and D) (Fig. S3A). Interestingly, ectopic expression of miR-30e significantly reduced the HBV replication in HepG2-NTCP cells as tested by HBV RNAs and HBV pgRNA (Fig. S3B). Notably, we found significant elevated levels of HBV DNA and HBV covalently closed circular DNA in HBV patient serum infected HepG2 cells and stably expressing HBV replicon HepG2215 cells compared to uninfected HepG2 cells (Fig S3C) to show the infection in cells. On another hand, expression of *IFNλ1* and *IFIT1* was enhanced in HepG2 and HepG2215 cells, respectively, in the presence of miR-30e (Fig. 1C and D) (Fig. S4A). Similarly, HBV infection in HepG2-NTCP cells (liver hepatoma cell line permissive for HBV infection) overexpressing miR-30e (ectopic), elevated IFNλ1 transcript (Fig. S4B). To study whether miR-30e was involved in controlling RNA virus infection, we infected human PBMCs (hPBMCs) with NDV to quantify the expression of miR-30e. We found that NDV infection elevated the expression

bioRxiv preprint doi: https://doi.org/10.1101/2020.02.29.969014; this version posted March 3, 2020. The copyright holder for this preprint (which was not certified by peer review) is the author/funder. All rights reserved. No reuse allowed without permission.

of miR-30e in time-dependent manner (Fig. 1E). Additionally, PBMCs infected with NDV in presence of miR-30e showed a significant reduction in NDV replication with a concomitant elevation of *IL6* expression whereas miR-30e inhibitor (AmiR-30e) reversed this phenomenon (Fig. 1F). Similar inhibition of viral replication was observed in multiple cell lines infected with NDV in the presence of miR-30e or AmiR-30e (Fig. S3D-F). Comparable results for antiviral responses were obtained after NDV infection in different cell-types at transcript level and protein levels (Fig. S4C-I) in presences of miR-30e and it also activate *ISRE, IFNβ* and *NFκB* promoters as tested by luciferase assay (Fig. S4J-L). Furthermore, miR-30e presence reduces NDV replication in terms NDV protein as tested by NDV-specific antibody estimated by western blot, microscopy and FACS analysis respectively (Fig. 1G-H and S3G). To further validate the function of miR-30e in controlling viral infections, we quantified the expression of miR-30e upon Sendai virus (SeV) infection in A549 cells. SeV induced the expression of miR-30e (Fig.1I) and ectopic expression of miR-30e (miR-30e mimic) inhibited the SeV replication as shown by qRT-PCR and FACS analysis (Fig. 1J-K) through enhancing antiviral genes such as the expression of *IFIT1* (Fig. 1J).

Next, role of miR-30e on DNA virus replication was determined, to this end, HFF cells were infected with DNA virus, HCMV, alone or along with miR-30e or miR-NC1. The viral replication was significantly reduced in the presence of miR-30e compared to the miR-NC1 treated HFF cells as quantified by HCMV transcript encoding viral glycoprotein gene (Gly B) by real-time PCR and analyzed by microscopy (Fig. S5A) and additionally the transcript levels of *IL-6* was enhanced (Fig. S5B).

bioRxiv preprint doi: https://doi.org/10.1101/2020.02.29.969014; this version posted March 3, 2020. The copyright holder for this preprint (which was not certified by peer review) is the author/funder. All rights reserved. No reuse allowed without permission.

To investigate, how miR-30e influence antiviral responses upon treatment with pure viral ligand such as poly IC and ssRNA, different cells including human PBMCs were stimulated along with miR-30e.The expression of various cytokines and ISGs such as *IFNβ, IP-10, IL-6* and *IFIT1* were elevated upon poly IC or ssRNA stimulation along with miR-30e transfection and similar results were found for the promoter activity of *ISRE* and *IFNβ* in presence of miR-30e (Fig. S6A-H). Collectively, our results demonstrate that miR-30e is upregulated in during virus infection and miR-30e inhibits viral replication by promoting the expression of innate antiviral genes.

miR-30e globally enhances innate immune responses during virus infection.

To investigate the effect of miR-30e on innate immune responses interms of innate immune immune genes upon virus infection, A549 cells were either mock transfected, or transfected with miR-NC1 and miR-30e for 24 hours, followed by infection with NDV for 24 hours and finally subjected to whole transcriptome sequencing using an illumina next-generation sequencer (NGS) and analyzed for differentially expressed genes as shown in the schematic (Fig. 2A, S7A). Notably, the transfection efficiency of miR-30e in both replicates was confirmed by qRT-PCR using miR-30e-5p Taqman and reduction in viral infection was confirmed by quantifying the NDV RNA in both the replicates to establish further analysis as per our previous findings (Fig. 2B). Principal component analysis for the samples resulted in formation of three distinct groups (miR-30e, miR-NC1 and uninfected) according to their treatment (Fig. 2C). Additional analysis of transcriptomic data showed that 1179 genes were significantly upregulated and 1206 genes were significantly downregulated upon miR-30e transfection in comparison to miR-NC1 (Fig. 2D (represented in volcano plot) and Fig. S7B

bioRxiv preprint doi: https://doi.org/10.1101/2020.02.29.969014; this version posted March 3, 2020. The copyright holder for this preprint (which was not certified by peer review) is the author/funder. All rights reserved. No reuse allowed without permission.

(represented in MA plot and shown in Table T2). Moreover, KEGG pathway analysis of significantly upregulated genes, upon miR-30e treatment and NDV infection indicated enrichment of genes belonging to key cellular mechanisms namely: cell cycle, NOD-like receptor signaling pathway, MAPK signaling pathway, TLR signaling pathway, RLR signaling pathway, PI3K-AKT signaling pathway, cytokine-cytokine receptor interaction pathway, NF-kappa B signaling pathways, TNF signaling pathway, etc. (Fig. 2E). Relative expression levels of top genes involved in these pathways is represented by heat map (Fig. S7C). Intriguingly, we noticed that a significant number of interferons stimulated genes (ISGs) like *IRF3, IRF7, CXCL10 (IP10), IFIT1, MX1, IL6, OAS1* among others were also predominantly upregulated (Fig. 2F) that confirmed with the initial findings of the study. Furthermore, our NGS results were verified by quantifying the expression level of type 1 interferon *IFNβ*, interferon stimulated genes: *IFIT1* and *OAS1* and pro-inflammatory cytokines: *IL6* and *IP10*. These outcomes intricate strongly that miR-30e reduces the viral replication by enhancing the innate immune responses upon activation of various signaling cascades. Additionally, miR-30e impacts innate immune responses during viral infection, prompted us to investigate transcriptome and gain mechanistic insight for the target of miR-30e.

miR-30e targets negative regulators of TLRs, RLRs, DNA sensing and interferon signaling pathways

To investigate underlying molecular mechanism for the reduction of viral burden and enhanced antiviral innate immune responses by miR-30e, we conducted unbiased rigorous screening using various bioinformatic tools for the identification of innate immune genes.

bioRxiv preprint doi: https://doi.org/10.1101/2020.02.29.969014; this version posted March 3, 2020. The copyright holder for this preprint (which was not certified by peer review) is the author/funder. All rights reserved. No reuse allowed without permission.

To filter the genes transcript targeted by miRNA, certain criteria for screening were applied. First of all, common genes involved in innate immune regulation upon viral infections and targeted by miR-30e were identified and subjected to KEGG pathway analysis. The analysis revealed that majority of genes (*TRIM38, TANK, ATG5, ATG12, BECN1, SOCS1, SOCS3, TRIM13* and *EPG5*) were involved in negative/down regulation of pattern recognition receptors (PRRs)-mediated signaling pathways (Fig. 3A). Additionally, our NGS analysis demonstrated that expression of identified negative regulators during NDV infection were reduced upon miR-30e treatment as compared to miR-NC1 group (Fig. 3B). This further concludes that negative regulators were targeted by mir-30e. The binding efficiency for miR-30e and identified targets genes are significantly high to alter any physiological functions by the miRNA that was tested by different *in-silico* tools such as miRanda, DIANA, targetscan, miRDB and BiBiServ2_RNAhybrid as reported (Table T3). Although few targets of miR-30e are not negative regulators however, binding energy for those target transcript and miRNA assembly are low (Fig. S8) and therefore, it may not significantly alter the cellular function. To test specificity of miRNA with the 3'UTR of identified negative regulator genes, the 3'UTR of the gene were cloned downstream of luciferase gene under the CMV promoter and performed luciferase assy. It was found that miR-30e significantly reduced luciferase activity of investigated genes compared to control miR (Fig. 3C). In contrast, introduction of mutation in cloned 3'UTR by site directed mutagenesis (SDM) did not change the luciferase activity in presence of miR-30e and it was comparable with miR-NC1 (Fig. S9A), moreover, it could be noted here that, the target sequence in each negative regulator genes were same. Additionally, we knockdown these negative regulators in HEK-293T cells and Infected them with NDV to further estimated the level of *IFNβ*, which clearly elucidated

bioRxiv preprint doi: https://doi.org/10.1101/2020.02.29.969014; this version posted March 3, 2020. The copyright holder for this preprint (which was not certified by peer review) is the author/funder. All rights reserved. No reuse allowed without permission.

their inhibitory effect on the mRNA levels of *IFNβ* within a cell, this effect was found to be significant with respect to the majority of the targets (Fig. 3D). And observed that the production of *IFNβ* is comparable after knockdown of target genes and introduction of miR-30e into the cells during viral infection suggesting the pivotal role of miR-30e in suppression of negative regulators transcripts. Furthermore, we scanned the 3'UTRs of identified negative regulators for RNA binding site for Ago2 protein in CLIP database, which is a key component of the miRNA-mediated silencing complex (RISC) and found that the miR-30e strongly complexes with the target genes as shown in (Table T4). To validate, miR-30e and negative regulator transcripts *(TRIM38, TANK, ATG5, ATG12, BECN1, SOCS1 and SOCS3)* interaction, Ago2 pull-down assay was performed as shown in schematic diagram (Fig. 3E) and found that introduction of miR-30e significantly enriches the transcript of negative regulators compared to the NDV alone infection or NDV infection along with control miRNA treated cells suggesting that miRNA directly interact with the transcript through the formation of RISC.

Next, the expression of identified negative regulators were examined in A549 cells upon NDV infection and found that at 12 hours there was increased in the expression of *TRIM38, TANK, ATG5, ATG12, BECN1, SOCS1* and *SOCS3* transcript and it was reduced at 24 hours due to induction of miR-30e as shown in left panel (Fig. S9B). Additionally, ectopic expression of miR-30e reduced the expression level of these targets in A549 cells compared to the control after NDV infection (Fig. S9C). Consistent with these results induction of targets was also reduced in HBV-patient serum treated HepG2 cells, HepG2215 cells (stably expressing HBV replicon cells and HepG2-NTCP cells infected with HBV, in presences of miR-30e compared to the control miRNA transfection (Fig. S10A-C), suggesting that miR-

bioRxiv preprint doi: https://doi.org/10.1101/2020.02.29.969014; this version posted March 3, 2020. The copyright holder for this preprint (which was not certified by peer review) is the author/funder. All rights reserved. No reuse allowed without permission.

30e targets these genes during HBV and NDV infection in HepG2, HepG2215, A549 cells, respectively. Similar results were obtained due to miR-30e transfection in NDV infected and poly IC treated HeLa cells (Fig. S10D-E). We not only confirmed the expression of negative regulators by analyzing transcripts but also tested for protein expression using specific antibodies by immunoblot analysis. The introduction of miR-30e significantly reduced the expression of *TRIM38, TANK, ATG12, BECN1, SOCS3* and *SOCS1* as shown (Fig. 3F). Therefore, our results strongly suggest that these key negative regulators of innate immunity are targeted by miR-30e, which are induced during virus infection and resulting to enhanced antiviral responses.

DAMPs induce miR-30e and enhance innate immune responses

Our observation for induction of miR-30e and subsequent heightened innate immune responses upon viral infection or pure PAMP stimulation prompted us to investigate the ability of host DAMPs for induction of miR-30e because sustained DAMPs production in the host can lead to enhance sterile inflammation and subsequently it may establish autoimmune disease[3]. To this end, ex-vivo experiment was performed using hPBMCs from three healthy volunteers. The genomic DNA were extracted from a portion of hPBMCs and sonicated to make small size (approx. 110-150 bps) for efficient transfection into the cells (Fig. 4A). The cultured hPBMCs were stimulated with the extracted small size DNA and tested for the induction of miR-30e and innate immune cytokines. The DAMP stimulation significantly induces the miR-30e and expression of *IFNα, IFNβ, IFIT1, IL6* genes in all 3 healthy volunteers (Fig. 4C-E). Next, to understand physiological significance of DAMP-induced innate immune cytokines, the DAMP-stimulated cells were infected by NDV and

bioRxiv preprint doi: https://doi.org/10.1101/2020.02.29.969014; this version posted March 3, 2020. The copyright holder for this preprint (which was not certified by peer review) is the author/funder. All rights reserved. No reuse allowed without permission.

NDV replication was measured. The dsDNA-stimulation significantly reduced the NDV replication (Fig. 4F) suggesting that inflammatory cytokines and type I interferons induced by dsDNA inhibited the viral replication. Although inhibition of viral replication could be the collective results of both dsDNA and virus-mediated induction proinflammatory cytokines, type I interferons and type I inducible genes. Finally, we examined the levels of apoptosis induced by autologous dsDNA in hPBMCs by Annexin-PI assay using FACS analysis as shown in Fig. S11A, dsDNA stimulation enhanced apoptosis compared to the mock stimulation and it is comparable to the positive control treated cells, by Camptothecin. Additionally, the levels of *TLRs 3/7/9* was estimated upon dsDNA treatment as previously it has been reported that DAMPs enhance the levels of these *TLRs.* Consistent with previous observation, we obtained similar results (Fig. S11B-D). Taken together, these results showed that DAMPs/dsDNA enhances miR-30e, innate immune responses as well as promote apoptosis and induce TLRs, the crucial characteristic features for the development of autoimmune disorder in co-occurrence with DAMPs/dsDNA and miR-30e might play pivotal role in autoimmune disease.

SLE patients and SLE mouse model show enhanced miR-30e expression

To investigate the role of miR-30e under physiological condition, an autoimmune disease, SLE was selected because SLE patients show enhanced inflammatory cytokines, type I interferons and type I interferon-inducible cytokines production[10]. The SLE patients also had elevated levels of several autoantibodies particularly antinuclear and anti-dsDNA antibodies. Therefore, PBMCs were isolated from clinically verified SLE patients (P: n=13) as shown (Table T5) and healthy controls (HC: n=13) and cultured for 48 hours, the expression levels

bioRxiv preprint doi: https://doi.org/10.1101/2020.02.29.969014; this version posted March 3, 2020. The copyright holder for this preprint (which was not certified by peer review) is the author/funder. All rights reserved. No reuse allowed without permission.

of *IFNβ, IFIT1 and IL6* were compared by qRT-PCR. As expected, we found that the expression levels of *IFNβ, IFIT1 and IL6* were significantly enhanced in SLE patients compared to healthy controls (Fig. 5A). The enhanced innate immune responses prompted us to investigate the expression levels of miR-30e. Interestingly, the expression of miR-30e is significantly enhanced (several fold) in patients (n=13) compared to healthy controls (n=13). Further to confirm our observations in SLE patients, the SLE mouse model was used. The New Zealand white/black (NZW/B) mice were extensively used for SLE studies. The splenocytes from both parents NZB and/or NZW mice (n=7) mice and lupus prone F1 (F1: NZW/B n=7) generation mice were tested for the expression levels of *Ip10, Tnfα and Il6* by qRT-PCR (Fig. 5B). The F1 mice showed significantly high level of inflammatory responses compared to non-SLE parent mice. Consistent with human SLE results, the expression of miR-30e is enhanced manifold both in F1 mouse splenocytes and serum compared to the parents. Additionally, GEO dataset: GSE79240 was utilized to observe the differential expression of microRNAs during SLE, especially, miR-30e expression level, that further revealed that expression of miR-30e modestly enhanced in dendritic cells of SLE patients (n=5) compared to healthy controls (n=5) (Fig. S12A). To understand the relevance of miR-30e in another autoimmune disease, we reanalyzed the previously submitted GEO dataset (GSE55099) for Type 1 Diabetes Mellitus patients. The reanalysis unveils that the expression of miR-30e significantly enhanced in PBMCs of patients (n=12) compared to healthy controls (n=10) (Fig. S12B). Collectively, these results suggest that enhanced innate immune responses are strongly linked with miR-30e expression under physiological condition and it might also play pivotal role in immune-pathogenesis of SLE in both human and mouse model.

bioRxiv preprint doi: https://doi.org/10.1101/2020.02.29.969014; this version posted March 3, 2020. The copyright holder for this preprint (which was not certified by peer review) is the author/funder. All rights reserved. No reuse allowed without permission.

miR-30e targets negative regulators of PRR-mediated signaling pathway in SLE patients and SLE mouse model

The enhanced expression of inflammatory cytokines, type I IFNs and type I IFN-inducible genes along with elevated miR-30e in SLE patients and SLE mouse model prompted us to examine the levels of our previously identified negative regulators as shown (Fig. 3A-B). Additionally, it has been reported that several negative regulators of innate immunity play a crucial role in the development of autoimmune disease. As expected, the expression of negative regulators of PRR-mediated signaling pathways namely *TRIM38, TANK, SOCS1 and SOCS3* was significantly reduced in the PBMCs of SLE patients compared to healthy controls (Fig. 6A). To support our observation, reanalysis of previously submitted GEO dataset, GSE11909 for SLE patients (n=103) and healthy controls (n=12) in PBMCs reveal that, in SLE, the identified negative regulators of innate immune signaling pathway maybe targeted by miR-30e, were significantly reduced in patients (n=103) compared to healthy controls (n=12) (Fig. S13). To confirm our observations, splenocytes from mouse model were analyzed for identified negative regulators. Consistent with human result for the expression of negative regulators, the expression of *Atg5* and *Atg12* were significantly reduced whereas expression of *Socs1* and *Socs3* was moderately reduced in SLE mouse (F1-NZW/B mice: n=7) compared to parent mice (PM-NZW-NZB: n=7) (Fig. 6B). Collectively, these results suggest that in SLE pathogenesis, in both human and mouse, enhanced expression of miR-30e might play a crucial role, by suppressing the expression of negative regulators of innate immune signaling pathway, which in turn enhance innate immune cytokines and contribute in development or severity to the disease. Therefore, manipulation of miR-30e expression might be key for the controlling SLE pathogenesis.

bioRxiv preprint doi: https://doi.org/10.1101/2020.02.29.969014; this version posted March 3, 2020. The copyright holder for this preprint (which was not certified by peer review) is the author/funder. All rights reserved. No reuse allowed without permission.

Prognostic and Therapeutic potential of miR-30e

To explore the prognostic and therapeutic potential of miR-30e, which modulate innate immune responses during infection and autoimmune diseases, particularly HBV infection and SLE, we tested prognostic potential of miR-30e. We validated the miR-30e expression by comparing the serum levels in pre- and post six months therapy (pegylated type I interferon) samples of HBV patients (demographic details mentioned in Table T6). Strikingly, we found significant reduction of miR-30e expression after interferon therapy (Fig. 7A), suggesting that, HBV infection triggers miR-30e over-expression in the host, to combat the which otherwise ablates upon Peg-IFN treatment, a well-established therapy that reduces the hepatitis B virus titer in patients. Additionally, GEO dataset GSE104126 supports the above finding in context to miR-30e expression level, as its reanalysis revealed, that there was significant reduction in the level of miR-30e in pegylated type I interferons treated and HBsAg-loss (reduction in viral titer) patients compared to pegylated type I interferons treated and non-HBsAg loss (no change in viral titer) patients (Fig. S14).

Next, we investigated the therapeutic potential of miR-30e modulator and have shown the importance of AmiR-30e (miR-30e inhibitor) that sequesters the activity of endogenous miR-30e. Our results showed that SLE patients and mouse model produce high inflammatory responses in terms of innate cytokines and it is linked to the elevated miR-30e expression (Fig. 5A) and contribute in reduction of negative regulators (Fig. 6A). Therefore, we introduce AmiR-30e into SLE patient's PBMCs. Interestingly, we found that ectopic expression of AmiR-30e sequester the expression of miR-30e in PBMCs of SLE patients and reduces the *IFNβ* expression as quantified by qRT-PCR (Fig. 7B). Next, we examined the

bioRxiv preprint doi: https://doi.org/10.1101/2020.02.29.969014; this version posted March 3, 2020. The copyright holder for this preprint (which was not certified by peer review) is the author/funder. All rights reserved. No reuse allowed without permission.

role of AmiR-30e in SLE mouse model, NZW/B. In *ex-vivo* experiment, transfection of splenocytes derived from the F1 mice (NZW/B) with AmiR-30e significantly reduces the expression levels of *Il6 and Tnfα* compared to the control AmiR-NC1 (Fig. 7C). Furthermore, to show the stable and specific sequestering effects of microRNAs for therapeutic relevance, previously it has been published that locked nucleic acid (LNA) based chemistry to design a potent inhibitor against the microRNA has showed promising effects in *in-vivo* studies[12]. Therefore, finally, we performed *in-vivo* experiments to test the effects of LNA-anti-mir-30e-5p (LNA Amir-30e) on innate immune responses in SLE mice, two groups of mice each consists of four mice were injected with LNA Amir-30e or LNA negative control (LNA NC) through retro-orbital route thrice with one day interval to sequester the endogenous expression of mir-30e to measure mir-30e and gene expression levels. The expression of mir-30e in serum and splenocytes of SLE induced F1 (NZW/B) mice was significantly reduced compared to the LNA NC treated mice. Additionally, innate immune cytokines namely *Il6 and Ip10* significantly reduced in LNA Amir-30e treated mice compared to the LNA NC. In contrast the expression of negative regulators, *Socs1 and Socs3* significantly enhanced in LNA Amir-30e treated mice compared to the LNA NC. (Fig. 7D). Taken together these findings conclude that LNA Amir-30e found to be stable under *in-vivo* conditions and significantly inhibits the activity of mir-30e in SLE mouse model, which further reduces the inhibition/targeting of negative regulators, contributing towards controlling of SLE phenomena.

bioRxiv preprint doi: https://doi.org/10.1101/2020.02.29.969014; this version posted March 3, 2020. The copyright holder for this preprint (which was not certified by peer review) is the author/funder. All rights reserved. No reuse allowed without permission.

Discussion

Innate immune responses to viral infection induces the production of pro-inflammatory cytokines and type I Interferons (IFNs) through cascade of complex signaling pathways that play critical roles in development of appropriate anti-viral immunity. In contrast, dysregulation of these signaling pathway results to inefficient clearance of microbial infection, immunopathology or autoimmune diseases[1,3]. Therefore, the expression and activation of signaling molecules in signaling pathways are tightly regulated at transcriptional, post-transcriptional, translational and post-translational levels. The non-coding small (micro) RNAs play a pivotal role in fine tuning of protein coding genes through, stability and translation of gene transcript. Here our study identifies a novel role of miR-30e in regulation of innate immune signaling pathway during HBV infection and immuno-pathogenesis of SLE. We also demonstrated the therapeutic and prognostic potential of AmiR-30e and miR-30e in SLE and HBV infection, respectively.

The miR-30e identified through unbiased *in-silico* screening using GEO datasets obtained from cell lines, primary cells, mice or human patients challenged by different viruses. Although, other miRNAs such as miR-27a-3p and miR-181a/2-3p are also induced, however, their complementation potency towards mRNA-miRNA targets was manifolds lower than miR-30e. The miR-30e has been reported to be associated with cancer[13-15], cardiac dysfunction[16], kidney malfunction[17], fatty acid deregulation, as a biomarker for SLE[18], a dysregulated micro RNA during Zika virus infection[19] and suppressor for Dengue virus[20]. However, its role in innate immune signaling pathway and innate immune responses during virus infection and pathogenesis of autoimmune diseases such as SLE are not clear.

bioRxiv preprint doi: https://doi.org/10.1101/2020.02.29.969014; this version posted March 3, 2020. The copyright holder for this preprint (which was not certified by peer review) is the author/funder. All rights reserved. No reuse allowed without permission.

Our results show that miR-30e induced manifold in the serum of (n=51) therapy naive chronic hepatitis B (CHB) patients compared to healthy control (n=24). This finding was also supported by another DNA and RNA virus such as HCMV, NDV, and SeV infection or stimulation with TLR or RLR viral PAMPs such as ssRNA and poly IC to various cell lines. Ectopic expression of miR-30e in primary cells or cell lines upon subsequent DNA or RNA virus infection significantly reduces the viral load through global enhancement of innate immune responses in terms of pro-inflammatory cytokines, type I interferons and type I interferons-inducible genes as shown by NGS data analysis. The enhanced miR-30e expression in therapy naive HBV (CHB) patients might elevate innate immune responses to combat HBV infection, however, it might be insufficient to control HBV infection. Therefore, HBV patients receiving pegylated interferon were sampled post six months therapy and were found to show significant reduction of viral load and miR-30e expression highlighting the link between HBV, miR-30e and innate immune responses. To establish the role of miR-30e under physiological condition, we selected SLE as a disease model. The SLE patients show enhanced expression of miR-30e, pro-inflammatory cytokines, type I interferons or type I interferons-inducible genes. Further to confirm our observations, we exploited SLE mouse model (NZW/ NZB F1) and obtained similar results for the expression of miR-30e that were consistent with SLE patients result suggesting the correlation of miR-30e with innate immune responses in SLE under physiological condition.

The transcriptomic analysis of our NGS data and GEO data sets using various bioinformatics tools shows that miR-30e directly targets several signal transducers and the negative regulators such as *TRIM38*[21-23], *TANK*[24], *ATG5, ATG12*[25, 26], *BECN1*[27], *SOCS1* and *SOCS3*[28]. The microRNA targeting reduces the expression negative regulators and enhance the innate

bioRxiv preprint doi: https://doi.org/10.1101/2020.02.29.969014; this version posted March 3, 2020. The copyright holder for this preprint (which was not certified by peer review) is the author/funder. All rights reserved. No reuse allowed without permission.

436 immune responses which play pivotal role in TLR, RLR, NLR, and type I interferon
437 signaling pathways. Although miR-30e also bind with few other gene transcripts which are
438 not negative regulator in the innate immune signaling pathway, however, the combined mean
439 free energy for these transcripts are lower than threshold binding energy necessary for
440 significant change in the expression of transcripts, for subsequently affecting the outcome of
441 signaling pathway. Notably, the expression of negative regulators such as *TRIM38, TANK,*
442 *SOCS1* and *SOCS3* in SLE patients are significantly reduced. Moreover, SLE mice also show
443 similar results for the expression of *Socs1, Socs3, Atg5* and *Atg12*. Collectively, human and
444 mouse results illustrate that miR-30e targets negative regulators to elevate innate immune
445 responses and dysregulation of miR-30e expression may be one of factor for the
446 establishment of SLE or other autoimmune diseases.
447 Previously, it has been shown that SLE patients has reduced ability to degrade DNA and
448 cellular chromatin[29]. Therefore, PBMCs from healthy donors were stimulated with partially
449 degraded self-DNA and these cells showed enhanced miR-30e and innate immune responses
450 suggesting the pathogenic role of miR-30e and suggested a link of self-DNA with the
451 pathogenesis of SLE. In contrast, sequestering endogenous miR-30e in PBMCs of SLE
452 patients by introducing antagomir/inhibitor significantly reduced the levels of miR-30e and
453 innate immune responses in terms of *IFNβ* production. Additionally, introduction of locked
454 nucleic acid (a stable form of antagomir) through retro-orbital route into SLE mice model
455 significantly reduced mir-30e and innate immune genes expression in splenocytes whereas
456 expression of negative regulators was enhanced, demonstrating the ability of mir-30e
457 antagomir to reduce innate immune responses under physiological condition. Finally, our
458 study identified miR-30e as a post-transcriptional regulator of negative regulation of PRR-

bioRxiv preprint doi: https://doi.org/10.1101/2020.02.29.969014; this version posted March 3, 2020. The copyright holder for this preprint (which was not certified by peer review) is the author/funder. All rights reserved. No reuse allowed without permission.

459 mediated innate immune signaling pathways and its diagnostic and prognostic potential
460 in HBV infection. Additionally, our study demonstrated the therapeutic implications of
461 miR-30e antagomir/inhibitor to immunologically complex autoimmune disease, SLE or
462 possibly other autoimmune diseases.
463

bioRxiv preprint doi: https://doi.org/10.1101/2020.02.29.969014; this version posted March 3, 2020. The copyright holder for this preprint (which was not certified by peer review) is the author/funder. All rights reserved. No reuse allowed without permission.

Materials and Methods

Ethical Statement. Experiments were performed after approval from the Institutional Ethical Committee (IEC)-Indian Institute of Science Education and Research (IISER) Bhopal: (IISERB/IEC/Certificate/20l6-IV/03), Institute Biosafety Committee (IBSC) - IISER-Bhopal: (IBSC/IISERB/2018/Meeting II/08), Bhopal Memorial Hospital & Research Centre Institutional Ethical Committee (IEC), BMHRC Research Projects/Clinical Studies (IRB/18/Research/10), Institutional Animal Ethical Committee (IAEC)-Small and Experimental Animal Facility National Institute of Immunology (NII): (IAEC#469/18) and Institutional Ethical Committee (IEC)- Sanjay Gandhi Post Graduate Institute of Medical Sciences (SGPGIMS): (2016-138-EMO-93).

Human blood samples. Blood samples from both healthy individuals and patients (HBV and SLE) were collected according to the ethics protocol in the respective hospitals by health professionals. Written informed consent was obtained from all patients and healthy participants before inclusion into the study at Bhopal Memorial Hospital & Research Center (BMHRC: for HBV samples: n = 51 Vs control samples: n = 24), Sanjay Gandhi Post Graduate Institute of Medical Sciences (SGPGIMS: for SLE samples: n = 13 Vs control samples: n = 13) and Institutional Ethical Committee (IEC)-Indian Institute of Science Education and Research (IISER) Bhopal. Reagents used for transfection/electroporation were Lipofectamine 2000, miRNA mimics, miRNA inhibitors, controls mimic/inhibitors and for RNA isolation were Trizol/Trizol-LS. All reagents used were procured from Ambion/Invitogen.

Mice. Systemic Lupus Erythematous (SLE) mouse model were procured from the Jackson Laboratory, USA and further breeding was done in approved pathogen- free, small animal

bioRxiv preprint doi: https://doi.org/10.1101/2020.02.29.969014; this version posted March 3, 2020. The copyright holder for this preprint (which was not certified by peer review) is the author/funder. All rights reserved. No reuse allowed without permission.

facility of National Institute of Immunology (NII). SLE mouse strains were used as follows: New Zealand White (NZW) and New Zealand Black (NZB) non-lupus bearing parent mice crossed to generate NZW/B F1 progenies, lupus induced mice. All the mice used in the study were from 6 to 12 weeks without any genders bias. Dendritic cell enriched low denisty fraction of splenocytes were prepared as described earlier[40,41]. Spleens were harvested and single cell suspension of splenocytes were cultured in RPMI based media containing either 50nM of miR-30e antagomir and miR-NC1 antagomir (transfected through RNAimax transfecting reagent) and plated in 24-well plate (3 x 10^6 cells/well) maintained at 37°C+5% CO_2. For the *in-vivo* experiments, four- 6 to 12 weeks old NZW/B F1 mice were randomly assigned into two groups. The mice in each group received four consecutives intravenous (retro-orbital) injections of either LNA antimiR-30e or LNA negative control (scrambled) compounds, formulated in TE Buffer (10mM Tris (pH: 7.5), 0.01mM EDTA) as per 25 mg LNA/kg mouse body weight on consecutive days as described previously. The mice were sacrificed within 24 h after the last dose. At selected time points, cells were harvested and relative abundances of miR-30e and other transcripts were quantified using qRT-PCR.

Cell lines, virus infections, transfection and reagents. A549 human alveolar basal epithelial cells (Cell Repository, NCCS, India), HEK293T/HEK293 human embryonic kidney cells (ATCC CRL-3216), Raw 264.7 (Cell Repository, NCCS, India), HeLa cervical cancer cells (Cell Repository, NCCS, India), HepG2-NTCP cells (from Dr. Takaji Wakita National Institute of Infectious Diseases Tokyo, Japan), HepG2 hepatoblastoma cells (from Dr. Nirupma Trehanpati's Laboratory, Institute of Liver & Biliary Sciences ILBS, New Delhi, India), HepG2215, HBV stably expressing hepatoblastoma cells (from Dr. Senthil Kumar Venugopal's Lab, South Asian University, New Delhi, India) and HFFs (from

bioRxiv preprint doi: https://doi.org/10.1101/2020.02.29.969014; this version posted March 3, 2020. The copyright holder for this preprint (which was not certified by peer review) is the author/funder. All rights reserved. No reuse allowed without permission.

Professor. Wade Gibson's Lab, Johns Hopkins, School of Medicine) were cultured in Dulbecco's modified Eagle's medium (DMEM) supplemented with 10% fetal bovine serum (FBS) and 1% Antibiotic-Antimycotic solution. HepG2-NTCP cells were infected with HBV in Professor Akinori Takaoka's Laoboratoy as per the standard protocol. Human PBMCs were isolated from whole blood and NDV LaSota viral stocks were accumulated as described previously[7]. NDV-GFP was a kind gift from Professor Peter Palese, Icahn School of Medicine at Mount Sinai. Sendai-RFP (SeV-RFP) were borrowed from Dr. Sunil Raghav, ILS, Bhubaneshwar, India, A single virus stock was used for all experiments. The cells were infected in serum-free DMEM with the NDV and SeV viruses at the MOIs indicated in the figure legends. After 60 min, the cells were washed with phosphate-buffered saline (PBS) and then were resuspended in DMEM, 1% FBS. HFFs were grown to full confluence and infected with GFP tagged HCMV at the MOIs indicated in the figure legends. HBV-positive sera were used to infect HepG2 cells as previously described[42-46]. HepG2 cells were made permissive to HBV virus infection by adding 3% PEG (polyethylglycol) and 0.5% DMSO (dimethylsulphoxide). The cells were infected in 1% FBS containing DMEM, 3% PEG and 0.5% DMSO with the HBV-positive sera. After 6-7 hours, the cells were washed with phosphate-buffered saline (PBS) and then were resuspended in DMEM, 10% FBS, 3% PEG and 0.5% DMSO. For electroporation of human PBMCs, 1 X 10^6 cells were suspended in Opti-MEM (Invitrogen) containing 50 nM mirVana miRNA mimics (Ambion). The cells were pulsed twice with 1000 V for 0.5 ms with a pulse interval of 5 s with the Gene Pulser Xcell electroporation system. The cells were then transferred to RPMI supplemented with 10% FBS[7]. Transfection of cells with miRNA mimics, inhibitors and control mimics/inhibitors and/or plasmids was performed with Lipofectamine 2000 or 3000

bioRxiv preprint doi: https://doi.org/10.1101/2020.02.29.969014; this version posted March 3, 2020. The copyright holder for this preprint (which was not certified by peer review) is the author/funder. All rights reserved. No reuse allowed without permission.

(Invitrogen) according to the manufacturer's protocol. Poly IC (Invivogen) was mixed with Lipofectamine2000 before being used to transfect cells. ssRNA (Invitrogen) were used to stimulate the cells as mentioned in the figure legends. DMEM, FBS, Opti-MEM, RPMI, and Lipofectamine 2000/3000 were purchased from Invitrogen. The miR-30e mimic (miR-30e) (Invitrogen) or a nonspecific miRNA negative control (miR-NC1) was used according to the manufacturer's instructions (Applied Biosystems). The miR-30e inhibitor (AmiR-30e) (Invitrogen) was used to inhibit miR-30e expression in transfected cells. The cDNA encoding the 3′-UTR of negative regulators was retrieved from the UCSC gene sorter and was sub-cloned into the pMIR-REPORT luciferase vector. A total of 2.0 kb of sequence upstream of the miR-30e gene was retrieved from the UCSC genome browser. This sequence was amplified by PCR from genomic DNA and was subcloned into the pGL3 basic vector between the KpnI and HindIII sites**.** Plasmids containing Firefly Luciferase gene under *IFNβ, ISRE* and *NFκB* promoters, were obtained from Professor Shizuo Akira's (Osaka University, Japan), *rhIFNβ* (bei resources) and *rhTNFα* (R&D Systems). All sh- clones, were obtained from the whole RNAi human library for shRNA mediating silencing (Sigma, Aldrich) maintained at IISER, Bhopal, India. *In-silico* analysis for miRNA target gene prediction was done as previously described[7].

Quantitative real-time reverse transcription PCR. Total RNA was extracted with the Trizol reagent (Ambion/Invitrogen) and used to synthesize cDNA with the iScript cDNA Synthesis Kit (BioRad, Hercules, CA, USA) according to the manufacturer's protocol. Gene expression was measured by quantitative real-time PCR using gene-specific primers and SYBR Green (Biorad, Hercules, CA, USA). For quantification of the abundances of miR-30e, real-time PCR analysis was performed with the TaqMan Universal PCR Master Mix

bioRxiv preprint doi: https://doi.org/10.1101/2020.02.29.969014; this version posted March 3, 2020. The copyright holder for this preprint (which was not certified by peer review) is the author/funder. All rights reserved. No reuse allowed without permission.

(Applied Biosystems) and the miR-30e-5p specific TaqMan miRNA assays. The Taqman U6 assay was used as a reference control. Real time quantification was done using StepOne Plus Real time PCR Systems by Applied BioSystems (Foster City, CA, USA). Primers used for qRT-PCR were listed in Supplementary Table T7.

Luciferase Reporter assays. HEK 293T and HeLa cells (5 X 10^4) were seeded into a 24-well plate and transiently transfected with 25 nM of mimics, 50 ng of the transfection control pRL-TK plasmid (*Renilla* luciferase containing plasmid) and 200 ng of the luciferase reporter plasmid (*Firefly* luciferase containing plasmid) together with/without 300 ng of the various expression plasmids or an empty plasmid as a control according to the respective experiments. The cells were lysed at 24 to 36 hours after transfection and/or infection or stimulations, and finally the luciferase activity in total cell lysates was measured with Glomax (Promega, Madison, WI, USA).

Enzyme-linked immunosorbent assay (ELISA). A549 and HeLa cells were transiently transfected with miR-30e and miR-NC1 and then were infected NDV virus. The culture media were harvested 36 to 40 hours after infection and were analyzed by specific ELISA kits (Becton Dickinson) according to the manufacturer's instructions to determine the amounts of *IP10* and *IL6* that were secreted by the cells.

RNA immunoprecipitations. RNA immunoprecipitations were performed as described previously[47,48]. The pIRESneo-Flag/HA Ago2 plasmid was a gift from Professor T. Tuschl (Addgene plasmid #10822). Briefly, HEK 293T cells transfected with miRNA and infected with NDV were lysed in 0.5% NP-40, 150 mM KCl, 25 mM tris-glycine (pH 7.5) and incubated with M2 Flag affinity beads (Sigma) overnight. The lysate was then washed with 300 mM NaCl, 50 mM tris-glycine (pH 7.5), 5 mM $MgCl_2$, and 0.05% NP-40. The extraction

bioRxiv preprint doi: https://doi.org/10.1101/2020.02.29.969014; this version posted March 3, 2020. The copyright holder for this preprint (which was not certified by peer review) is the author/funder. All rights reserved. No reuse allowed without permission.

of RNA from the immunoprecipitated RNPs was performed with the Trizol reagent (Ambion, Invitrogen) according to the manufacturer's protocol.

Fluorescence-activated cell sorting (FACS) Cytometry Analysis. A549 and HeLa cells were grown to 70-80% confluence, then treated with mimics and negative control reagents and finally infected with SeV-RFP and NDV-GFP. After 24 hours of infection, cells were trypsinized, harvested and then washed with PBS thrice and finally resuspended in PBS for FACS analysis as described in figure legends. Human PBMCs were treated with DNA and or camptothecin (0.3μM) to estimate apoptosis levels. At desired time points, cells were analyzed by staining with FITC-labeled Annexin V and propidium iodide (Becton Dickinson, USA) as per manufacturer's instructions and stained cells were analyzed using a FACS Aria III (Becton Dickinson) and data were analyzed by using FlowJo software (FlowJo, Ashland, OR, USA).

Immunoblotting analysis. After cells were transfected with miRNA mimic and controls then after infected with NDV and/or NDV-GFP (as indicated in figures), lysates were collected and subjected to western blotting analysis as previously described[7,49]. Cells were harvested after 36 hours of infection with standard ice-cold cell lysis buffer supplemented with 1 X protease inhibitor cocktail (obtained from Sigma, Aldrich). Immunoblotting were done as previously described[49]. Immunoblotted nitrocellulose membrane was imaged with LI-COR system. Anti–GFP antibody was obtained from Sigma-Aldrich, anti-TRIM38 (from ImmunoTag,), anti-TANK, SOCS3, BECN1 (from Cloud-Clone Corporation), anti-ATG12 (from Cell Signaling Technology), anti-SOCS1 (from Santa Cruz) and anti γ-Tubulin (from Sigma, Aldrich). IR dye labeled anti-Rabbit and anti-Mouse IgG (secondary antibody), were purchased from LI-COR.

bioRxiv preprint doi: https://doi.org/10.1101/2020.02.29.969014; this version posted March 3, 2020. The copyright holder for this preprint (which was not certified by peer review) is the author/funder. All rights reserved. No reuse allowed without permission.

Microscopy. HeLa cells were transfected with miRNA mimic and infected with NDV-GFP were fixed with 4% PFA for 15 min at room temperature; permeabilized with 0.05% Triton X-100 in 1 x PBS for 10 min at room temperature; blocked with bovine serum albumin (5 mg/ml) in PBS, 0.04% Tween 20 for 30 min and incubated for 1 hour with the relevant primary antibodies diluted in blocking buffer. The cells were then washed three times with PBS and incubated for 1 hour with the appropriate secondary antibodies at room temperature. Nuclei were stained with DAPI, and the cells were then analyzed with an LSM 780 confocal laser microscope (Carl Zeiss). The images were analyzed using ImageJ processing software. HCMV infection (GFP fluorescence) in HFFs miRNA mimic and control mimic transfected cells was visualized with Inverted microscope Vert.A1 (AXIO) by Zeiss.

RNA-Sequencing data analysis. Trizol reagent (Ambion, Invitrogen) was used to isolate total RNA that was processed to prepare cDNA libraries using TruSeq technology according to the manufacturer's instructions protocol (Illumina, San Diego, CA). Libraries were sequenced using Illumina NovaSeq 6000, with a read length of 101 bp, by Bencos Research Solutions Pvt. Ltd., Bangalore, India. FastQC (0.11.5) was used to access the read quality of the raw data. Trimmomatic was used to remove Illumina adaptors and sliding-window approach was used for the quality filtering of reads. Approximately 20 million cleaned pair-end sequencing reads from each sample were uploaded to the Galaxy web platform and were analyzed at https://usegalaxy.org. HISAT2 was used to map the reads with the reference human genome (hg38). StringTie was used to assemble the aligned RNA-Seq reads into transcripts and estimate the abundance of the assembled transcripts. DESeq2 was used for differential expression analysis of genes between groups[30]. Various R packages were used to visualize the expression and differential expression outcomes. Gene ontology (GO) analysis

bioRxiv preprint doi: https://doi.org/10.1101/2020.02.29.969014; this version posted March 3, 2020. The copyright holder for this preprint (which was not certified by peer review) is the author/funder. All rights reserved. No reuse allowed without permission.

was done using the web-based Gene Set Analysis toolkit, and analysis of upregulated KEGG pathways was done using Enrichr. Cluster 3.0 and TreeView 1.1.6 were used for making heat maps. All the addressed analysis were demonstrated as described previously[50].

Statistical analysis. All experiments were carried out along with the appropriate controls, indicated as untreated/untransfected cells (Ctrl) or transfected with the transfection reagent alone (Mock). Experiments were performed in duplicates or triplicates for at least two or three times independently. GraphPad Prism 5.0 (GraphPad Software, La Jolla, CA, USA) was used for statistical analysis. The differences between two groups were compared by using an unpaired two-tailed Student's t-test and/or Mann Whitney test additionally the paired data was analyzed using paired t-test and/or Wilcoxon sign rank test. While the differences between three groups or more were compared by using analysis of variance (ANOVA)w ith Tukey test. Differences were considered to be statistically significant when $P < 0.05$. Statistical significance in the figures is indicated as follows: $***P < 0.001$, $**P < 0.01$, $*P < 0.05$; *ns*, not significant.

bioRxiv preprint doi: https://doi.org/10.1101/2020.02.29.969014; this version posted March 3, 2020. The copyright holder for this preprint (which was not certified by peer review) is the author/funder. All rights reserved. No reuse allowed without permission.

References

1. Akira, S., Uematsu, S. & Takeuchi, O. Pathogen recognition and innate immunity. *Cell* 124, 783-801 (2006).
2. Alvarez, K. & Vasquez, G. Damage-associated molecular patterns and their role as initiators of inflammatory and auto-immune signals in systemic lupus erythematosus. *International reviews of immunology* 36, 259-270 (2017).
3. He, L. & Hannon, G.J. MicroRNAs: small RNAs with a big role in gene regulation. *Nature reviews. Genetics* 5, 522-531 (2004).
4. Treiber, T., Treiber, N. & Meister, G. Regulation of microRNA biogenesis and its crosstalk with other cellular pathways. *Nature reviews. Molecular cell biology* 20, 5-20 (2019).
5. Li, C. *et al.* Competitive virus and host RNAs: the interplay of a hidden virus and host interaction. *Protein & cell* 5, 348-356 (2014).
6. Zheng, Z. *et al.* Human microRNA hsa-miR-296-5p suppresses enterovirus 71 replication by targeting the viral genome. *Journal of virology* 87, 5645-5656 (2013).
7. Ingle, H. *et al.* The microRNA miR-485 targets host and influenza virus transcripts to regulate antiviral immunity and restrict viral replication. *Science signaling* 8, ra126 (2015).
8. Porritt, R.A. & Hertzog, P.J. Dynamic control of type I IFN signalling by an integrated network of negative regulators. *Trends in immunology* 36, 150-160 (2015).
9. Kondo, T., Kawai, T. & Akira, S. Dissecting negative regulation of Toll-like receptor signaling. *Trends in immunology* 33, 449-458 (2012).
10. Moulton, V.R. *et al.* Pathogenesis of Human Systemic Lupus Erythematosus: A Cellular Perspective. *Trends in molecular medicine* 23, 615-635 (2017).
11. Shen, N., Liang, D., Tang, Y., de Vries, N. & Tak, P.P. MicroRNAs--novel regulators of systemic lupus erythematosus pathogenesis. *Nature reviews. Rheumatology* 8, 701-709 (2012).
12. Garchow, B.G. *et al.* Silencing of microRNA-21 in vivo ameliorates autoimmune splenomegaly in lupus mice. *EMBO molecular medicine* 3, 605-615 (2011).
13. Ning, Z.Q. *et al.* MicroRNA-30e reduces cell growth and enhances drug sensitivity to gefitinib in lung carcinoma. *Oncotarget* 8, 4572-4581 (2017).
14. Feng, G.X. *et al.* Hepatitis B virus X protein promotes the development of liver fibrosis and hepatoma through downregulation of miR-30e targeting P4HA2 mRNA. *Oncogene* 36, 6895-6905 (2017).
15. Liu, M.M. *et al.* MiR-30e inhibits tumor growth and chemoresistance via targeting IRS1 in Breast Cancer. *Scientific reports* 7, 15929 (2017).
16. Su, Q., Ye, Z., Sun, Y., Yang, H. & Li, L. Relationship between circulating miRNA-30e and no-reflow phenomenon in STEMI patients undergoing primary coronary intervention. *Scandinavian journal of clinical and laboratory investigation* 78, 318-324 (2018).
17. Wu, J. *et al.* MicroRNA-30 family members regulate calcium/calcineurin signaling in podocytes. *The Journal of clinical investigation* 125, 4091-4106 (2015).
18. Kim, B.S., Jung, J.Y., Jeon, J.Y., Kim, H.A. & Suh, C.H. Circulating hsa-miR-30e-5p, hsa-miR-92a-3p, and hsa-miR-223-3p may be novel biomarkers in systemic lupus erythematosus. *Hla* 88, 187-193 (2016).
19. Kozak, R.A. *et al.* MicroRNA and mRNA Dysregulation in Astrocytes Infected with Zika Virus. *Viruses* 9 (2017).
20. Zhu, X. *et al.* MicroRNA-30e* suppresses dengue virus replication by promoting NF-kappaB-dependent IFN production. *PLoS neglected tropical diseases* 8, e3088 (2014).

bioRxiv preprint doi: https://doi.org/10.1101/2020.02.29.969014; this version posted March 3, 2020. The copyright holder for this preprint (which was not certified by peer review) is the author/funder. All rights reserved. No reuse allowed without permission.

21. Versteeg, G.A., Benke, S., Garcia-Sastre, A. & Rajsbaum, R. InTRIMsic immunity: Positive and negative regulation of immune signaling by tripartite motif proteins. *Cytokine & growth factor reviews* 25, 563-576 (2014).
22. Zhao, W., Wang, L., Zhang, M., Yuan, C. & Gao, C. E3 ubiquitin ligase tripartite motif 38 negatively regulates TLR-mediated immune responses by proteasomal degradation of TNF receptor-associated factor 6 in macrophages. *J Immunol* 188, 2567-2574 (2012).
23. Hu, M.M. *et al.* TRIM38 inhibits TNFalpha- and IL-1beta-triggered NF-kappaB activation by mediating lysosome-dependent degradation of TAB2/3. *Proceedings of the National Academy of Sciences of the United States of America* 111, 1509-1514 (2014).
24. Kawagoe, T. *et al.* TANK is a negative regulator of Toll-like receptor signaling and is critical for the prevention of autoimmune nephritis. *Nature immunology* 10, 965-972 (2009).
25. Li, M. *et al.* Respiratory Syncytial Virus Replication Is Promoted by Autophagy-Mediated Inhibition of Apoptosis. *Journal of virology* 92 (2018).
26. Jounai, N. *et al.* The Atg5 Atg12 conjugate associates with innate antiviral immune responses. *Proceedings of the National Academy of Sciences of the United States of America* 104, 14050-14055 (2007).
27. Cui, J., Jin, S. & Wang, R.F. The BECN1-USP19 axis plays a role in the crosstalk between autophagy and antiviral immune responses. *Autophagy* 12, 1210-1211 (2016).
28. Pothlichet, J., Chignard, M. & Si-Tahar, M. Cutting edge: innate immune response triggered by influenza A virus is negatively regulated by SOCS1 and SOCS3 through a RIG-I/IFNAR1-dependent pathway. *J Immunol* 180, 2034-2038 (2008).
29. Gheita, T.A. *et al.* Anti-dsDNA titre in female systemic lupus erythematosus patients: relation to disease manifestations, damage and antiphospholipid antibodies. *Lupus* 27, 1081-1087 (2018).
30. Love, M.I., Huber, W. & Anders, S. Moderated estimation of fold change and dispersion for RNA-seq data with DESeq2. *Genome Biology*, 15, 550 (2014).
31. Morel, L. Genetics of SLE: evidence from mouse models. *Nature reviews. Rheumatology* 6, 348-357 (2010).
32. Vela, E.M. *et al.* MicroRNA expression in mice infected with seasonal H1N1, swine H1N1 or highly pathogenic H5N1. *Journal of medical microbiology* 63, 1131-1142 (2014).
33. Gao, L. *et al.* Dynamic expression of viral and cellular microRNAs in infectious mononucleosis caused by primary Epstein-Barr virus infection in children. *Virology journal* 12, 208 (2015).
34. Wang, Y. *et al.* Elevated expression of miR-142-3p is related to the pro-inflammatory function of monocyte-derived dendritic cells in SLE. *Arthritis research & therapy* 18, 263 (2016).
35. Chaussabel, D. *et al.* A modular analysis framework for blood genomics studies: application to systemic lupus erythematosus. *Immunity* 29, 150-164 (2008).
36. Yang, Y. *et al.* Pretreatment microRNA levels can predict HBsAg clearance in CHB patients treated with pegylated interferon alpha-2a. *Virology journal* 15, 73 (2018).
37. Wang, Y. *et al.* TRIM35 negatively regulates TLR7- and TLR9-mediated type I interferon production by targeting IRF7. *FEBS letters* 589, 1322-1330 (2015).
38. Narayan, K. *et al.* TRIM13 is a negative regulator of MDA5-mediated type I interferon production. *Journal of virology* 88, 10748-10757 (2014).
39. Lu, Q. *et al.* Homeostatic Control of Innate Lung Inflammation by Vici Syndrome Gene Epg5 and Additional Autophagy Genes Promotes Influenza Pathogenesis. *Cell host & microbe* 19, 102-113 (2016).
40. Aliberti, J. *et al.* Essential role for ICSBP in the in vivo development of murine $CD8\alpha^+$ dendritic cells. *Blood* 101, 305-310 (2003).
41. Tamura, T. *et al.* IFN Regulatory Factor-4 and -8 Govern Dendritic Cell Subset Development and Their Functional Diversity. *Journal of Immunology* 175 (5), 2573-2581 (2005).

bioRxiv preprint doi: https://doi.org/10.1101/2020.02.29.969014; this version posted March 3, 2020. The copyright holder for this preprint (which was not certified by peer review) is the author/funder. All rights reserved. No reuse allowed without permission.

42. Paran, N., Geiger, B. & Shaul, Y. HBV infection of cell culture: evidence for multivalent and cooperative attachment. *The EMBO journal* 20, 4443-4453 (2001).
43. Bchini, R., Capel, F., Dauguet, C., Dubanchet, S. & Petit, M.A. In vitro infection of human hepatoma (HepG2) cells with hepatitis B virus. *Journal of virology* 64, 3025-3032 (1990).
44. Gripon, P. *et al.* Hepatitis B virus infection of adult human hepatocytes cultured in the presence of dimethyl sulfoxide. *Journal of virology* 62, 4136-4143 (1988).
45. Vivekanandan, P., Daniel, H.D., Kannangai, R., Martinez-Murillo, F. & Torbenson, M. Hepatitis B virus replication induces methylation of both host and viral DNA. *Journal of virology* 84, 4321-4329 (2010).
46. Zhu, X. *et al.* TMEM2 inhibits hepatitis B virus infection in HepG2 and HepG2.2.15 cells by activating the JAK-STAT signaling pathway. *Cell death & disease* 7, e2239 (2016).
47. Meister, G. *et al.* Human Argonaute2 mediates RNA cleavage targeted by miRNAs and siRNAs. *Molecular cell* 15, 185-197 (2004).
48. Beitzinger, M. & Meister, G. Experimental identification of microRNA targets by immunoprecipitation of Argonaute protein complexes. *Methods Mol Biol* 732, 153-167 (2011).
49. Kumar, S. *et al.* IPS-1 differentially induces TRAIL, BCL2, BIRC3 and PRKCE in type I interferons-dependent and -independent anticancer activity. *Cell death & disease* 6, e1758 (2015).
50. Kumar, A. *et al.* MicroRNA hsa-miR-324-5p Suppresses H5N1 Virus Replication by Targeting the Viral PB1 and Host CUEDC2. *Journal of virology* 92 (2018).

bioRxiv preprint doi: https://doi.org/10.1101/2020.02.29.969014; this version posted March 3, 2020. The copyright holder for this preprint (which was not certified by peer review) is the author/funder. All rights reserved. No reuse allowed without permission.

Figure Legends

Figure 1 - Viral infection induces miRNA-30e that inhibits virus replication by promoting innate immunity: (A) Quantification (as determined by qRT-PCR analysis) of the fold changes in the abundances of miR-30e as indicated, in the serum collected from hepatitis B patients (n=51) compared to healthy controls (n=24). (B-F; I and J) Quantification of the fold changes in the relative abundances of miR-30e , viral transcripts and respective innate immune transcripts (*IFNλ1, IL6 and IFIT1)* at the indicated times after treatment or infection with (B) HBV patient's serum (HBV PS) in HepG2 cells, (C) HepG2 cells were transfected with miR-30e (50 nM) or miR-NC1 (50 nM) prior to infection (D) HepG2215 cells, stably expressing HBV replicon HepG2 cells transfected with miR-30e or miR-NC1, (E) NDV (MOI 5) in human PBMCs, (F) hPBMCs transfected with miR-30e or AmiR-30e (50 nM) prior to infection and (I) SeV (MOI 5) in A549 cells (J) A549 cells transfected with miR-30e or AmiR-30e prior to infection. (G, H and K) Quantification of viral infection as indicated in (G) HEK293 cells (transfected with miR-30e or AmiR-30e for 24 hours then infected with GFP-tagged NDV (NDV-GFP) (MOI 5) for 36 hours and subjected to immunoblot analysis using antibodies specific for GFP (anti-GFP antibody) and γ-tubulin (used as a loading control), (H) HeLa cells transfected with miR-30e or infected with NDV-GFP and subsequently subjected to confocal microscopic analysis for NDV particles with anti-GFP antibody (green) and, nuclei were visualized with 4′,6-diamidino-2-phenylindole (DAPI; blue) and (K) A549 cells were transfected with miR-30e or AmiR-30e for 24 hours then infected with RFP tagged SeV (MOI 5) for 24 hours and analyzed by flow cytometery. Ctrl represents control untreated sample, D; represents number of days, *dpi*; represents days post infection and *hpi*; represents hours post infection. Data are mean +/- SEM of triplicate samples from single experiment and are representative of three (A-C, E, F, I, J) two (D, G, H, K) independent experiments. ***$P<0.001$, **$P<0.01$ and *$P<0.05$ by one-way ANOVA Tukey test, Mann-Whitney test and unpaired t-test.

Figure 2 - Transcriptomic analysis shows miR-30e enhances innate immune responses during NDV infection: (A) Schematic outline of transfection with control (miR-NC1) or miR-30e and NDV infection (MOI 5) in A549 cells at indicated time and subjected to whole transcriptome sequencing and gene analysis (Inf: infected and Un-inf: uninfected). (B) Quantification of the fold changes in the abundances of miR-30e is measured by qRT-PCR and normalized by U6 control and NDV viral transcripts in both the replicate samples

bioRxiv preprint doi: https://doi.org/10.1101/2020.02.29.969014; this version posted March 3, 2020. The copyright holder for this preprint (which was not certified by peer review) is the author/funder. All rights reserved. No reuse allowed without permission.

used for transcriptome sequencing and analysis. (C) Plot showing first two components from principal component analysis of all the 6 samples, distance between samples indicate how different they are from each other in terms of gene expression. (D) Volcano plot represents differential expression of genes between two groups of samples (miR-30e and miR-NC1 overexpression) during NDV infection in A549 cells. For each gene: *P-value* is plotted against fold change (miR-30e vs miR-NC1). Genes significantly changed (>1.5-fold) are colored in red (upregulated) and blue (downregulated). (E) KEGG pathway analysis of upregulated genes, outer circle indicates top upregulated pathways and the inner circle represents corresponding combined score (a derivative of *P-value* and Z-score). (F) Heat map represents relative abundance of top upregulated interferon stimulated genes across different samples. (G) Quantification (measured by qRT-PCR) of the fold changes in the abundances of type 1 interferon and pro-inflammatory cytokines in the samples, A549 cells transfected with miR-NC1 or miR-30e and infected with NDV as indicated (NDV+NC1) and (NDV+30e), analyzed by RNA-Sequencing.

Figure 3 - miR-30e targets 3'UTR of negative regulators of innate immune signaling pathways: (A) Screening pipeline used for identification of miR-30e target genes based on the indicated schematic workflow, final hits 09 genes corresponds to negative regulators targeted by miRNA-30e. (B) Reanalysis of previous transcriptome data for identification of negative regulators (targeted by miR-30e) upon miR-30e transfection and NDV infection (MOI 5) compared to miR-NC1 in two replicate samples. (C) HEK293 cells were transfected with 50 ng of pRL-TK and 300ng of 3'UTR_WT (of indicated genes) together with 25 nM miR-30e or miR-NC1, 24 hours after transfection, the cell was lysed and subjected to luciferase assay. (D) HEK293T cells were transiently transfected with 1.5µg of *sh*-clones of indicated genes or scrambled control for 48 hours then infected with NDV (MOI 5) for 24 hours and subjected to the quantification of the indicated transcripts or genes and *IFNβ*. (E) Schematic for RNA-immunoprecipitation assay. HEK293 cells were transfected with plasmid encoding Flag-Ago2 in presence of miR-30e (50 nM) and miR-NC1 (50 nM) and then infected with NDV (MOI 5). 24 hours after transfection cells were subjected to RNA immunoprecipitation with ant-Flag antibody and quantified for *TRIM38, TANK, ATG5, ATG12, BECN1, SOCS1* and *SOCS3* transcripts. (F) A549 cells were transfected with miR-30e or miR-NC1 mimic and then infected with NDV (MOI 5) for 36 hours before being subjected to immunoblot analysis with antibodies specific for indicated protein or γ-tubulin (used as a loading control). Data are mean +/- SEM of triplicate samples from single experiment and are

bioRxiv preprint doi: https://doi.org/10.1101/2020.02.29.969014; this version posted March 3, 2020. The copyright holder for this preprint (which was not certified by peer review) is the author/funder. All rights reserved. No reuse allowed without permission.

representative of three (C) two (D, E, F) independent experiments. ***P<0.001, **P<0.01 and *P<0.05 by one-way ANOVA Tukey test and unpaired t-test.

Figure 4 - Human PBMCs stimulated with DAMPs induce miRNA-30e and enhance innate immune responses: PBMCs from three healthy individuals were transfected with their own genomic DNA (ds DNA). (A) Isolated genomic DNA sonicated into small fragments of dsDNA of approximately 100-150 bps each (as shown) and transfected using Lipofectamine 2000. (B-F) Quantification (by qRT-PCR analysis) of the fold changes in the relative abundances of (B) miR-30e, (C-E) respective innate immune transcripts (*IFNα, IFNβ, IFIT1* and *IL6)* in all individuals and (F) NDV viral transcript (shown as per schematic workflow). Data are mean +/- SEM of triplicate samples from single experiment and are representative of three independent experiments in three different individuals. ***P<0.001, **P<0.01 and *P<0.05 by one-way ANOVA Tukey test and unpaired t-test, N.D. correspond to not detected.

Figure 5 - SLE patients and mouse model show enhanced innate immune responses: (A-C) Quantification of the fold changes by qRT-PCR analysis of indicated transcripts *IFNβ, IFIT1* and *IL6* (in SLE patients) and *Ip10, Tnfα* and *Il6* (in SLE mice) and miR-30e at indicated times as represented in the schematic workflow in, (A) PBMCs from SLE diagnosed patients (P) (n=13) and healthy controls (HC) (n=13), (B) Splenocytes from parent (New Zealand White and Black-NZW and NZB) (PM) (n=7) and lupus induced mice (NZW/B -F1 progeny) (F1) (n=7) and (C) Splenocytes from PM (n= 9) and F1 (n=12) and serum from PM (n=16) and F1 (n=21). Data are mean +/- SEM of triplicate samples from single experiment (A) and are representative of two independent experiments (B and C). ***P<0.001, **P<0.01 and *P<0.05 by unpaired t-test and Mann-Whitney test.

Figure 6 - Enhanced miRNA-30e suppresses negative regulators in SLE patients and mouse model: (A-B) Schematic representation of the workflow for quantification of the fold changes by qRT-PCR analysis of indicated transcripts in (A) PBMCs of SLE patients (*TRIM38, TANK, SOCS1* and *SOCS3*) and (B) Splenocytes of SLE mice (*Socs1, Socs3, Atg5* and *Atg12*). Data are mean +/- SEM of triplicate samples from single

bioRxiv preprint doi: https://doi.org/10.1101/2020.02.29.969014; this version posted March 3, 2020. The copyright holder for this preprint (which was not certified by peer review) is the author/funder. All rights reserved. No reuse allowed without permission.

869 experiment (A) and are representative of two independent experiments (B). ***P<0.001, **P<0.01 and
870 *P<0.05 by unpaired t-test.

871 **Figure 7 - Prognostic and therapeutic potential of miR-30e:** (A) Schematic representation of the workflow
872 for quantification of the fold changes by qRT-PCR analysis of miR-30e as indicated, in the serum collected
873 from hepatitis B (HBV) naive patients (n=7) compared to HBV treated (with pegylated IFNs) patients (n=7).
874 (B) Schematic representation of workflow for quantification of the fold changes in the relative abundances of
875 miR-30e and *IFNβ* as indicated, in the PBMCs from SLE patients treated with/without AmiR-30e (miR-30e
876 inhibitor). (C) Schematic representation of the *ex-vivo* experiment workflow for quantification of the fold
877 changes in the relative abundances of *Il6* and *Tnfα* as indicated, in the splenocytes from SLE mice model (as
878 described previously) treated with AmiR-30e (miR-30e inhibitor) and AmiR-NC1. (D) Schematic
879 representation of the *in-vivo* experiment workflow for quantification of the fold changes of miR-30e, *Il6*, *Ip10*,
880 *Socs1* and *Socs3* as indicated, in the splenocytes and serum from SLE mice model (as described previously);
881 four mice distributed in each group were subjected to LNA-miR-30e-antagomir (LNA Amir-30e) and LNA-
882 negative control antagomir (LNA NC) treatment (explained in materials and methods). Data are mean +/- SEM
883 of triplicate samples from single experiment (A-B and D) and are representative of two independent
884 experiments (C). All the *P-values*/***P<0.001 defined by paired t-test.

885 **Figure 8 – Regulation of innate immune responses by miRNA-30e during virus infection and SLE:**
886 PAMPs (green) and DAMPs (red) sensed by Pattern recognition receptors (PRRs) to activate cascade of innate
887 immune signaling pathways to induce pro-inflammatory cytokines (yellow), type I and type III interferons
888 (blue) and miRNA-30e (purple). miRNA-30e regulates both PAMPs and DAMPs induced immune responses
889 by targeting the 3'-UTR of negative regulators (dark blue) of innate immune signaling pathways and reducing
890 the expression of these negative regulators (grey). During viral infection, miR-30e is induced which reduces
891 the cellular abundance of negative regulators to enhance innate immune responses and facilitate viral clearance.
892 The endogenous host DNA induces miR-30e and subsequently enhances innate immune responses for the
893 development of autoimmune disease, SLE.
894

bioRxiv preprint doi: https://doi.org/10.1101/2020.02.29.969014; this version posted March 3, 2020. The copyright holder for this preprint (which was not certified by peer review) is the author/funder. All rights reserved. No reuse allowed without permission.

Supplementary Figure Legends

Figure S1 - miRNA-30e induced during viral infection: (A) Schematic representation for the selection and screening pipeline of common miRNAs during viral infections. (B) Table and Venn diagram represent miR-30e, miR-27a and miR-181a as commonly upregulated miRNAs during indicated infections. Abundance of miR-30e-5p as log fold change (Log FC) and transcripts per million (TPM) in indicated infections, (C) Log FC (fold change) of the selected miRNAs and efficiency (represented by [*] asterisk) by which they target the negative regulation of innate immune signaling pathways as per indicated GEO dataset (GSE65694) and algorithms. (D) miR-30e is conserved among the wide range of species (green); has, Homo sapiens (Human); mmu, Mus musculus (Mouse); rno, Rattus norvegicus (Norway Rat); mml, Macaca mulatta (Rhesus monkey); gga, Gallus gallus (chicken); chi, Capra hircus (Goat); dre, Danio rerio (Zebrafish) and bta, Bos Taurus (Cattle).

Figure S2 - Induction of miRNA-30e in different cells by DNA, RNA virus and viral PAMPs: (A-E) Quantification of the fold changes by qRT-PCR in the abundances of miR-30e (at the indicated times and cells) after indicated viral infections and viral PAMPs treatment (A and B) NDV (MOI 5) in A549 and Raw 264.7 cells respectively, (C) HCMV-GFP (MOI 5) in HFF. (D and E) indicated synthetic PAMPs [poly IC (10μg/ml) {stimulation (S) and transfection (T)}; ssRNA (2μg/ml)] in (D) HeLa and (E) Raw 264.7 cells. (F) Schematic representation of workflow for quantification of miR-30e promoter activity and ISRE/IFNβ/NFκB promoter activity by luciferase assay as indicated in (G, I-K) HEK293 cells and (H) HeLa cells. Data are mean +/- SEM of triplicate samples from single experiment and are representative of three (A-C, I-M) two (D-G) independent experiments. ***$P<0.001$, **$P<0.01$ and *$P<0.05$ by one-way ANOVA Tukey test and unpaired t-test.

Figure S3 - miR-30e inhibits viral replication: (A-F) Quantification of the fold changes in the relative abundances of viral transcripts measured by qRT-PCR after treatment or infection in indicated cells with (A) HepG2215 cells were transfected with/without miR-30e as described previously, (B) HepG2-NTCP cells transfected with miR-30e and miR-NC1 to quantify relative expression (RE) of HBV viral transcripts (HBV RNA and pgRNA), (C) HBV patient serum in HepG2 compared with HepG2215 cells as indicated. (D-F) NDV (MOI 5) in HeLa, A549 and Raw264.7 cells respectively transfected with miR-NC1 or miR-30e prior to infection as described previously. (G) Quantification of NDV viral signals detected by flow cytometery in HeLa cells mock transfected or transfected with miR-30e for 24 hours then subjected to NDV (GFP tagged) infection (MOI 5) for 24 hours. HBV DNA, HBV cccDNA and HBV copy number represent different primers set used

bioRxiv preprint doi: https://doi.org/10.1101/2020.02.29.969014; this version posted March 3, 2020. The copyright holder for this preprint (which was not certified by peer review) is the author/funder. All rights reserved. No reuse allowed without permission.

to measure HBV viral transcripts. Data are mean +/- SEM of triplicate samples from single experiment and are representative of three (D-F) two (A, B,C and G) independent experiments. ***P<0.001 and **P<0.01 by one-way ANOVA Tukey test and unpaired t-test.

Figure S4 - miR-30e enhances innate immune responses during viral infection (A-F) Quantification of the fold changes in the relative abundances of indicated genes and cells measured by qRT-PCR after viral infection and transfection with/without miR-30e as described previously. (G-I) A549 and HeLa cells were mock transfected, transfected with miR-30e or miR-NC1 mimics and then infected with NDV (MOI 5), 24 hours after infection, the amounts of *IP10* and *IL6* protein secreted into the cell culture supernatant were measured by enzyme-linked immunosorbent assay (ELISA). (J-L) Schematic representation of workflow for quantification of ISRE/IFNβ/NFκB promoter activity by luciferase assay as indicated in (I-K) HEK293 cells. Data are mean +/- SEM of triplicate samples from single experiment and are representative of two (A-B) and three (C-L) independent experiments. ***P<0.001, **P<0.01 and *P<0.05 by one-way ANOVA Tukey test.

Figure S5 - miR-30e inhibits DNA virus replication: HFF (Human foreskin fibroblast) cells were cultured in DMEM and transfected with miR-30e or miR-NC1 mimics then infected with HCMV-GFP virus (MOI = 5) and RNA were isolated to quantify the (A) HCMV transcript (Glycoprotein B) by using qRT-PCR and GFP signals (of HCMV-GFP tagged virus) by microscopy, (B) *IL6* transcript in indicated transfected groups and compared with control. Data are mean +/- SEM of triplicate samples from single experiment and are representative of two independent experiments. ***P<0.001 and **P<0.01 by one-way ANOVA Tukey test.

Figure S6 - miR-30e enhances innate immune responses upon viral PAMPs stimulation: (A-F) Quantification of indicated transcripts in indicated cells (measured by qRT-pCR) transfected with mir-30e or miR-NC1 for 24 hours and then stimulated with (A-D) poly IC (10μg/ml) and (E-F) ssRNA (2μg/ml) treatment respectively. (G, H) HEK 293T cells transfected with miR-30e (25 nM) or miR-NC1 (25 nM) mimics, pRL-TK (50 ng) and indicated luciferase reporters for ISRE/IFNβ (200 ng) then stimulated with poly IC for 24 hours. Cells were then lysed to analyze the promoter activity by luciferase assay. Data are mean +/- SEM of triplicate samples from single experiment and are representative of three independent experiments. ***P<0.001, **P<0.01 and *P<0.05 by one-way ANOVA Tukey test.

bioRxiv preprint doi: https://doi.org/10.1101/2020.02.29.969014; this version posted March 3, 2020. The copyright holder for this preprint (which was not certified by peer review) is the author/funder. All rights reserved. No reuse allowed without permission.

Figure S7 – miR-30e differentially expressed genes during NDV infection: (A) Workflow for the analysis of RNA-Sequencing data from raw sequencing reads to expression profiles of differentially expressed genes represented through different plots and heat maps. (B) MA (M=log ratio and A=mean average) plot for differential expression of genes, indicating upregulated (in red) and downregulated (in green) genes. (C) Heat map representing relative abundance of genes involved in top enriched KEGG pathways in figure 2E.

Figure S8 – Minimum free energy (mfe) for binding efficiency of miR-30e to negative regulators: Representative of minimum free energy diagrams for negative regulators (*TRIM38, TRIM13, TANK, ATG5, ATG12, BECN1, EPG5, SOCS1* and *SOCS3*) and positive regulators (*JAK1* and *STAT1*) targeted by miR-30e.

Figure S9 – Quantification of innate immune negative regulators in presence of miR-30e: (A) HEK293 cells were transfected with miR-30e (25nM) mimic and 50 ng of pRL-TK along with 300ng of 3'UTR_WT or 300ng of 3'UTR_MUT for 24 hours, the cell was lysed and subjected to luciferase assay. 3'-UTRs of all selected target genes having binding sites for seed sequence in miR-30e were conserved throughout (shown in red). (B and C) Quantification of the fold changes by qRT-PCR analysis in the relative abundances of miR-30e (at the indicated times), and negative regulator transcripts (*TRIM38, TANK, ATG5, ATG12, BECN1, SOCS1* and *SOCS3*) after infection of (B) NDV (MOI = 5) in A549 cells and (C) NDV (MOI = 5) for 24 hours in A549 cells remain untransfected, transfected with miR-30e or miR-NC1 as indicated. Data are mean +/- SEM of triplicate samples from single experiment and are representative of two independent experiments. ***$P<0.001$, **$P<0.01$ and *$P<0.05$ by one-way ANOVA Tukey test.

Figure S10 – Quantification of innate immune negative regulators in presence of miR-30e: (A-D) Quantification of the fold changes by qRT-PCR analysis in the relative abundances of negative regulator transcripts (*TRIM38, TANK, ATG5, ATG12, BECN1, SOCS1* and *SOCS3*) in (A) HepG2 cells remain untransfecd, transfected with miR-30e, AmiR-30e or miR-NC1 for 48 hours then treated with HBV-PS for HBV infection, (B) HepG2215 cells transfected as described previously, (C) HepG2-NTCP cells transfected with miR-30e and miR-NC1 for 48 hours then infected with HBV infection. (D-E) HeLa cells remain untransfecd, transfected with miR-30e, AmiR-30e or miR-NC1 for 24 hours then (D) infected with NDV (MOI = 5) or (E) treated with poly IC for 24 hours. D; represents number of days, *dpi*; days post infection and *hpi*; hours post infection. Data are mean +/- SEM of triplicate samples from single experiment and are representative of two independent experiments. ***$P<0.001$, **$P<0.01$ and *$P<0.05$ by one-way ANOVA Tukey test.

bioRxiv preprint doi: https://doi.org/10.1101/2020.02.29.969014; this version posted March 3, 2020. The copyright holder for this preprint (which was not certified by peer review) is the author/funder. All rights reserved. No reuse allowed without permission.

Figure S11 – DAMPs induce apoptosis and TLR 3/7/9: (A) Human PBMCs remain untreated or treated with camptothecin, dsDNA separately from two different individuals (as indicated 1 and 2) and subjected to Annexin PI assay to detect the apoptosis level within the PBMCs using flow cytometery. (B-D) Quantification of the fold changes by qRT-PCR analysis in the relative abundances of respective transcripts (*TLR3, TLR7* and *TLR9)* in all individuals. Data is the representative of three independent experiments. Data are mean +/- SEM of triplicate samples from single experiment and are representative of three independent experiments. ***$P<0.001$ and **$P<0.01$ by unpaired t-test.

Figure S12 – GEO Datasets re-analyzed to demonstrate the expression level of miR-30e in autoimmune disorder: (A) SLE (GSE79240) - Non-coding RNA profiling by microarray in dendritic cells of SLE patients (P) compared to healthy controls (HC). Data points include fold change of miR-30e among 5 patients. (B) Type 1 Diabetes Mellitus (GSE55099) - Non-coding RNA profiling by microarray in PBMCs of patients (P) compared to healthy controls (HC). Data points include fold change of miR-30e among 12 patients compared to 10 healthy controls (*P-value* = 0.0086).

Figure S13 – GEO Dataset-GSE11909 re-analyzed to demonstrate the transcript levels of innate negative regulators in SLE: (A) Expression profiling by microarray to estimate the log fold change of following innate negative regulators during SLE pathogenesis in patients (P) compared to healthy controls (HC); ATG5, ATG12, BECN1, TANK, SOCS1, SOCS3, TRIM13 and TRIM38.

Figure S14 – GEO Dataset-GSE104126 re-analyzed to demonstrate the expression level of miR-30e: (A) Non-coding RNA profiling by microarray in PBMCs of two types of chronic hepatitis B (CHB) patients (HBsAg loss and non-HBsAg loss) after treatment with pegylated interferon (peg-IFNα2a). Data points include fold change of miR-30e among 10 patients.

bioRxiv preprint doi: https://doi.org/10.1101/2020.02.29.969014; this version posted March 3, 2020. The copyright holder for this preprint (which was not certified by peer review) is the author/funder. All rights reserved. No reuse allowed without permission.

Supplementary Tables

Table T1: Demographic data of chronic hepatitis B (CHB) cohort and controls

Table T2: Differentially expressed genes by RNA sequencing analysis

Table T3: *In-silico* analysis of miR-30e targets using indicated algorithms

Table T4: CLIP database analysis for miR-30e targets

Table T5: SLE patients details used in the study

Table T6: Demographic data of chronic hepatitis B (CHB) patients after Peg-interferon treatment

Table T7: List of primers used in the study

bioRxiv preprint doi: https://doi.org/10.1101/2020.02.29.969014; this version posted March 3, 2020. The copyright holder for this preprint (which was not certified by peer review) is the author/funder. All rights reserved. No reuse allowed without permission.

Acknowledgments: We acknowledge Professor Akinori Takaoka for valuable discussions. We thank Dr. Takaji Wakita for providing the HepG2-NTCP cell lines. We thank Dr. Nirupma Trehanpati and Dr. Senthil Kumar Venugopal for providing the HepG2 and HepG2215 cell lines. We thank Dr. Sunil Raghav for providing Sendai-RFP, Professor. Peter Palese for providing NDV-GFP and Professor. Wade Gibson for providing HCMV-GFP and HFFs. We thank Professor. T. Tuschl for providing the Ago2-Flag construct through Addgene and BEI Resources for providing human rIFNβ. We are grateful to Indian Institute of Science Education and Research (IISER) Bhopal for providing the Central Instrumentation Facility. We also thank all members of the laboratory for helpful discussions. Finally, we are eternally grateful to all the patients and healthy donors for proving their blood samples for the study.

bioRxiv preprint doi: https://doi.org/10.1101/2020.02.29.969014; this version posted March 3, 2020. The copyright holder for this preprint (which was not certified by peer review) is the author/funder. All rights reserved. No reuse allowed without permission.

1058 **Funding:** This work was partially supported by IISER Bhopal–IGM Hokkaido University
1059 Grant for General Joint Research Program of the Institute for Genetic Medicine, Hokkaido
1060 University, Japan and by an Intramural Research Grant of IISER, Bhopal, India, to H.K.
1061 Start-up grant, IISER Bhopal to A.C. R.M. is supported by the IISER Bhopal institutional
1062 fellowship.

bioRxiv preprint doi: https://doi.org/10.1101/2020.02.29.969014; this version posted March 3, 2020. The copyright holder for this preprint (which was not certified by peer review) is the author/funder. All rights reserved. No reuse allowed without permission.

Author contributions: R.M. and H.K. conceptualized the study and designed the experiments; R.M. performed the experiments; S.B. and D.K. performed the mutation experiments; R.M., A.K. and H.K. analyzed the data; R.M., P.G. and H.K. designed the HBV experiments; P.G. provided the HBV patients samples; R.M., K.N. and P.G. performed the HBV experiments; R.M., A.A., P.T. and H.K. designed the SLE experiments; A.A. provided the SLE patients samples and executed SLE patient samples experiments; R.M. and A.K. performed the SLE *in-vitro* experiments; B.S.R., R.M. and P.T. performed the SLE mice related experiments; A.C. helped in procuring critical reagents; R.M. and H.K. wrote the manuscript; and H.K. supervised the entire project.

Conflict of interests: The authors declare no conflict of interests.

Data and materials availability: The NGS (RNA-Sequencing) data for expression profiling reported in this paper have been deposited in the GenBank database (accession no. GSE130005).

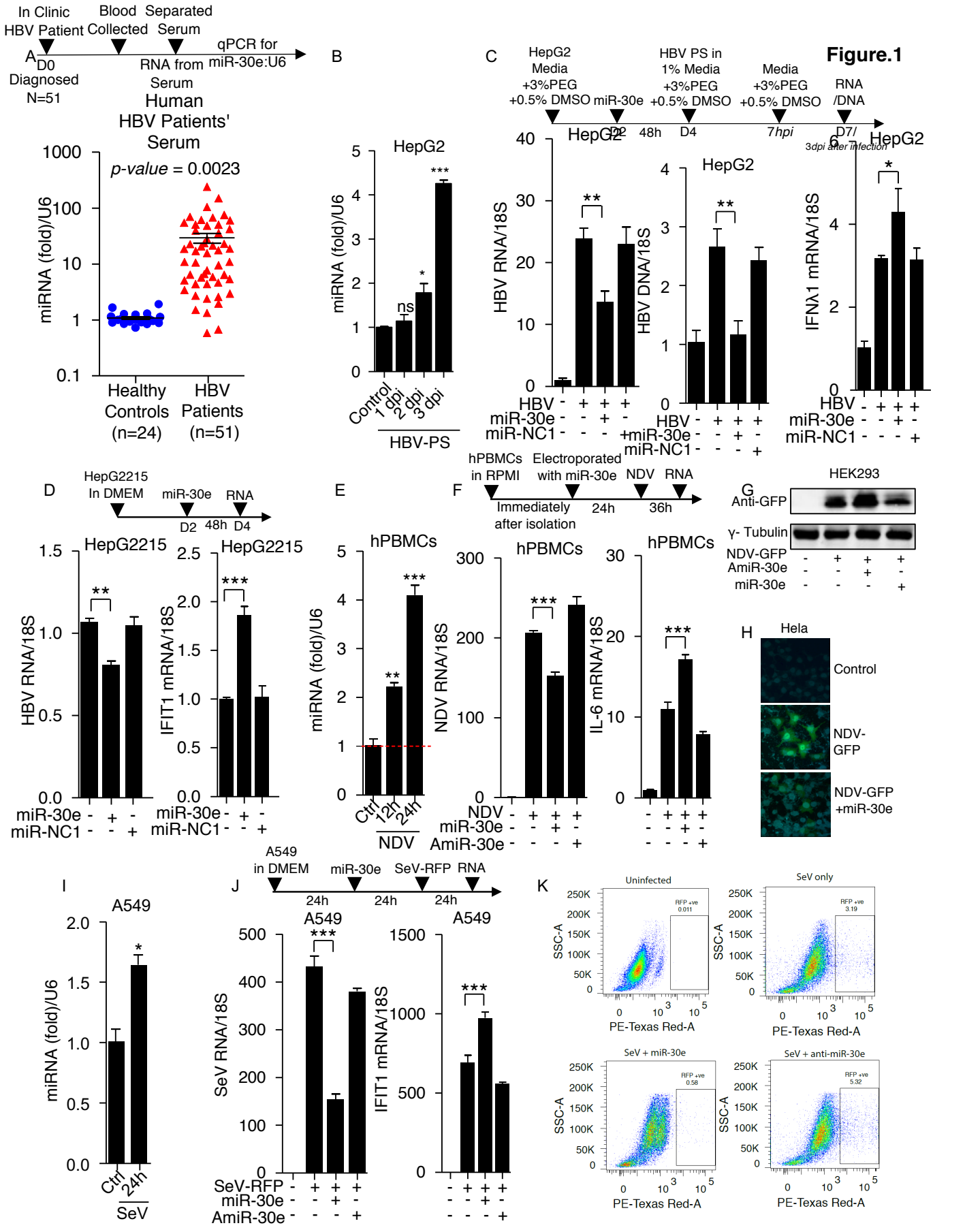
Figure.1
A
In Clinic HBV Patient
Blood Collected
Separated Serum
qPCR for miR-30e:U6
D0 Diagnosed N=51
RNA from Serum
Human HBV Patients' Serum
p-value = 0.0023
miRNA (fold)/U6
Healthy Controls (n=24)
HBV Patients (n=51)
B
HepG2
miRNA (fold)/U6
ns
Control
1 dpi
2 dpi
3 dpi
HBV-PS
C
HepG2 Media +3%PEG +0.5% DMSO
miR-30e
HBV PS in 1% Media +3%PEG +0.5% DMSO
Media +3%PEG +0.5% DMSO
RNA /DNA
D2
48h
D4
7hpi
D7/ 3dpi after infection
HepG2
HBV RNA/18S
HBV DNA/18S
IFNλ1 mRNA/18S
HBV
miR-30e
miR-NC1
D
HepG2215
In DMEM
miR-30e
RNA
D2
48h
D4
HepG2215
HBV RNA/18S
IFIT1 mRNA/18S
E
hPBMCs
miRNA (fold)/U6
Ctrl
12h
24h
NDV
F
hPBMCs in RPMI
Electroporated with miR-30e
NDV
RNA
Immediately after isolation
24h
36h
hPBMCs
NDV RNA/18S
IL-6 mRNA/18S
NDV
AmiR-30e
G
HEK293
Anti-GFP
γ- Tubulin
NDV-GFP
AmiR-30e
miR-30e
H
Hela
Control
NDV-GFP
NDV-GFP +miR-30e
I
A549
miRNA (fold)/U6
Ctrl
24h
SeV
J
A549
in DMEM
miR-30e
SeV-RFP
RNA
24h
24h
24h
A549
SeV RNA/18S
IFIT1 mRNA/18S
SeV-RFP
miR-30e
AmiR-30e
K
Uninfected
SeV only
SeV + miR-30e
SeV + anti-miR-30e
SSC-A
PE-Texas Red-A
RFP +ve

Figure. 2

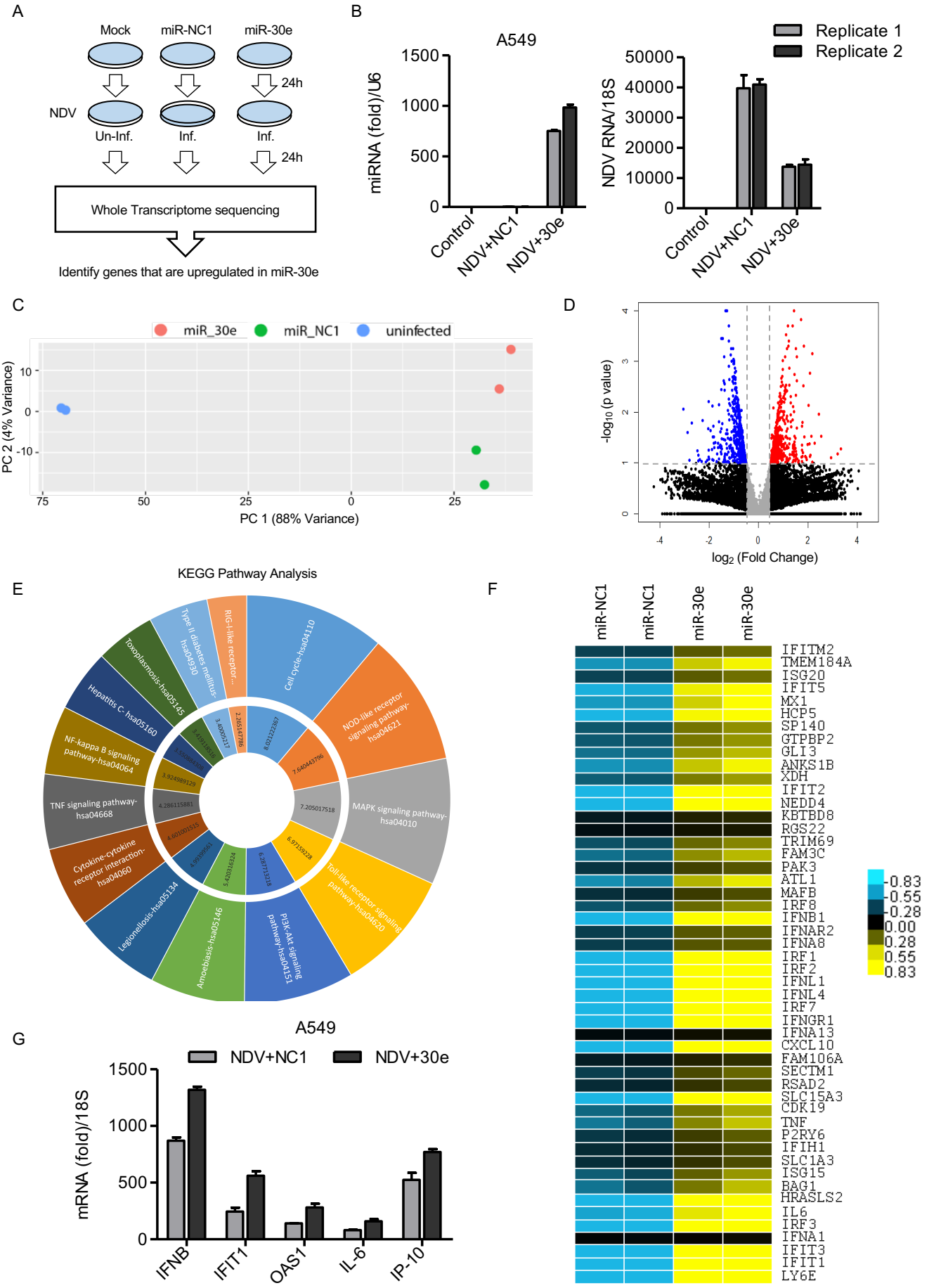
A
Mock
miR-NC1
miR-30e
24h
NDV
Un-Inf.
Inf.
Inf.
24h
Whole Transcriptome sequencing
Identify genes that are upregulated in miR-30e
B
A549
Replicate 1
Replicate 2
miRNA (fold)/U6
NDV RNA/18S
Control
NDV+NC1
NDV+30e
C
miR_30e
miR_NC1
uninfected
PC 2 (4% Variance)
PC 1 (88% Variance)
D
-log10 (p value)
log2 (Fold Change)
E
KEGG Pathway Analysis
Cell cycle-hsa04110
NOD-like receptor signaling pathway-hsa04621
MAPK signaling pathway-hsa04010
Toll-like receptor signaling pathway-hsa04620
PI3K-Akt signaling pathway-hsa04151
Amoebiasis-hsa05146
Legionellosis-hsa05134
Cytokine-cytokine receptor interaction-hsa04060
TNF signaling pathway-hsa04668
NF-kappa B signaling pathway-hsa04064
Hepatitis C-hsa05160
Toxoplasmosis-hsa05145
Type II diabetes mellitus-hsa04930
RIG-I-like receptor...
F
miR-NC1
miR-NC1
miR-30e
miR-30e
IFITM2
TMEM184A
ISG20
IFIT5
MX1
HCP5
SP140
GTPBP2
GLI3
ANKS1B
XDH
IFIT2
NEDD4
KBTBD8
RGS22
TRIM69
FAM3C
PAK3
ATL1
MAFB
IRF8
IFNB1
IFNAR2
IFNA8
IRF1
IRF2
IFNL1
IFNL4
IRF7
IFNGR1
IFNA13
CXCL10
FAM106A
SECTM1
RSAD2
SLC15A3
CDK19
TNF
P2RY6
IFIH1
SLC1A3
ISG15
BAG1
HRASLS2
IL6
IRF3
IFNA1
IFIT3
IFIT1
LY6E
-0.83
-0.55
-0.28
0.00
0.28
0.55
0.83
G
A549
NDV+NC1
NDV+30e
mRNA (fold)/18S
IFNB
IFIT1
OAS1
IL-6
IP-10

Figure. 3

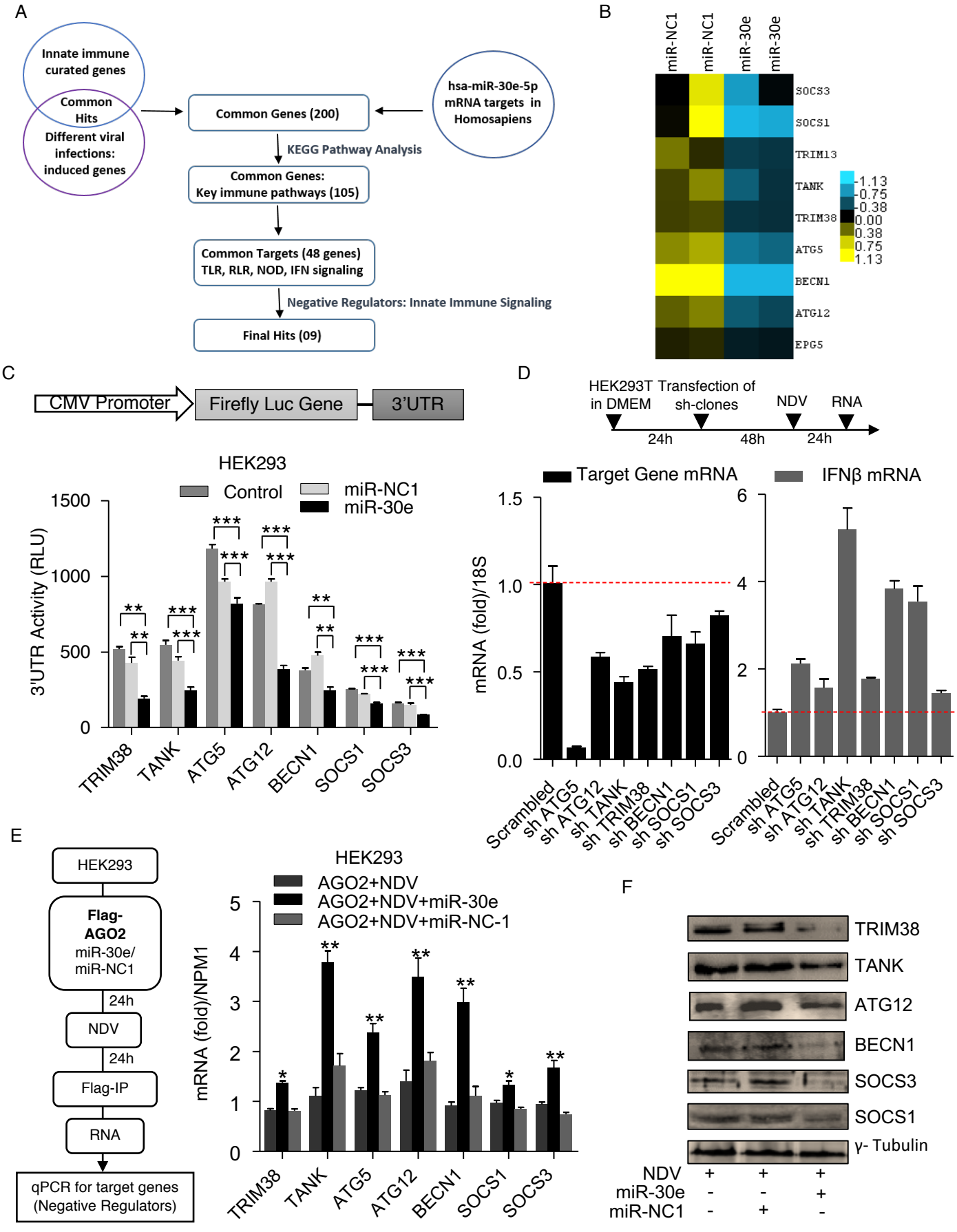
A
Innate immune curated genes
Common Hits
Different viral infections: induced genes
Common Genes (200)
hsa-miR-30e-5p mRNA targets in Homosapiens
KEGG Pathway Analysis
Common Genes: Key immune pathways (105)
Common Targets (48 genes) TLR, RLR, NOD, IFN signaling
Negative Regulators: Innate Immune Signaling
Final Hits (09)
B
miR-NC1
miR-NC1
miR-30e
miR-30e
SOCS3
SOCS1
TRIM13
TANK
TRIM38
ATG5
BECN1
ATG12
EPG5
1.13
0.75
0.38
0.00
0.38
0.75
1.13
C
CMV Promoter
Firefly Luc Gene
3'UTR
HEK293
Control
miR-NC1
miR-30e
3'UTR Activity (RLU)
1500
1000
500
0
TRIM38
TANK
ATG5
ATG12
BECN1
SOCS1
SOCS3
D
HEK293T Transfection of sh-clones in DMEM
NDV
RNA
24h
48h
24h
Target Gene mRNA
IFNβ mRNA
mRNA (fold)/18S
1.5
1.0
0.5
0.0
6
4
2
0
Scrambled
sh ATG5
sh ATG12
sh TANK
sh TRIM38
sh BECN1
sh SOCS1
sh SOCS3
E
HEK293
Flag-AGO2 miR-30e/ miR-NC1
24h
NDV
24h
Flag-IP
RNA
qPCR for target genes (Negative Regulators)
HEK293
AGO2+NDV
AGO2+NDV+miR-30e
AGO2+NDV+miR-NC-1
mRNA (fold)/NPM1
5
4
3
2
1
0
TRIM38
TANK
ATG5
ATG12
BECN1
SOCS1
SOCS3
F
TRIM38
TANK
ATG12
BECN1
SOCS3
SOCS1
γ- Tubulin
NDV + + +
miR-30e - - +
miR-NC1 - + -

Figure. 4

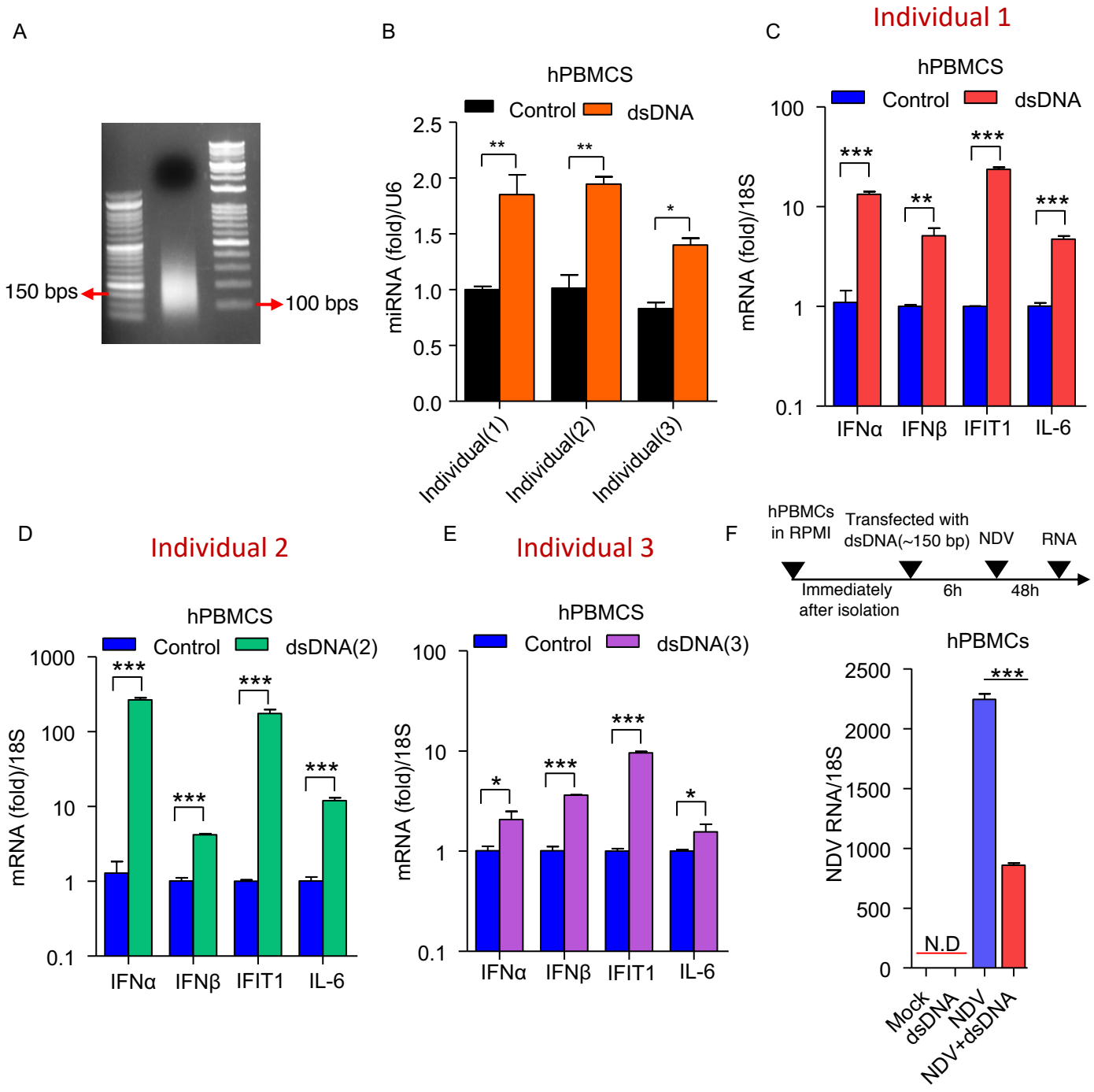
A
150 bps
100 bps
B
hPBMCS
Control
dsDNA
miRNA (fold)/U6
Individual(1)
Individual(2)
Individual(3)
C
Individual 1
hPBMCS
Control
dsDNA
mRNA (fold)/18S
IFNα
IFNβ
IFIT1
IL-6
D
Individual 2
hPBMCS
Control
dsDNA(2)
mRNA (fold)/18S
IFNα
IFNβ
IFIT1
IL-6
E
Individual 3
hPBMCS
Control
dsDNA(3)
mRNA (fold)/18S
IFNα
IFNβ
IFIT1
IL-6
F
hPBMCs in RPMI
Transfected with dsDNA(~150 bp)
NDV
RNA
Immediately after isolation
6h
48h
hPBMCs
NDV RNA/18S
N.D
Mock
dsDNA
NDV
NDV+dsDNA

Figure. 5

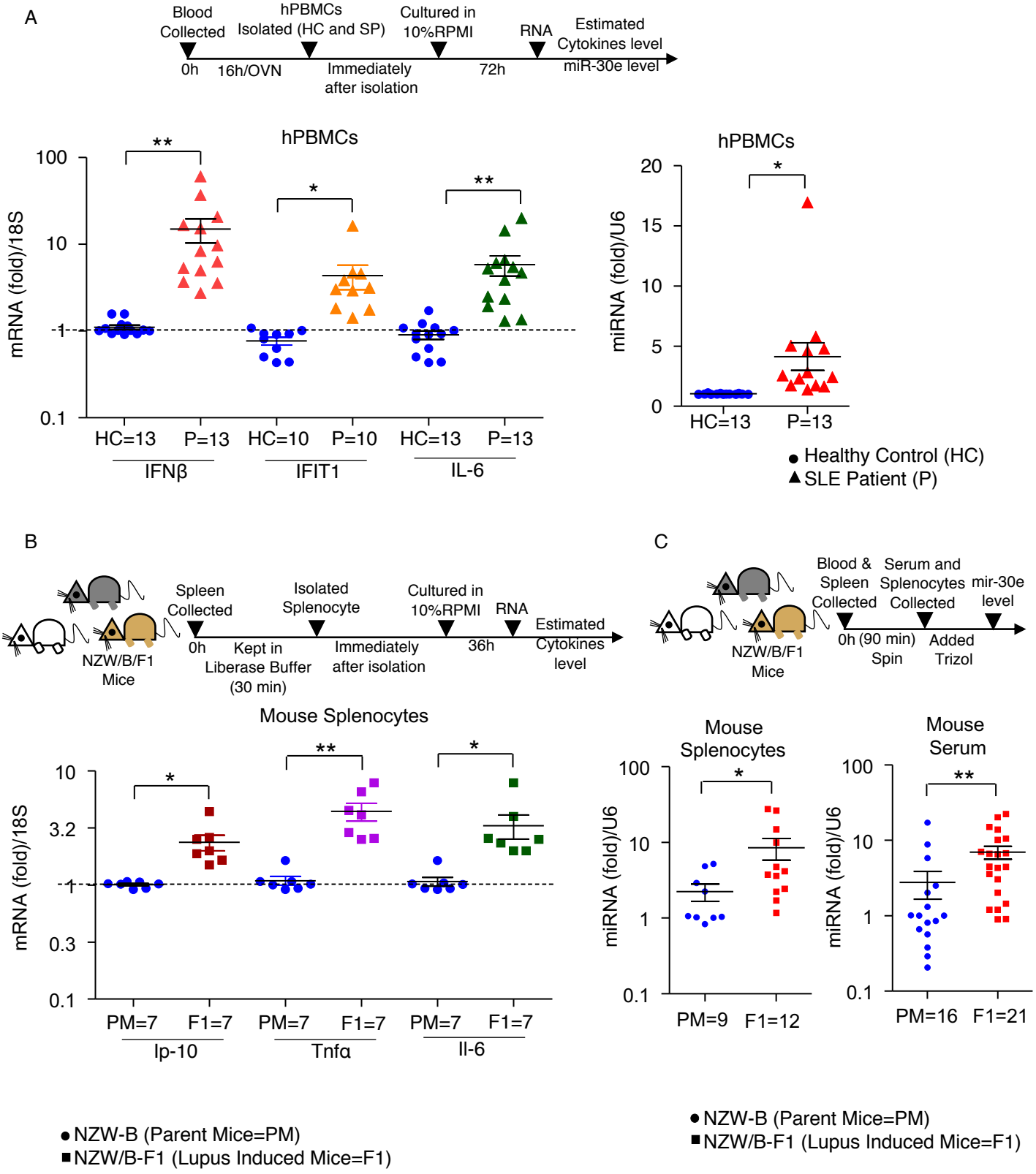
A
Blood Collected
hPBMCs Isolated (HC and SP)
Cultured in 10%RPMI
RNA
Estimated Cytokines level
miR-30e level
0h
16h/OVN
Immediately after isolation
72h
hPBMCs
mRNA (fold)/18S
HC=13
P=13
HC=10
P=10
IFNβ
IFIT1
IL-6
hPBMCs
miRNA (fold)/U6
Healthy Control (HC)
SLE Patient (P)
B
Spleen Collected
Isolated Splenocyte
Cultured in 10%RPMI
RNA
Estimated Cytokines level
NZW/B/F1 Mice
0h
Kept in Liberase Buffer (30 min)
Immediately after isolation
36h
Mouse Splenocytes
PM=7
F1=7
Ip-10
Tnfα
Il-6
NZW-B (Parent Mice=PM)
NZW/B-F1 (Lupus Induced Mice=F1)
C
Blood & Spleen Collected
Serum and Splenocytes Collected
mir-30e level
NZW/B/F1 Mice
0h (90 min) Spin
Added Trizol
Mouse Splenocytes
Mouse Serum
miRNA (fold)/U6
PM=9
F1=12
PM=16
F1=21
NZW-B (Parent Mice=PM)
NZW/B-F1 (Lupus Induced Mice=F1)

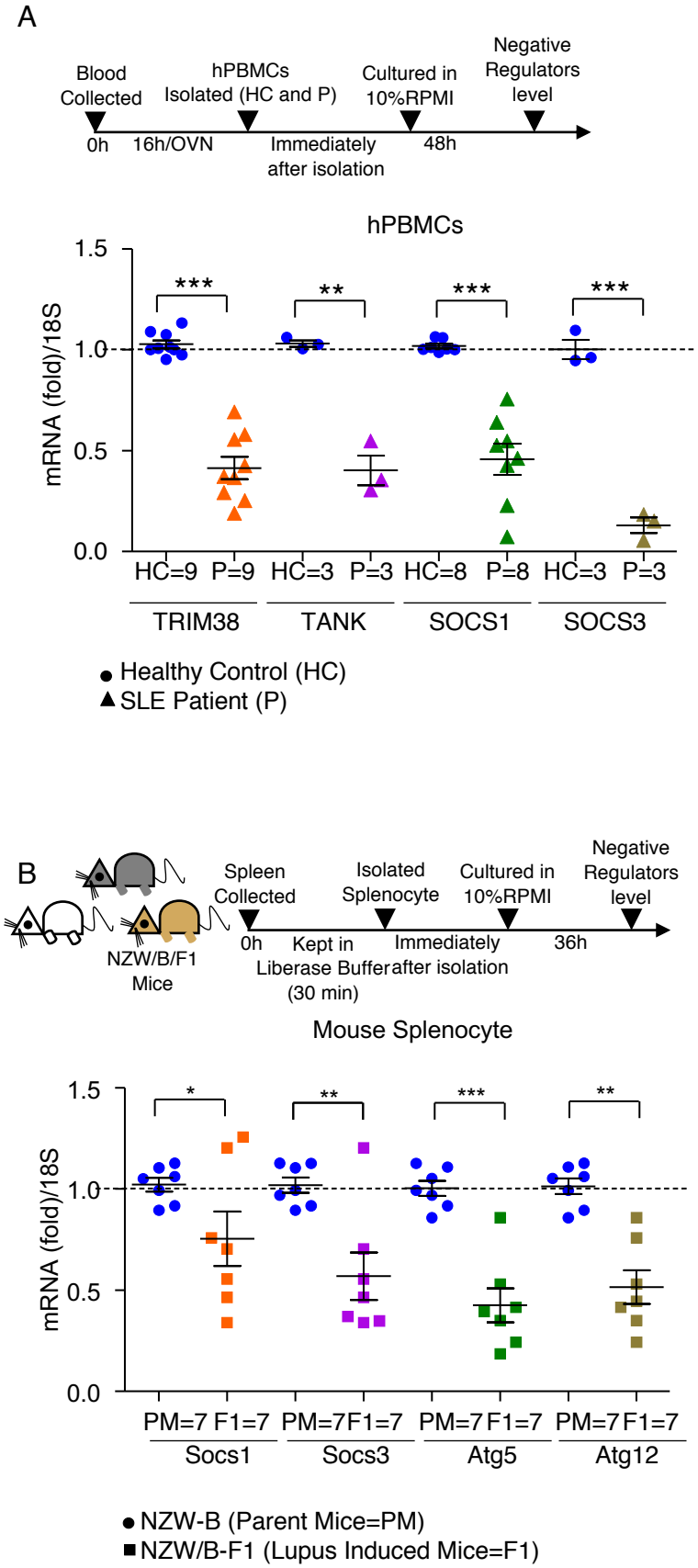
A
Blood Collected
hPBMCs Isolated (HC and P)
Cultured in 10%RPMI
Negative Regulators level
0h
16h/OVN
Immediately after isolation
48h
hPBMCs
mRNA (fold)/18S
1.5
1.0
0.5
0.0
***
**
***
***
HC=9 P=9 HC=3 P=3 HC=8 P=8 HC=3 P=3
TRIM38
TANK
SOCS1
SOCS3
Healthy Control (HC)
SLE Patient (P)
B
NZW/B/F1 Mice
Spleen Collected
Isolated Splenocyte
Cultured in 10%RPMI
Negative Regulators level
0h
Kept in Liberase Buffer (30 min)
Immediately after isolation
36h
Mouse Splenocyte
mRNA (fold)/18S
1.5
1.0
0.5
0.0
*
**
***
**
PM=7 F1=7 PM=7 F1=7 PM=7 F1=7 PM=7 F1=7
Socs1
Socs3
Atg5
Atg12
NZW-B (Parent Mice=PM)
NZW/B-F1 (Lupus Induced Mice=F1)

Figure. 7

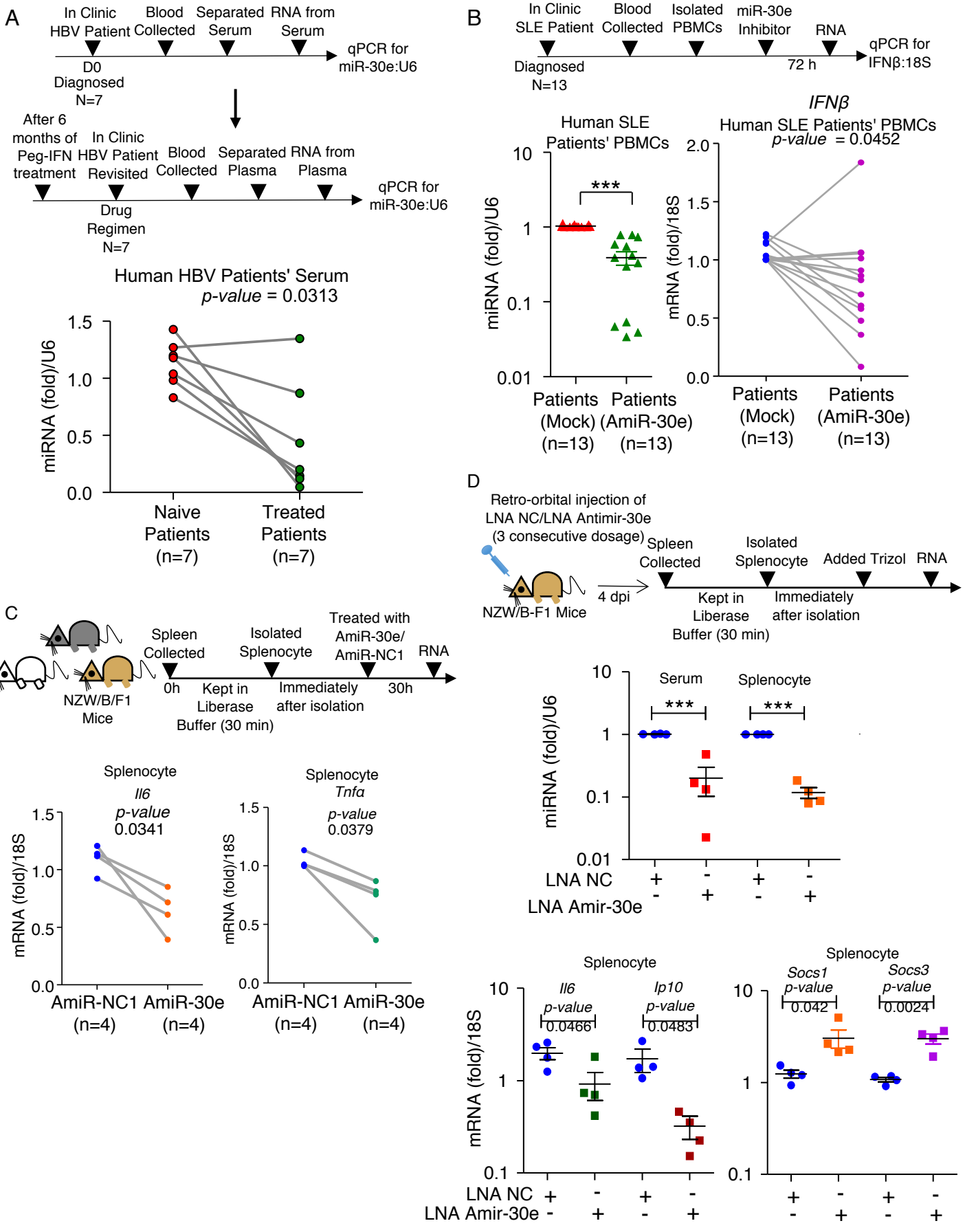
A
In Clinic HBV Patient
Blood Collected
Separated Serum
RNA from Serum
qPCR for miR-30e:U6
D0 Diagnosed N=7
After 6 months of Peg-IFN treatment
In Clinic HBV Patient Revisited
Blood Collected
Separated Plasma
RNA from Plasma
qPCR for miR-30e:U6
Drug Regimen N=7
Human HBV Patients' Serum
p-value = 0.0313
miRNA (fold)/U6
Naive Patients (n=7)
Treated Patients (n=7)
B
In Clinic SLE Patient
Blood Collected
Isolated PBMCs
Treated with miR-30e Inhibitor
RNA
qPCR for IFNβ:18S
Diagnosed N=13
72 h
IFNβ
Human SLE Patients' PBMCs
Human SLE Patients' PBMCs
p-value = 0.0452
miRNA (fold)/U6
mRNA (fold)/18S
Patients (Mock) (n=13)
Patients (AmiR-30e) (n=13)
C
NZW/B/F1 Mice
Spleen Collected
Isolated Splenocyte
Treated with AmiR-30e/ AmiR-NC1
RNA
0h
Kept in Liberase Buffer (30 min)
Immediately after isolation
30h
Splenocyte
Il6
p-value 0.0341
Splenocyte
Tnfa
p-value 0.0379
mRNA (fold)/18S
AmiR-NC1 (n=4)
AmiR-30e (n=4)
D
Retro-orbital injection of LNA NC/LNA Antimir-30e (3 consecutive dosage)
NZW/B-F1 Mice
4 dpi
Spleen Collected
Isolated Splenocyte
Added Trizol
RNA
Kept in Liberase Buffer (30 min)
Immediately after isolation
Serum
Splenocyte
miRNA (fold)/U6
LNA NC
LNA Amir-30e
Splenocyte
Il6
p-value 0.0466
Ip10
p-value 0.0483
Socs1
p-value 0.042
Socs3
p-value 0.0024
mRNA (fold)/18S

Figure. 8

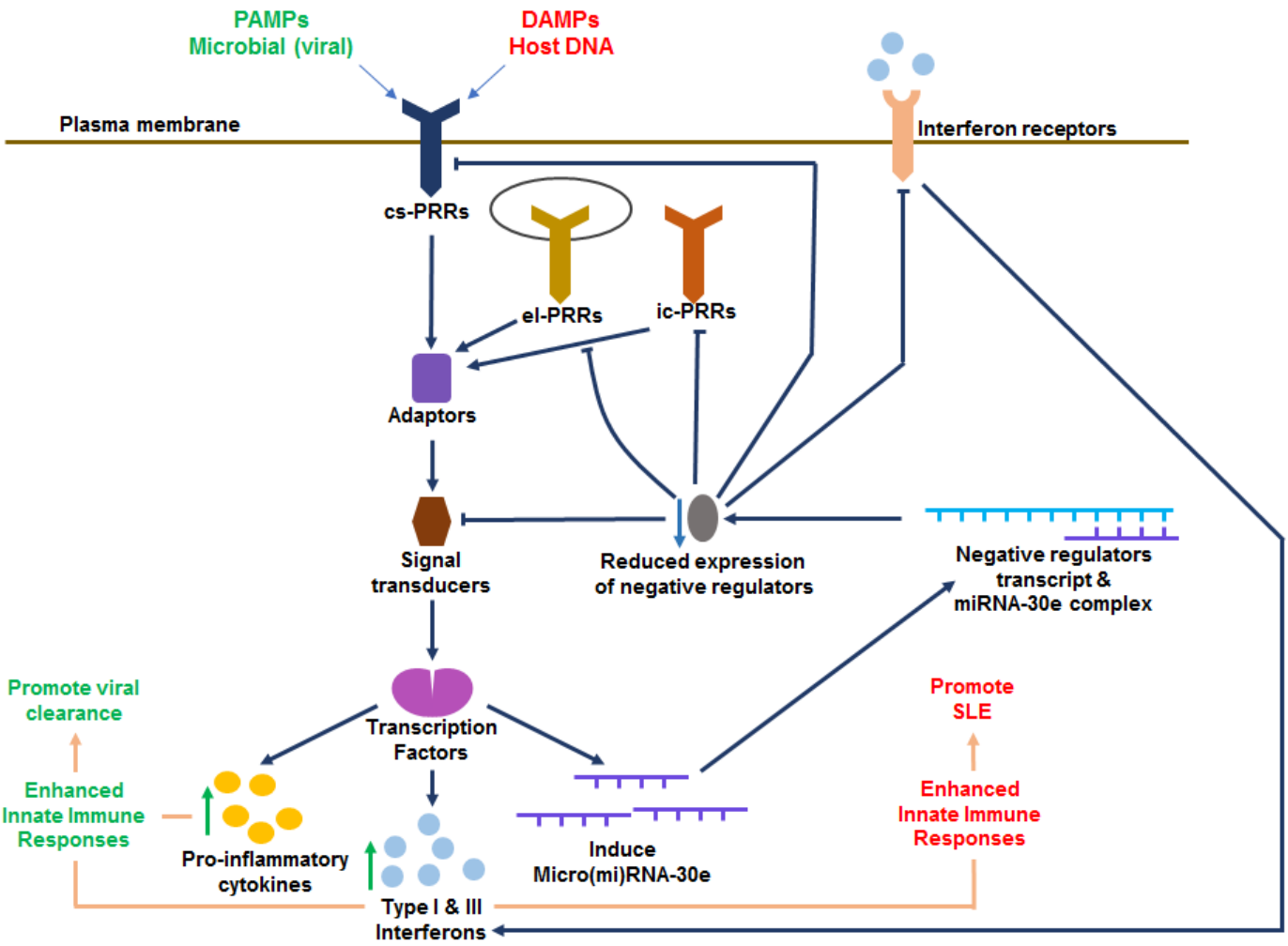
PAMPs
Microbial (viral)
DAMPs
Host DNA
Plasma membrane
Interferon receptors
cs-PRRs
el-PRRs
ic-PRRs
Adaptors
Signal
transducers
Reduced expression
of negative regulators
Negative regulators
transcript &
miRNA-30e complex
Promote viral
clearance
Transcription
Factors
Promote
SLE
Enhanced
Innate Immune
Responses
Pro-inflammatory
cytokines
Induce
Micro(mi)RNA-30e
Enhanced
Innate Immune
Responses
Type I & III
Interferons

Figure. S1

A

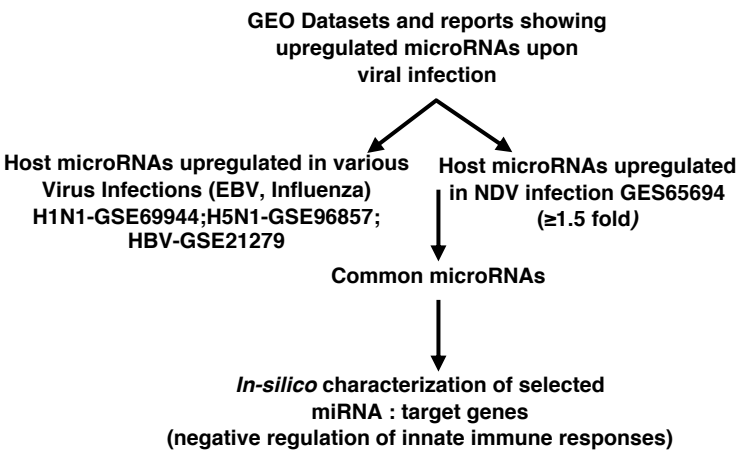

B

S.No.	Viral Infection	Model or Cell line	Upregulated miRs	Reference
1.	H5N1	Mice	51	(31)
2.	EBV	Patients (IM)	84	(32)
3.	NDV	HEK-293	209	(7)

Common microRNAs

miR-30e-5p
miR-27a-3p
miR-181a/2-3p

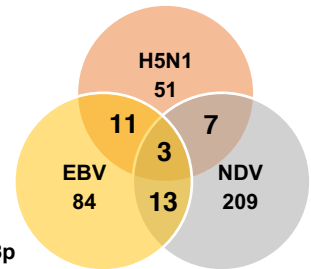

C

miRNA	Log FC during NDV Infection GSE65694	Significantly Target Negative Regulation Of Innate Immune Responses (miRanda, DIANA, TargetScan, miRDB, RNA hybrid)
miR-30e-5p	1.69	**** (majority of targets with high binding efficiency towards miRNAs)
miR-27a-3p	1.54	*
miR-181a/2-3p	1.5	*

Common microRNA

miR-30e-5p

D

```
                5′ ******** 3′
hsa-miR-30e-5p  UGUAAACAUCCUU
mmu-miR-30e-5p  UGUAAACAUCCUU
rno-miR-30e-5p  UGUAAACAUCCUU
mml-miR-30e-5p  UGUAAACAUCCUU
gga-miR-30e-5p  UGUAAACAUCCUU
chi-miR-30e-5p  UGUAAACAUCCUU
dre-miR-30e-5p  UGUAAACAUCCUU
bta-miR-30e-5p  UGUAAACAUCCUU
```

E

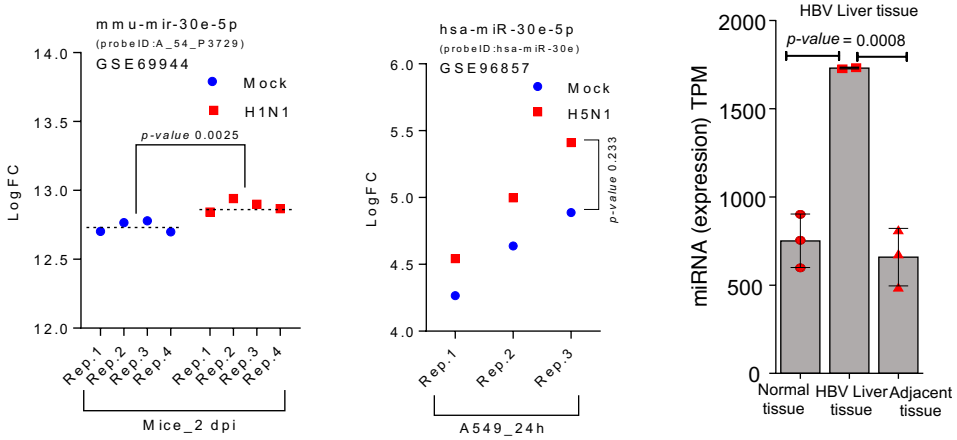

Figure. S2

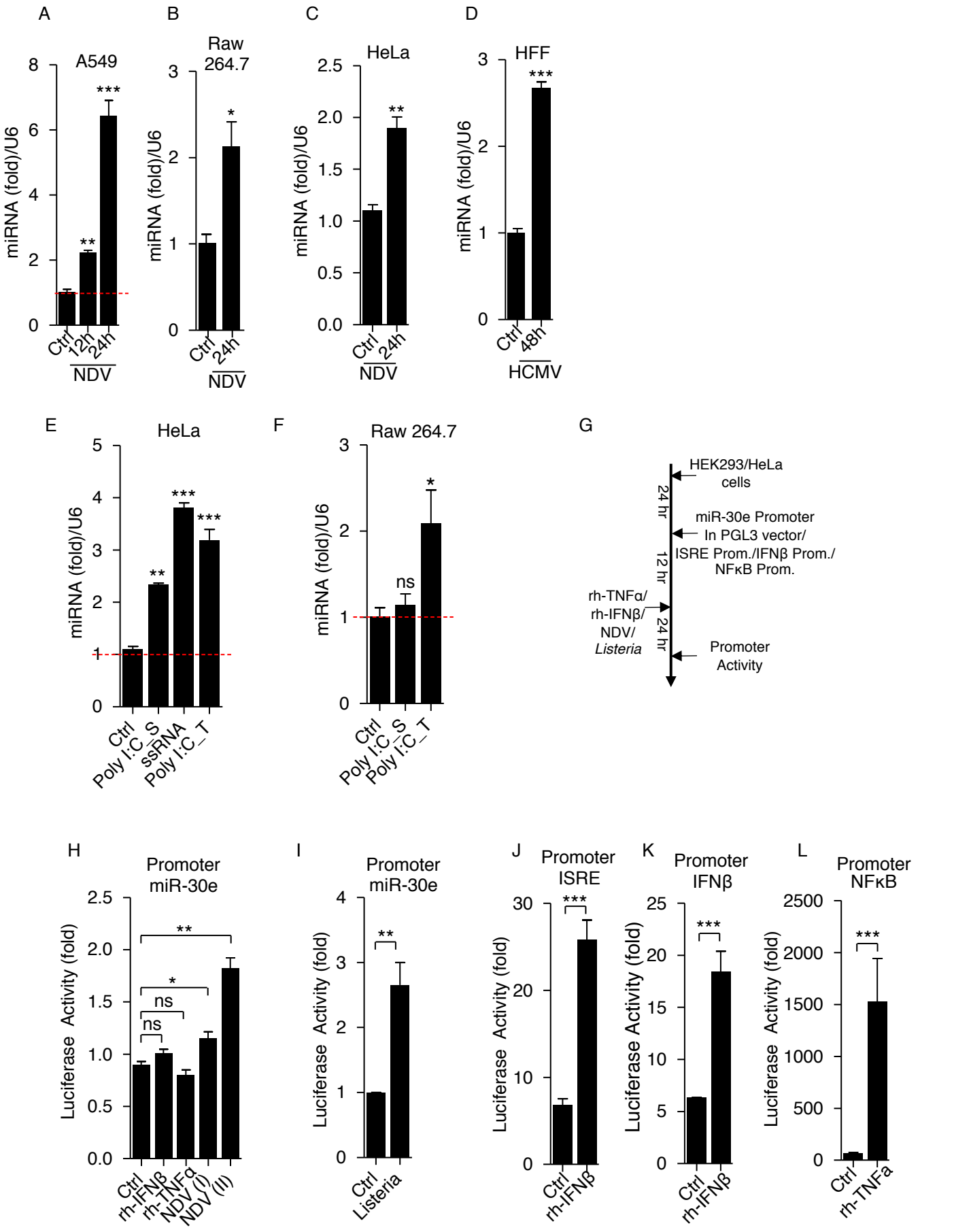
A
A549
miRNA (fold)/U6
Ctrl
12h
24h
NDV
B
Raw 264.7
Ctrl
24h
NDV
C
HeLa
Ctrl
24h
NDV
D
HFF
Ctrl
48h
HCMV
E
HeLa
Ctrl
Poly I:C_S
ssRNA
Poly I:C_T
F
Raw 264.7
ns
G
HEK293/HeLa cells
24 hr
miR-30e Promoter In PGL3 vector/ ISRE Prom./IFNβ Prom./ NFκB Prom.
12 hr
rh-TNFα/ rh-IFNβ/ NDV/ Listeria
24 hr
Promoter Activity
H
Promoter miR-30e
Luciferase Activity (fold)
Ctrl
rh-IFNβ
rh-TNFα
NDV (I)
NDV (II)
I
Promoter miR-30e
Ctrl
Listeria
J
Promoter ISRE
Ctrl
rh-IFNβ
K
Promoter IFNβ
Ctrl
rh-IFNβ
L
Promoter NFκB
Ctrl
rh-TNFa

Figure. S3

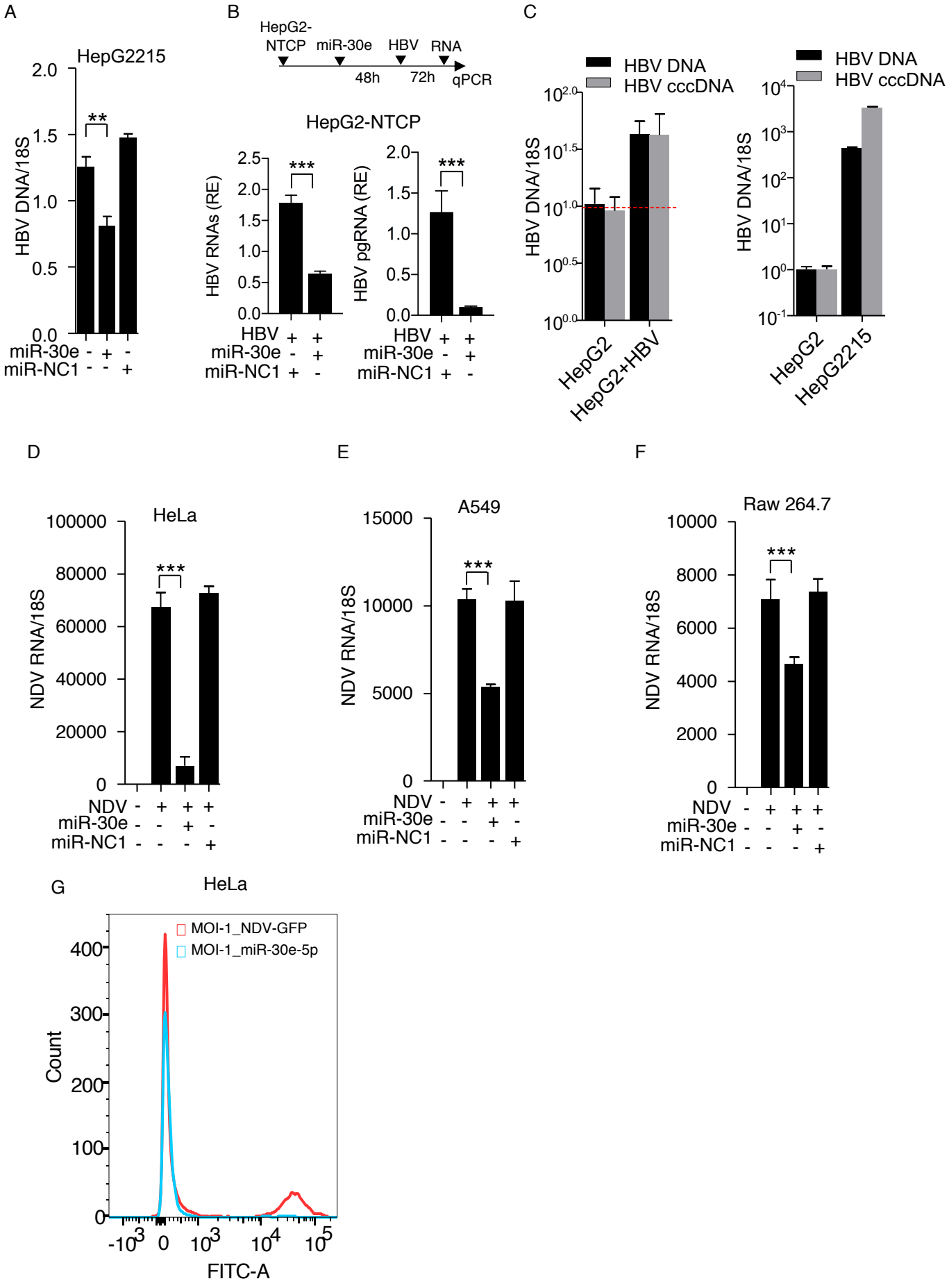
A
HepG2215
HBV DNA/18S
miR-30e
miR-NC1
B
HepG2-NTCP
miR-30e
HBV
RNA
48h
72h
qPCR
HepG2-NTCP
HBV RNAs (RE)
HBV pgRNA (RE)
HBV
miR-30e
miR-NC1
C
HBV DNA
HBV cccDNA
HBV DNA/18S
HepG2
HepG2+HBV
HepG2215
D
HeLa
NDV RNA/18S
NDV
miR-30e
miR-NC1
E
A549
F
Raw 264.7
G
HeLa
MOI-1_NDV-GFP
MOI-1_miR-30e-5p
Count
FITC-A

Figure. S4

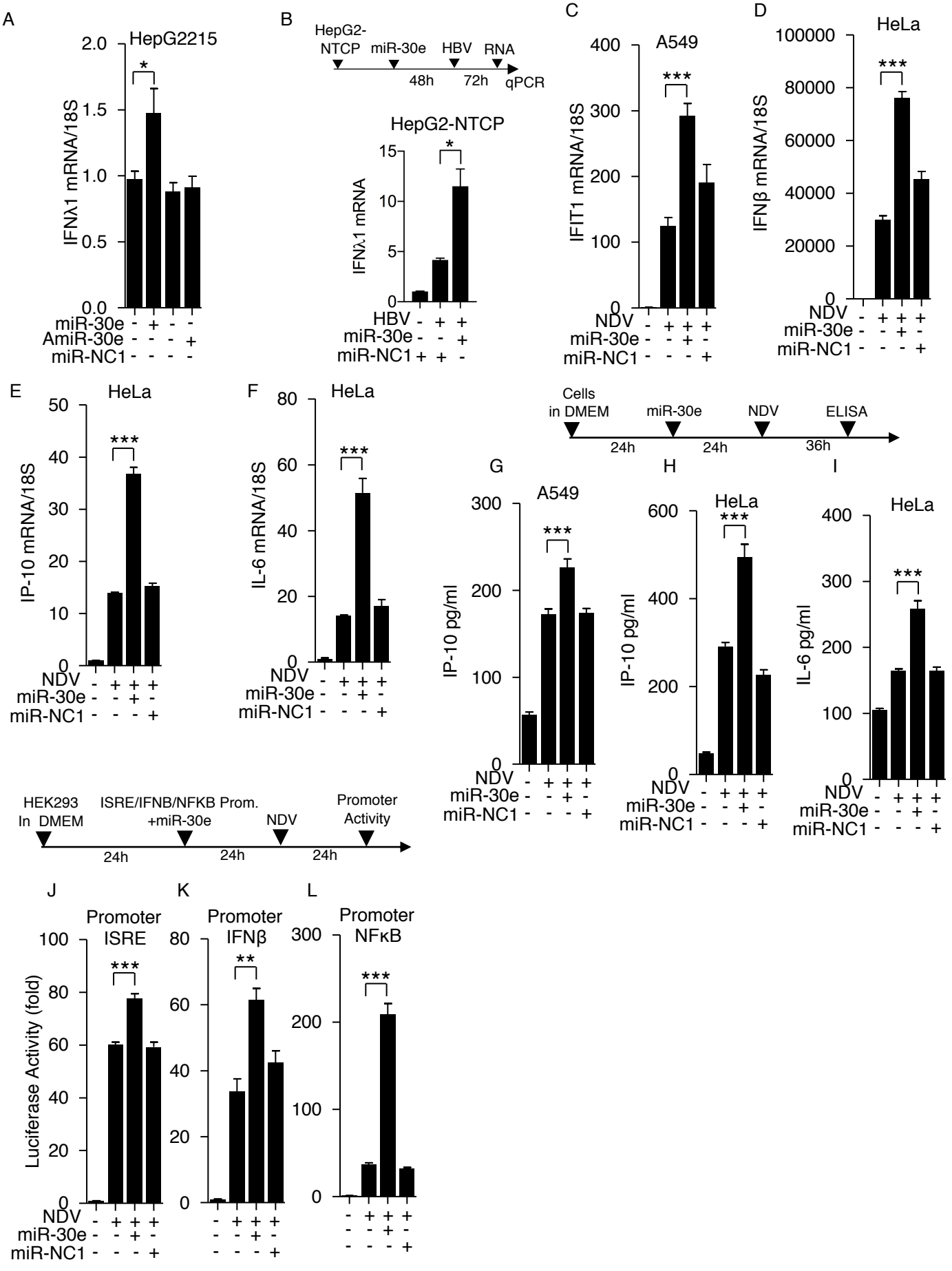
A
HepG2215
IFNλ1 mRNA/18S
miR-30e
AmiR-30e
miR-NC1
B
HepG2-NTCP
miR-30e
HBV
RNA
48h
72h
qPCR
HepG2-NTCP
IFNλ1 mRNA
HBV
miR-30e
miR-NC1
C
A549
IFIT1 mRNA/18S
NDV
miR-30e
miR-NC1
D
HeLa
IFNβ mRNA/18S
NDV
miR-30e
miR-NC1
E
HeLa
IP-10 mRNA/18S
NDV
miR-30e
miR-NC1
F
HeLa
IL-6 mRNA/18S
NDV
miR-30e
miR-NC1
Cells in DMEM
miR-30e
NDV
ELISA
24h
24h
36h
G
A549
IP-10 pg/ml
NDV
miR-30e
miR-NC1
H
HeLa
IP-10 pg/ml
NDV
miR-30e
miR-NC1
I
HeLa
IL-6 pg/ml
NDV
miR-30e
miR-NC1
HEK293 In DMEM
ISRE/IFNB/NFKB Prom. +miR-30e
NDV
Promoter Activity
24h
24h
24h
J
Promoter ISRE
Luciferase Activity (fold)
NDV
miR-30e
miR-NC1
K
Promoter IFNβ
L
Promoter NFκB

Figure. S5

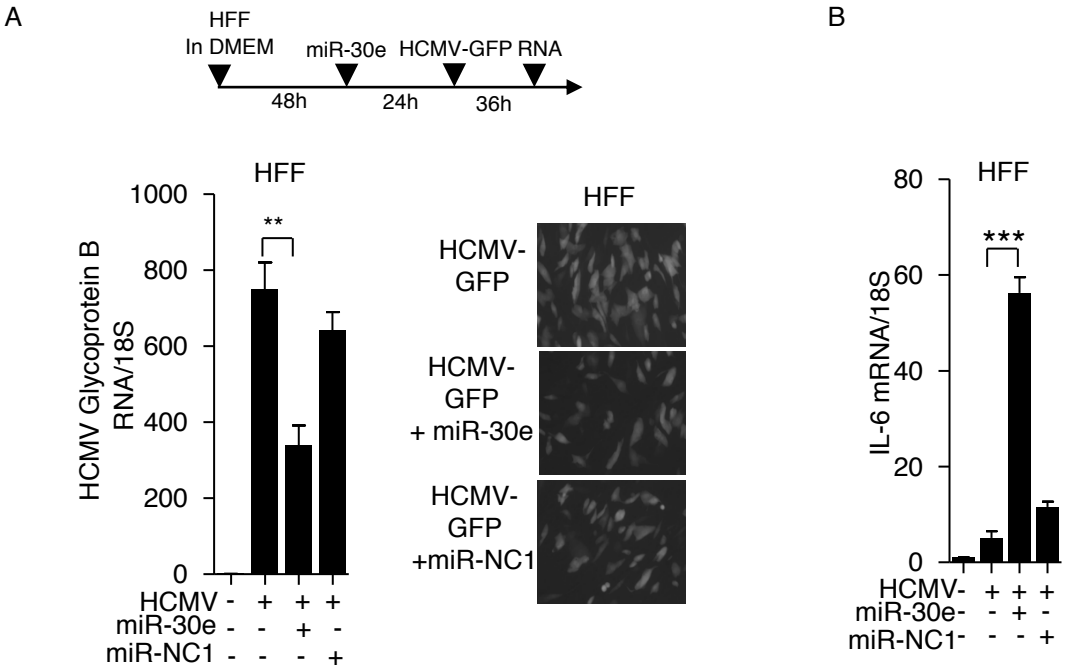
A
HFF
In DMEM
miR-30e
HCMV-GFP RNA
48h
24h
36h
HFF
HCMV Glycoprotein B RNA/18S
1000
800
600
400
200
0
**
HCMV - + + +
miR-30e - - + -
miR-NC1 - - - +
HFF
HCMV-GFP
HCMV-GFP + miR-30e
HCMV-GFP +miR-NC1
B
HFF
IL-6 mRNA/18S
80
60
40
20
0
***
HCMV- + + +
miR-30e- - + -
miR-NC1- - - +

Figure. S6

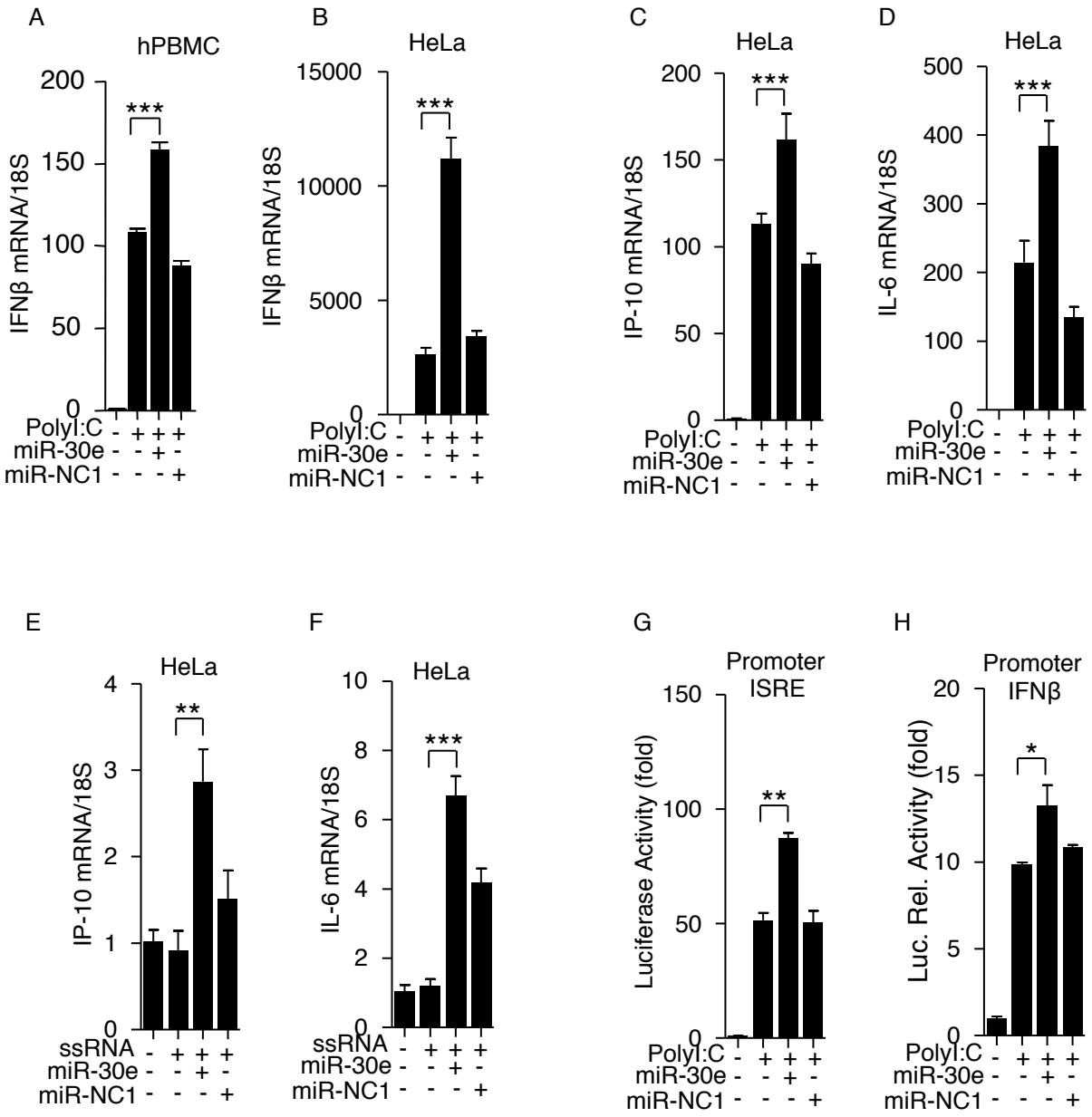
A
hPBMC
IFNβ mRNA/18S
200
150
100
50
0
***
PolyI:C - + + +
miR-30e - - + -
miR-NC1 - - - +
B
HeLa
IFNβ mRNA/18S
15000
10000
5000
0
***
PolyI:C - + + +
miR-30e - - + -
miR-NC1 - - - +
C
HeLa
IP-10 mRNA/18S
200
150
100
50
0
***
PolyI:C - + + +
miR-30e - - + -
miR-NC1 - - - +
D
HeLa
IL-6 mRNA/18S
500
400
300
200
100
0
***
PolyI:C - + + +
miR-30e - - + -
miR-NC1 - - - +
E
HeLa
IP-10 mRNA/18S
4
3
2
1
0
**
ssRNA - + + +
miR-30e - - + -
miR-NC1 - - - +
F
HeLa
IL-6 mRNA/18S
10
8
6
4
2
0
***
ssRNA - + + +
miR-30e - - + -
miR-NC1 - - - +
G
Promoter
ISRE
Luciferase Activity (fold)
150
100
50
0
**
PolyI:C - + + +
miR-30e - - + -
miR-NC1 - - - +
H
Promoter
IFNβ
Luc. Rel. Activity (fold)
20
15
10
5
0
*
PolyI:C - + + +
miR-30e - - + -
miR-NC1 - - - +

Figure. S7

A

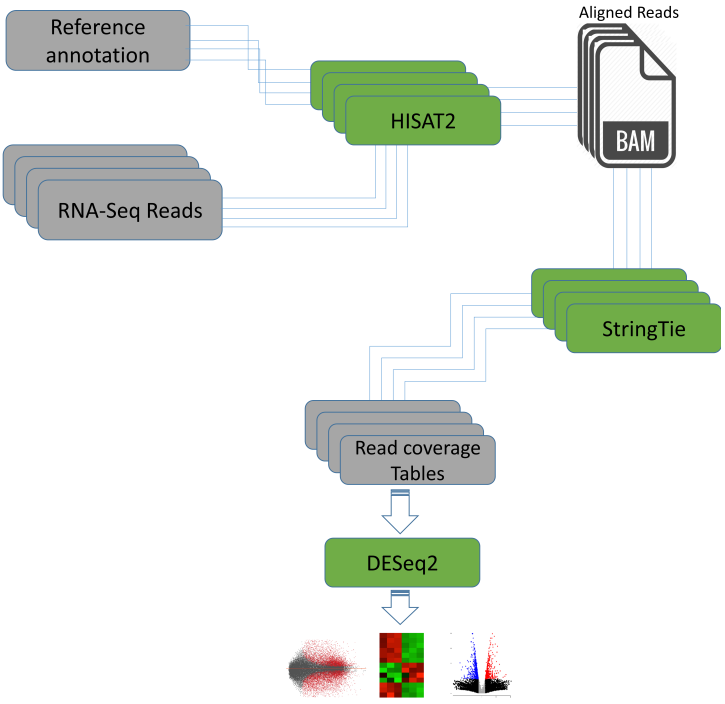

Representation of differentially expressed genes in plots and heat maps

B

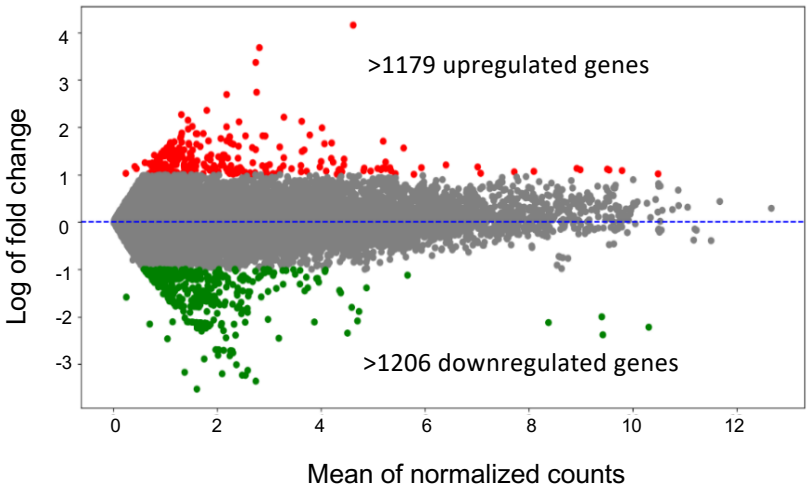

C

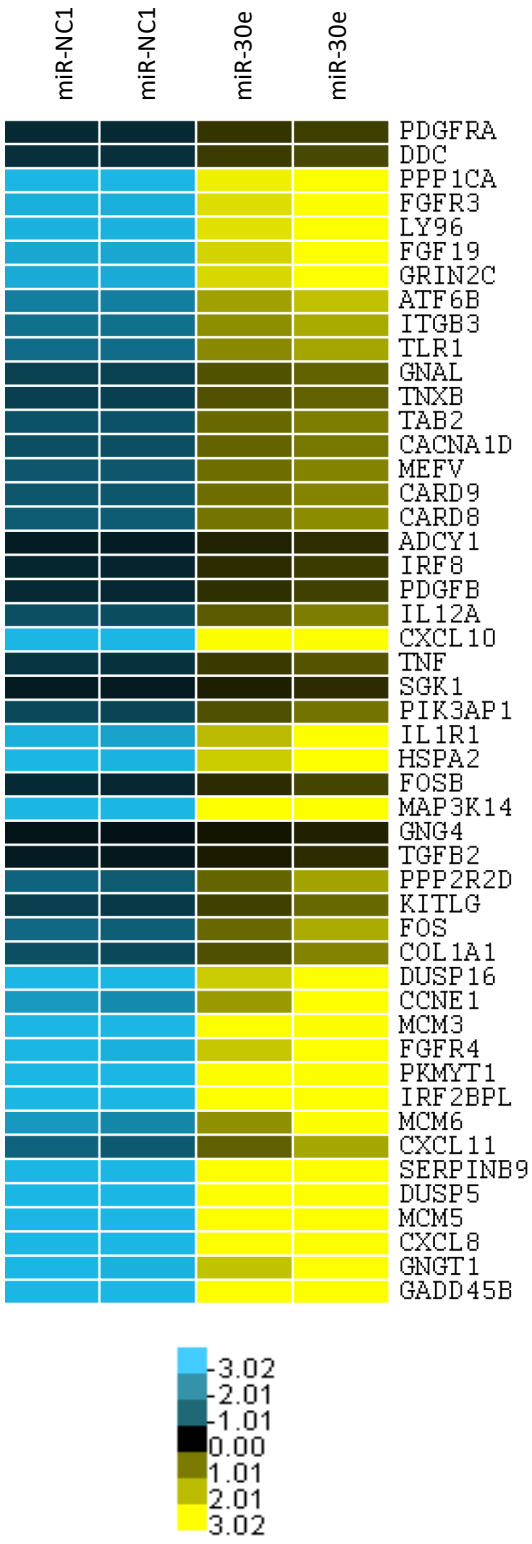

Top genes involved in KEGG Pathway Enrichment

Figure. S8

TRIM 38

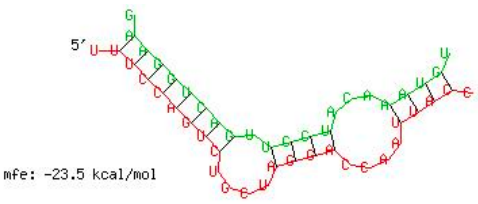

TRIM13

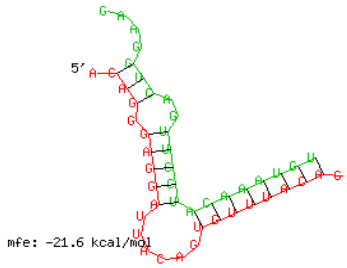

TANK

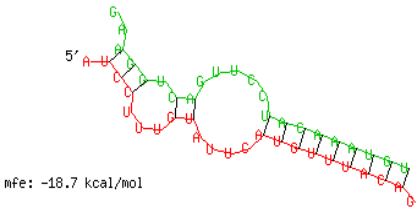

ATG 5

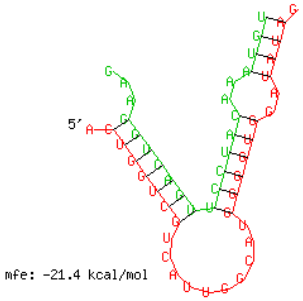

ATG 12

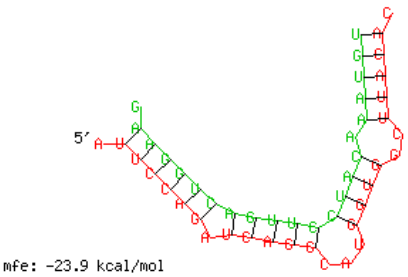

BECN1

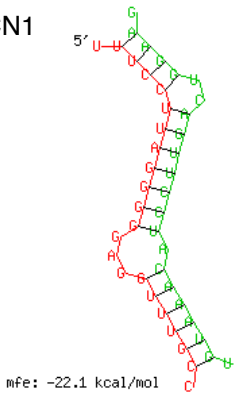

EPG5

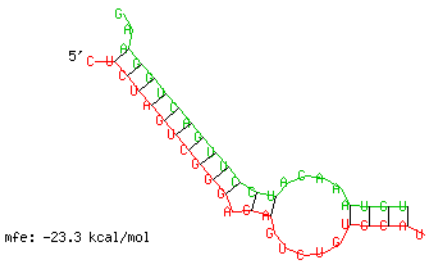

SOCS1

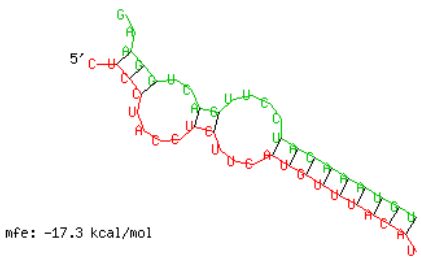

SOCS3

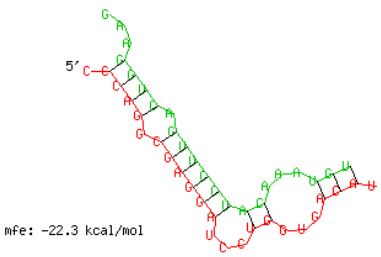

JAK1

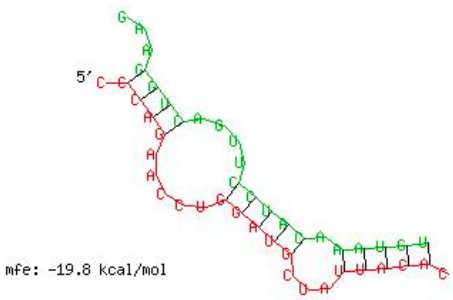

STAT1

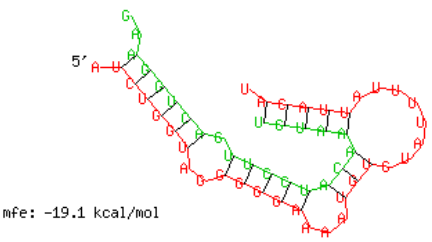

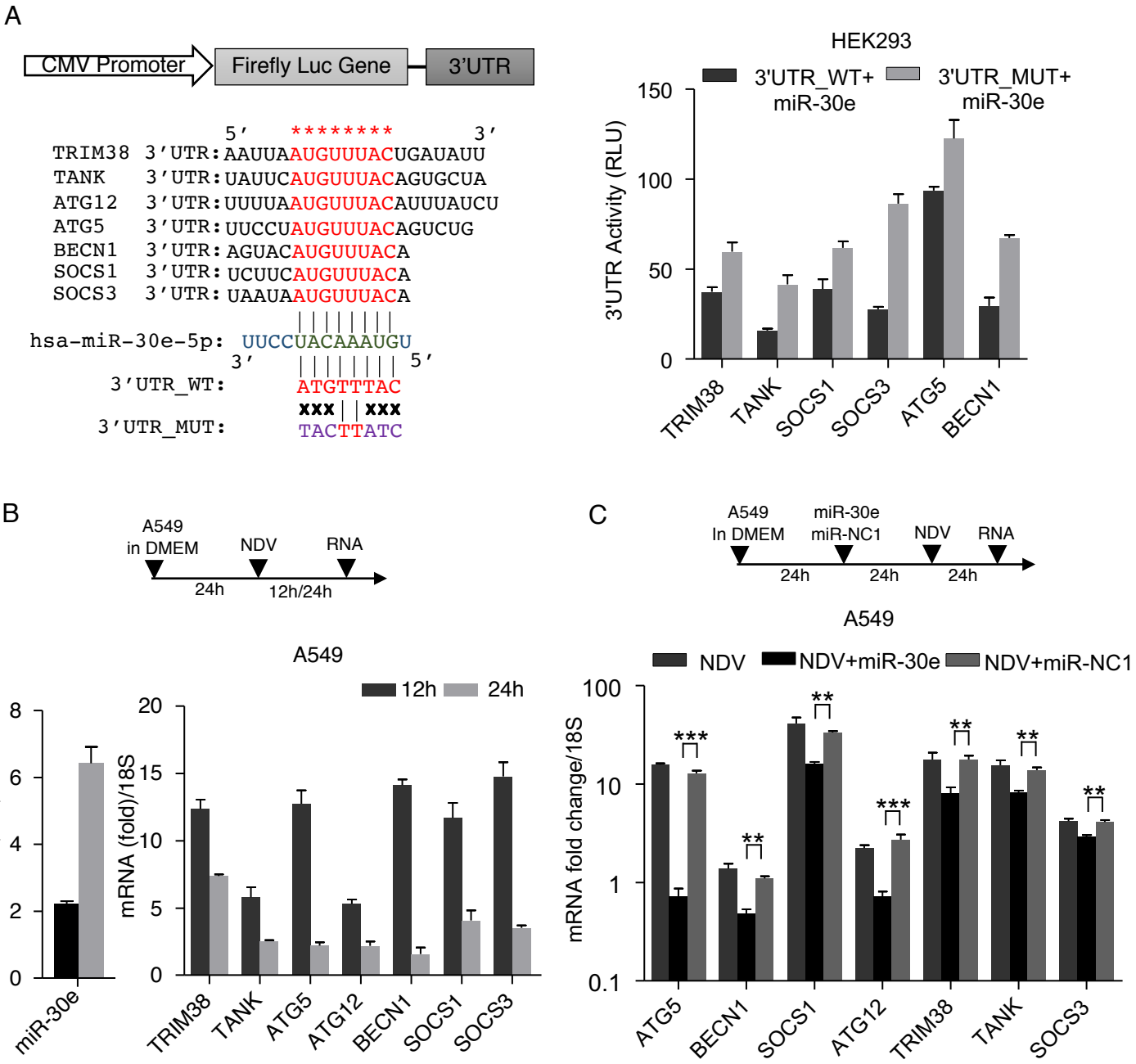
A
CMV Promoter
Firefly Luc Gene
3'UTR
5' ******** 3'
TRIM38 3'UTR: AAUUAAUGUUUACUGAUAUU
TANK 3'UTR: UAUUCAUGUUUACAGUGCUA
ATG12 3'UTR: UUUUAAUGUUUACAUUUAUCU
ATG5 3'UTR: UUCCUAUGUUUACAGUCUG
BECN1 3'UTR: AGUACAUGUUUACA
SOCS1 3'UTR: UCUUCAUGUUUACA
SOCS3 3'UTR: UAAUAAUGUUUACA
hsa-miR-30e-5p: UUCCUACAAAUGU
3' 5'
3'UTR_WT: ATGTTTAC
xxx xxx
3'UTR_MUT: TACTTATC
HEK293
3'UTR_WT+ miR-30e
3'UTR_MUT+ miR-30e
3'UTR Activity (RLU)
150
100
50
0
TRIM38
TANK
SOCS1
SOCS3
ATG5
BECN1
B
A549 in DMEM
NDV
RNA
24h
12h/24h
A549
12h
24h
miRNA (fold)/U6
mRNA (fold)/18S
miR-30e
TRIM38
TANK
ATG5
ATG12
BECN1
SOCS1
SOCS3
C
A549 In DMEM
miR-30e miR-NC1
NDV
RNA
24h
24h
24h
A549
NDV
NDV+miR-30e
NDV+miR-NC1
mRNA fold change/18S
100
10
1
0.1
***
**
ATG5
BECN1
SOCS1
ATG12
TRIM38
TANK
SOCS3

Figure. S10

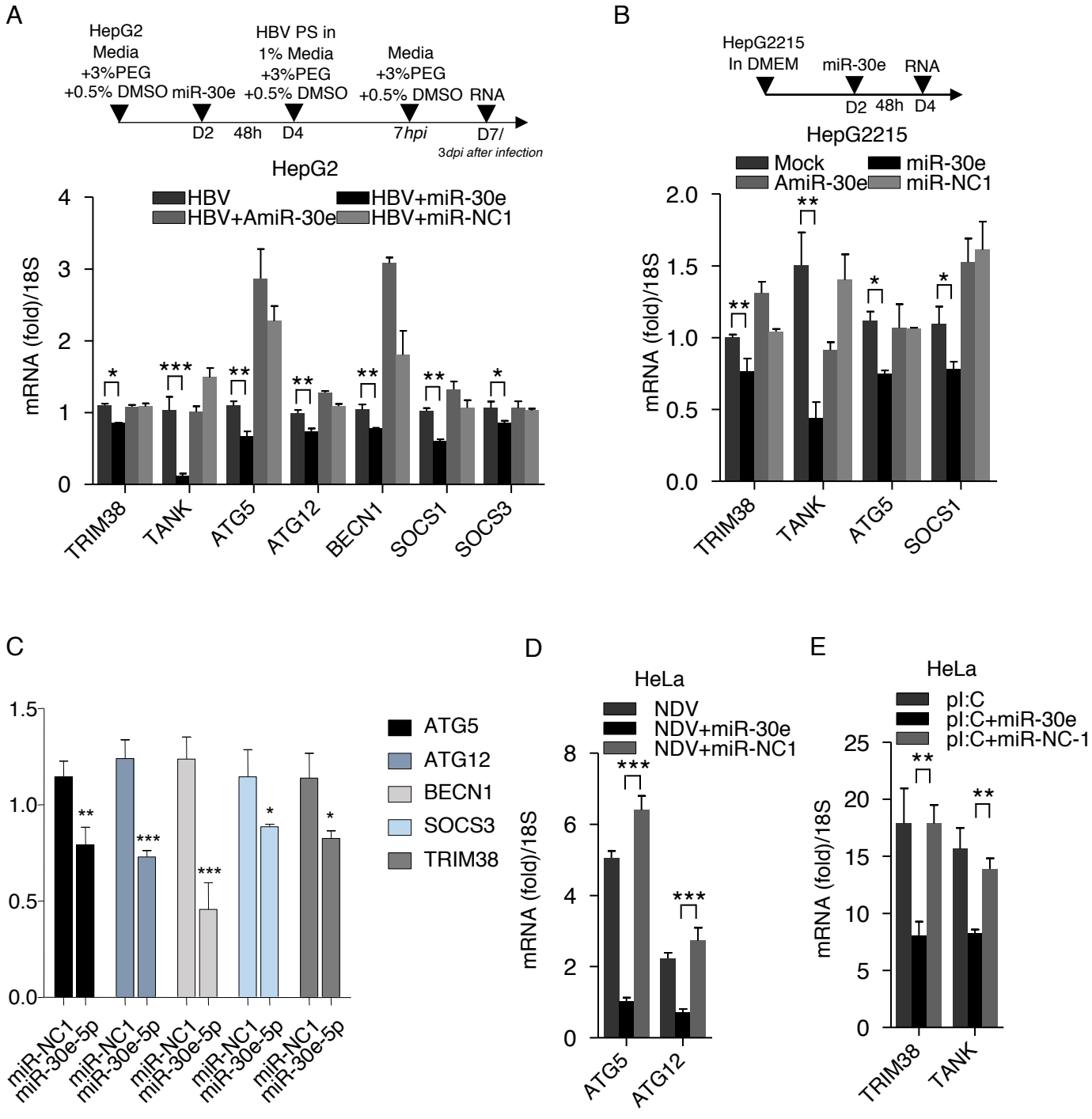
A
HepG2
Media
+3%PEG
+0.5% DMSO miR-30e
HBV PS in
1% Media
+3%PEG
+0.5% DMSO
Media
+3%PEG
+0.5% DMSO RNA
D2
48h
D4
7hpi
D7/
3dpi after infection
HepG2
HBV
HBV+miR-30e
HBV+AmiR-30e
HBV+miR-NC1
mRNA (fold)/18S
TRIM38
TANK
ATG5
ATG12
BECN1
SOCS1
SOCS3
B
HepG2215
In DMEM
miR-30e
RNA
D2 48h D4
HepG2215
Mock
miR-30e
AmiR-30e
miR-NC1
mRNA (fold)/18S
TRIM38
TANK
ATG5
SOCS1
C
mRNA (fold)
ATG5
ATG12
BECN1
SOCS3
TRIM38
miR-NC1
miR-30e-5p
D
HeLa
NDV
NDV+miR-30e
NDV+miR-NC1
mRNA (fold)/18S
ATG5
ATG12
E
HeLa
pI:C
pI:C+miR-30e
pI:C+miR-NC-1
mRNA (fold)/18S
TRIM38
TANK

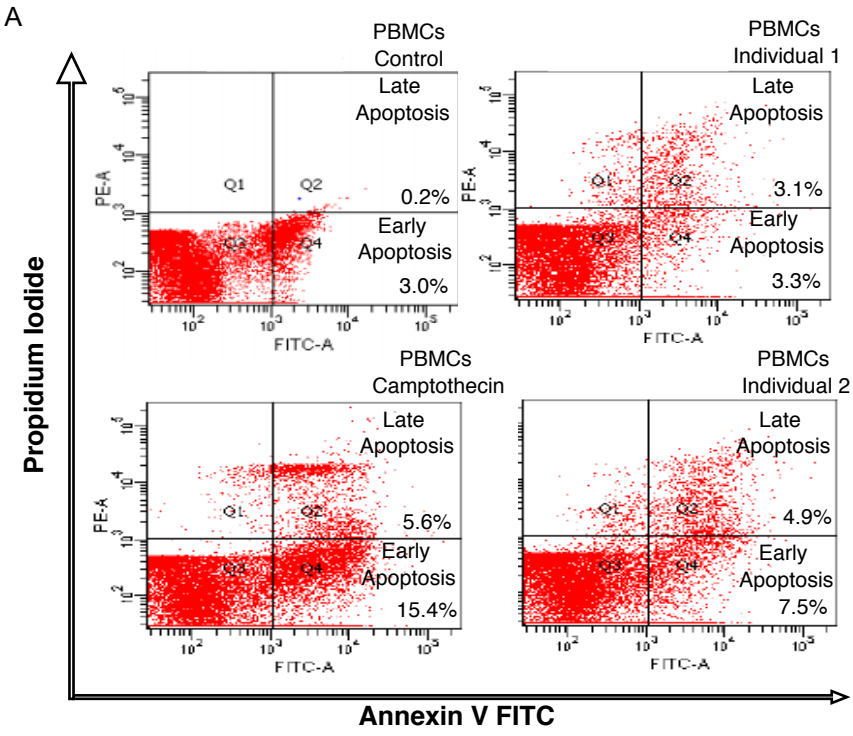
A
PBMCs
Control
Late
Apoptosis
0.2%
Early
Apoptosis
3.0%
PBMCs
Individual 1
Late
Apoptosis
3.1%
Early
Apoptosis
3.3%
PBMCs
Camptothecin
Late
Apoptosis
5.6%
Early
Apoptosis
15.4%
PBMCs
Individual 2
Late
Apoptosis
4.9%
Early
Apoptosis
7.5%
Propidium Iodide
Annexin V FITC
PE-A
FITC-A
Q1
Q2
Q3
Q4

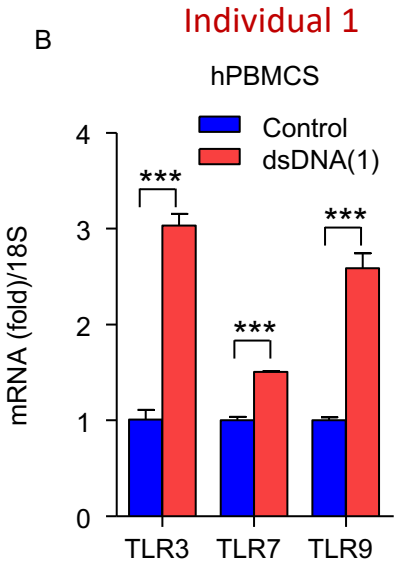
B
Individual 1
hPBMCS
Control
dsDNA(1)
mRNA (fold)/18S
TLR3
TLR7
TLR9
***

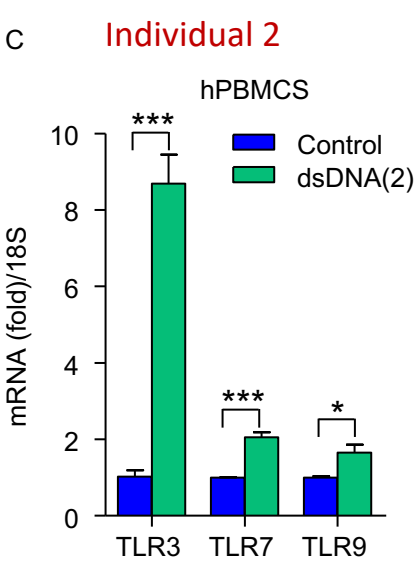
C
Individual 2
hPBMCS
Control
dsDNA(2)
mRNA (fold)/18S
TLR3
TLR7
TLR9
***
*

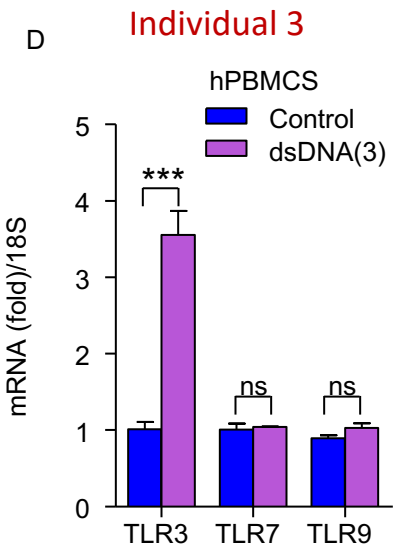
D
Individual 3
hPBMCS
Control
dsDNA(3)
mRNA (fold)/18S
TLR3
TLR7
TLR9
***
ns

Figure. S12

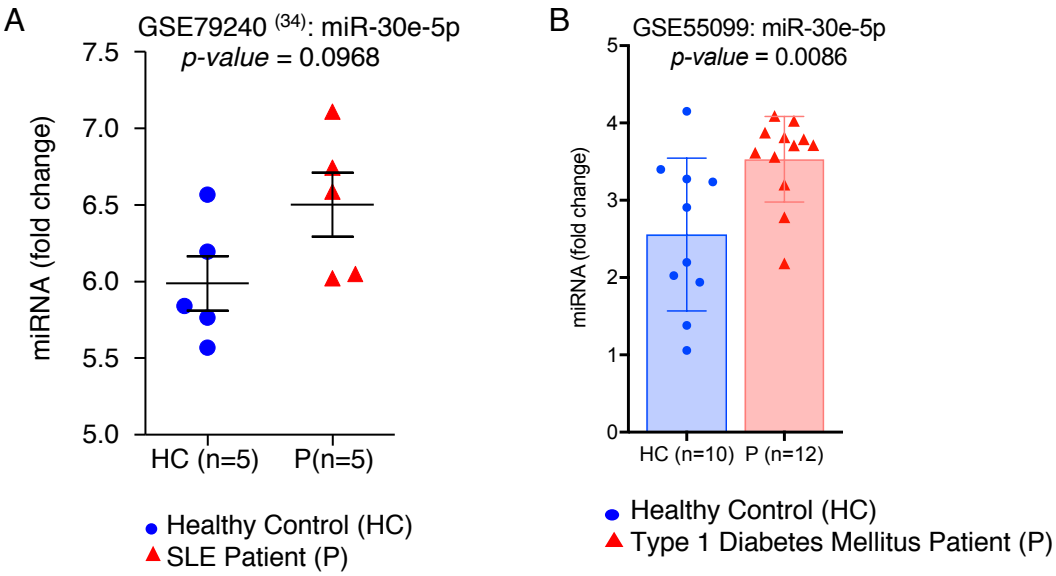
A
GSE79240 (34): miR-30e-5p
p-value = 0.0968
miRNA (fold change)
7.5
7.0
6.5
6.0
5.5
5.0
HC (n=5)
P(n=5)
Healthy Control (HC)
SLE Patient (P)
B
GSE55099: miR-30e-5p
p-value = 0.0086
miRNA (fold change)
5
4
3
2
1
0
HC (n=10)
P (n=12)
Healthy Control (HC)
Type 1 Diabetes Mellitus Patient (P)

Figure. S13

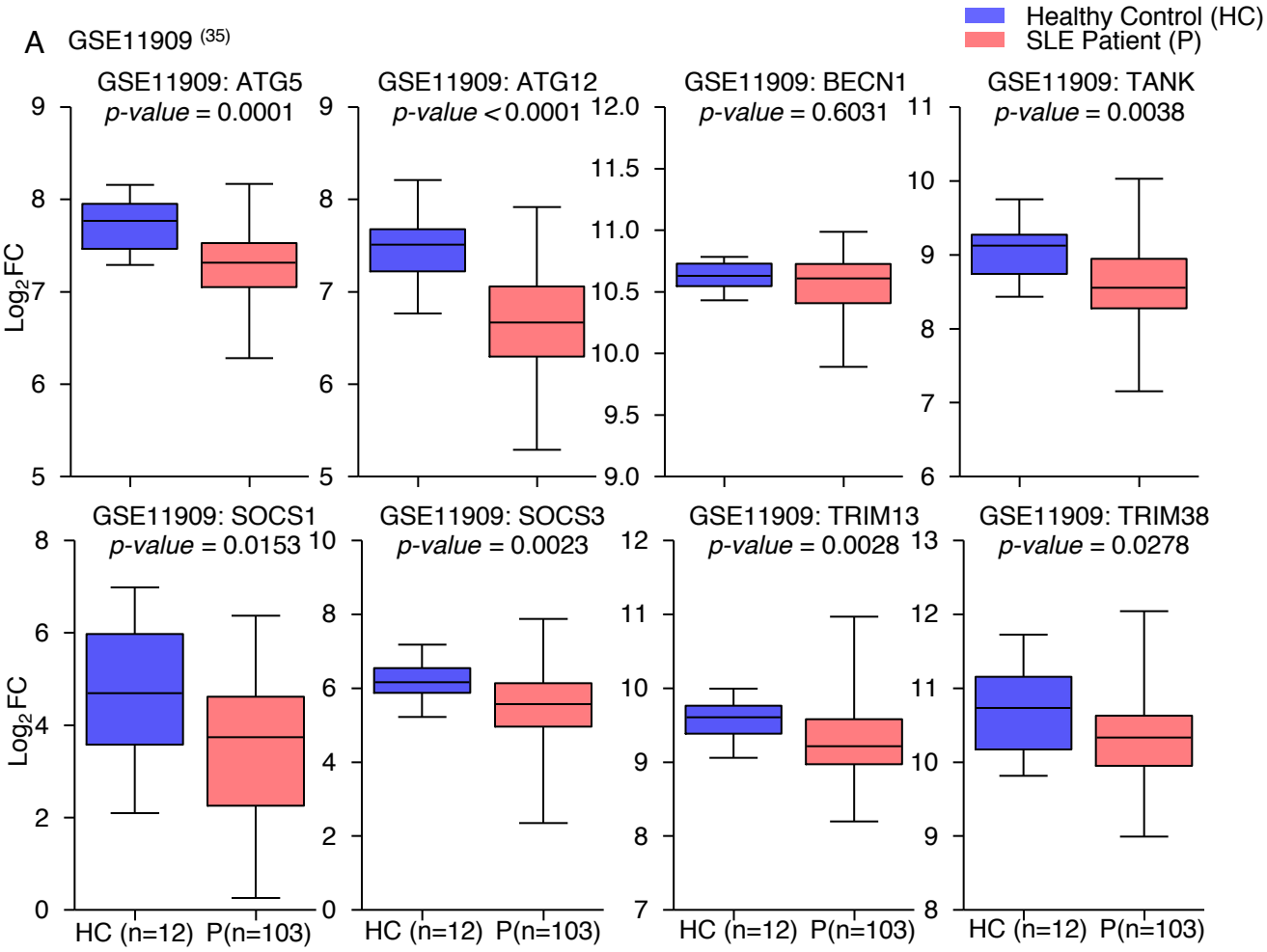
A GSE11909 (35)
Healthy Control (HC)
SLE Patient (P)
GSE11909: ATG5
p-value = 0.0001
GSE11909: ATG12
p-value < 0.0001
GSE11909: BECN1
p-value = 0.6031
GSE11909: TANK
p-value = 0.0038
GSE11909: SOCS1
p-value = 0.0153
GSE11909: SOCS3
p-value = 0.0023
GSE11909: TRIM13
p-value = 0.0028
GSE11909: TRIM38
p-value = 0.0278
Log2FC
HC (n=12)
P(n=103)

A

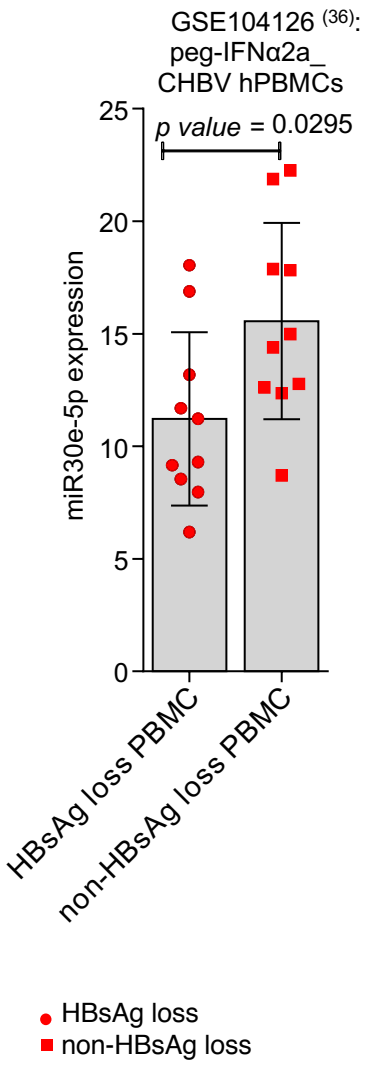
GSE104126 (36):
peg-IFNα2a_
CHBV hPBMCs
p value = 0.0295
miR30e-5p expression
25
20
15
10
5
0
HBsAg loss PBMC
non-HBsAg loss PBMC
HBsAg loss
non-HBsAg loss

Table T1

	Therapy naive CHB (n=51)	Control (n=24)	*p-value*
Median age (range)	48(19-68)	31(23-55)	
Male/Female	36/15	10/14	
AST (reference range: 10 - 40 U/L)	37(18-166)	24(16-42)	
ALT (reference range:7-56U/L)	36(15-130)	23.5(12-48)	
HBsAg	Positive	Negative	
Anti-HBcIgM	Negative	…….	
HbeAg	16 positive	…….	
HBV DNA Load log10 (IU/mL)	5.03(1.36-9.2)	…….	
hsa-miR-30e-5p (fold change/U6)	18.2(0.63-269.12)	1.01(0.712-1.92)	0.0023***

Data expressed as median (range); CHB (Chronic Hepatitis B); AST (aspartate transaminase); ALT (alanine transaminase); HBsAg (Hepatitis B surface Antigen); Anti-HBcIgM (IgM antibody to hepatitis B core antigen); HBeAg (Hepatitis B e-Antigen); hsa-miR-30e-5p (Human Micro(mi)-RNA-30e).

Table 2

Down Regulated genes

NBPF19	CYP4F11	DIABLO	TWF1	UPK1B	NT5E	HDAC5	AXIN2
ALPL	PRR5L	HOXB8	AC027698.1	LINC00707	PRRG1	SLC38A6	RARS2
OR2B6	CD99	SEMA3E	ST3GAL5	SNX29	STC2	CD9	SPOCK3
DLEU1	TBPL1	PADI3	HOXB8	PTPRH	PTGFRN	AC130456.3	STEAP1
LNPK	COPZ2	AC092608.1	MEX3B	GOLGA7B	AC084871.1	C9orf72	RAB32
ZDHHC8P1	GM2A	GALNT9	TMEM158	AP4B1	AC106820.5	NT5E	F8
BORCS7-ASMT	FOXD3	AC093677.2	UPK1B	FAM110B	P4HA2	SLC5A4-AS1	MIR210HG
FBXO48	AVEN	GNG10	C12orf66	TSEN15	SLC19A3	CREG1	TMEM87B
TM6SF2	WNT7B	ZDHHC20	TCP11L2	ACSL1	NEIL2	MORN4	TMED10
CLEC2D	AC243964.2	TRAPPC2	AP4B1-AS1	TSEN15	VPS26B	STK39	EVA1A
LRRC27	TWF1P1	CPT1C	CDK5R2	AC016042.1	ST3GAL5	AC072022.1	B4GALT5
CORO2A	PDIK1L	RTN4R	ACVRL1	PADI2	AC008537.2	PORCN	NEIL2
IDH1	AC005606.2	WISP2	CRTAC1	AC005726.4	SLC6A6	RNA5SP39	TMCO3
AL390879.1	FAM81A	GALNT7	LPXN	ZFP90	ABHD6	CREG1	SMIM20
AC021733.1	JAK3	SMPDL3A	PPP1R18	KCNC3	APLP1	GFOD1	NEU1
MAP3K7CL	RTN4R	HMGB2	SFXN3	TMEM156	ABHD14B	AL445483.1	NAGPA
PAX6	HERC2P4	DHRS2	ACHE	AC027097.1	MAP1LC3B	BCHE	SEL1L3
ATP6V0E2-AS1	TTC21A	AC138466.4	UPRT	STAG1	AL136084.2	ATP6V1B2	CFDP1
PCBD2	AC099489.1	DUSP28	EXOC4	RNU6-527P	ARID5B	FADS2	CAMK2N1
EFCAB13	SNAI3-AS1	ADAT1	AC010655.4	CKAP4	KLHL20	SCARA5	CD70
STX3	KIAA2012	GATA2	FUCA1	ATP8B1	AC011120.1	DESI2	TFAP4
IDH1	CTHRC1	MALL	VIM	S100A2	FRRS1	AL049780.2	SEMA3F
BX088651.4	UGT2B26P	PPIL3	AC008676.3	FOXD1	B4GALT4-AS1	PSMD10	TNFSF13B
SH3PXD2A	FO393400.1	LNPK	RARG	RUNX2	ENO2	REEP2	NIPAL4
PPFIA4	GNAI2	SAR1AP2	FTH1P8	B3GNT5	AC093388.1	C17orf75	ABCA7
ASTE1	PIP4K2A	ARID5B	MALL	PHOSPHO1	RNU6-1333P	ADAM19	TFPI
ACKR3	SEC23A-AS1	VAV3	AC007790.1	TIMP2	VWA8	RF00019	LPIN1
MYO15B	SFRP5	LMBR1L	TWF1	NPC1	CCNF	METTL2B	FOXD1-AS1
AC097467.3	NOV	ZNF34	CTH	UAP1L1	C11orf45	B3GNT5	CD70
METTL8	CCDC184	FBXO32	TTLL12	AC007319.1	TRAF3IP2-AS1	SPP1	MINPP1
B3GALT4	LRRK2	ALDOC	MPHOSPH6	BNIP3L	STX7	UBE2V2	AC116634.1
NBPF19	AC132872.1	CAPS2	SLC20A1	CEACAM6	RAB32	AL121929.2	PPP1R18
PIGC	C3orf18	SAP30	FUCA1	P4HA2-AS1	PTGES	RNA5SP118	UAP1L1
NIPAL2	ACACA	CAPN5	GSTM4	AC243967.2	PIK3IP1-AS1	GALNT1	ABCG2
ZNF77	GNAI2	ITPK1-AS1	NTNG2	RNA5SP55	E2F7	IGFL4	DSG2
PRDM13	WNT7B	MID2	TRIB3	SEC22C	CRCP	RN7SL798P	ABCG2
CNTNAP3C	SEC23A	CDKN2D	GNPDA1	STK39	AC106801.1	LSS	LYN
TNFSF12	GGT8P	AC092570.1	AC099489.1	RASGEF1A	ABCA5	ABCA17P	ARPC5
GM2A	AP3S1	PADI2	ENDOD1	TMEM205	AC002996.1	ALG1	PQLC3
MMP16	TWF1P1	RARG	AC100788.1	TTLL7	BEGAIN	ENO2	ANKRD29
AC107373.2	RGS11	MMP23A	TMEM59L	DLK2	RMC1	DGKA	EIF4EP1
MLIP	TMEM59L	HSD17B7	RRAD	TMEM156	AL357673.1	HILPDA	BAIAP2-DT
THCAT158	SLC35C1	CAPN5	TBC1D2	TRIB3	AP2A1	PTPN13	ANXA10
CD99	AC069113.2	VGF	DNAJC25	KLK10	FBXO45	SPP1	RAB7A
SETDB2	PIP4K2A	SLC35C1	TEX2	LCLAT1	IRAK4	DBF4	MRPL46
ADAM12	NEFL	ITPK1	RTN2	CAMKK1	CPLANE2	GSDME	CA12
SFRP5	SCML1	AMPD3	F12	ATP8B2	STX4	SLC35D1	MTDH
SYNGR3	AC098582.1	AL360081.1	SLC20A1	LRRC75B	ATP8B2	RAD23B	DPY19L1
RRAD	PPP2R5B	VIM-AS1	RN7SL462P	CAMKK1	RHEBL1	SOGA1	SOGA1
GDPD5	MINCR	AC007406.4	SDAD1P1	TMEM158	ATP6V1B2	RAD23B	HYAL3
SPATC1L	AP3S1	GNPDA1	B4GALNT4	ENDOD1	CYFIP2	TMEM231	PDP2

Table 2. Continued

CLIP2	UBAC1	PLPPR2	HK1	SPINT1	NINJ2	AP000487.1	MST1L
ELF3	WDR54	LDHAP4	DHCR7	STK31	PAFAH1B3	ATRNL1	NRG1
JCAD	NEU1	ACVR1	RAP2B	STXBP1	PTGR1	ATRNL1	PARD6G-AS1
FAM162A	AC027682.5	AC010531.3	JMJD1C	TRIM69	SAP30L-AS1	C3orf20	PRKCH
CNTN1	UPRT	SERINC3	AC020907.6	TRPV3	SPAG4	CRISPLD2	PROSER3
SLC6A15	TM4SF1	ARPC5	AOC2	ENPEP	AK3	DICER1-AS1	PRRT2
GABRA5	RF00019	ITGB3BP	CERKL	GPR135	CC2D1B	GPLD1	RAB30-AS1
DPY19L1	AL163636.1	PFKFB4	MYH7B	MSC-AS1	FAM95C	GRASP	RAB40A
GPI	PGM1	NSMAF	FAM129A	PRKAR2B	LINC00539	LINC01091	RAD51B
SLC8B1	MARK2P8	VAMP3	PLA2R1	RRN3P2	MAP7D2	MPRIP	RBM4
HK2	HAGH	AL031714.1	ARFGEF3	ZNF574	SLC9B2	SLIT3	RN7SL644P
GLI2	AC079203.2	LAMA3	IGDCC4	ARHGEF26	ZFHX3	STIM1	SORCS2
PHOSPHO1	TLCD2	AC005253.1	RAB30-AS1	AC131097.3	AC006486.1	TBX19	SPDYE18
STXBP5-AS1	RPA2	INSIG2	AC058822.1	ACBD5	AC068234.1	TPCN2	STXBP5-AS1
FUZ	TTLL12	KCNAB2	PTPRCAP	ENSA	AC133552.2	ZBED5	TLN2
ESCO1	CNTN1	OLFML2A	RAD51B	GPR135	AC242426.2	ZNF511-PRAP1	TXK
NCAPH	MYDGF	AC090541.1	MCOLN3	LINC02585	ALS2CL	ZNF708	URGCP-MRPS24
YWHAZ	FAM102A	CDCA2	STXBP1	MAPK6-DT	ARHGEF6	ZNF800	ZBTB7C
SNX30	GJA1	TM4SF1-AS1	IFNA1	PDE11A	C17orf75	AC007000.3	ZFPM2-AS1
BMP6	OGFRL1	AC010260.1	ERMP1	PHKG1	C1QTNF6	AC007318.2	ARHGAP23P1
DSG2-AS1	CAT	IRF2BP2	SERPINE3	ZAN	DCHS1	AC007785.1	MIR100HG
VAMP3	CDCA2	AL160408.2	TMC5	RNH1	FAM86HP	AC008663.2	SLC16A8
DLG4	TMEM170A	AC027319.1	HIVEP2	VPS25	INSL3	AC011481.1	SLC5A11
CSTB	TMEM106B	GLYCTK-AS1	VILL	CDH23	KATNBL1	AC015687.1	SNX24
B4GALT5	HMOX1	SPOCK1	DLEU2	RAB3B	KLHL30	AC040174.1	AC003002.1
ELF3	AL354740.1	CARS-AS1	PLEKHM3	SPRED3	KPNA7	ADAMTS6	ACAD9
AP4E1	SPAST	FTH1P7	GREB1L	SPTBN4	MED12	ANKRD24	ADAMTS14
SYT5	LIMA1	AL445488.1	POLN	AC022893.1	MIATNB	APIP	AL683807.2
PTGES	MBNL1	CCDC97	ZNF678	AC139149.1	MUC6	ARMH3	BAIAP3
STXBP1	CBX2	CBFB	CEMIP	ANKRD34A	PELI2	ATF3	C2
TRAPPC9	GSKIP	KNSTRN	AC026464.1	CATSPER3	PRCC	BACH1	CCDC88B
HK1	FER1L4	SUCLG2-AS1	ERV3-1	LGI3	SGSM1	BACH1-IT1	CD55
LINC00472	UCP2	HMOX1	ISM2	RCOR2	STARD7-AS1	CAPN12	CDH16
KDELC2	STEAP1	ZNRF1	ITFG2	TTN	STXBP1	CTR9	CMPK2
GJA1	KXD1	PLBD2	TET1	TANK	TRIOBP	CYP2F1	DLEU1
AMZ2	WDR82	KRIT1	MORC4	AC138150.1	ZDHHC8P1	DNHD1	DYRK4
SLC6A15	TLE1	GNA13	RNF187	LRRFIP2	ZNF346	DYNLRB2	EIF1B-AS1
AC113386.1	TRAF3IP2	DLGAP5	SNAP25-AS1	APOBEC3A	ZNF398	EFCAB13	EXOG
NDEL1	AL845552.2	SERINC5	EFCAB13	AC073107.1	ZNF503	ELK4	FRMD8
YWHAZ	AC037487.2	KLF13	SPG7	AC244230.2	AC009690.1	FRMPD2B	FRMPD2B
AGFG2	CBFB	NPTXR	TRIM13	IDH3A	CACNA1A	GREB1L	GATD1
STXBP5	KCNAB2	AP001469.1	AC087482.1	KREMEN2	DUBR	HACD4	HS1BP3
PPP3CA	DHRS3	XPR1	AC106869.1	MIRLET7BHG	ENSA	HOXB-AS4	IKZF4
HR	RPA2	RRM2	BORCS7-ASMT	ZDHHC8P1	RAB27A	KCNAB1	KANSL1L
TK2	ABCA3	MTDH	CA14	ABCA5	SAP30L-AS1	KNDC1	LCA5
DYRK4	CD82	UCP2	CATSPERG	AC009690.1	TPCN2	LMO3	LINC00680
B4GALT4	HKDC1	EDEM2	CEP72	AL032819.3	VPS53	LRRC8C-DT	LINC02532
ITGA2	KATNB1	GTSE1	KIAA2026	ANKRD24	AC007773.1	MAP1A	LMNA
C3orf58	SAT2	TRIM38	LINC01521	CLDN18	AC137936.1	MED6	MIR222HG
MINPP1	HR	SIGMAR1	PRUNE2	GNGT1	AMPD3	MIR29B2CHG	MYO1D
PLIN3	PLPPR2	CAT	SALL4	LRMDA	AP000487.1	MIRLET7BHG	NALCN

Table 2. Continued

NFATC2	ZBTB20-AS5	AC009133.2	DNAJA3	PRB1	ZNF674	DSCAML1	SLC4A3
POLR2J4	AC009065.4	AC009404.1	DNM1P47	PSMB5	ZNF718	EPHX3	SLCO1B3
PTOV1-AS1	AC025048.4	AC009690.1	DOP1A	PUM3	AC011466.1	FGF12	SNHG28
PXDNL	AC104389.4	AC009690.2	DPY19L1P1	PYCR3	AC073569.2	GGA3	TRIM66
RAB3GAP1	AC145285.3	AC021660.3	DPY19L2P2	RAD51B	AC124944.3	GLRA3	ZNF620
RAD51B	ADAMTS14	AC026412.3	DRAM1	RAD9A	AC138150.1	GRTP1	CPLX2
RBM45	ADRA1D	AC068205.2	ENSA	RALGAPA2	AL391684.1	INSL6	RPL39P40
RCOR2	AK9	AC068533.4	EXD3	RBFOX3	BCL2L13	KCNIP2	MFSD2A
RCOR3	AL049629.1	AC079447.1	EXO1	RDH16	CCDC162P	KIF9	LSMEM1
RIF1	APLF	AC079781.5	FAM45A	RETREG1	COA5	KIF9-AS1	AL356489.2
RMI2	ATF3	AC091045.1	FAXDC2	RFX3-AS1	DACT3-AS1	L3MBTL4	GNG13
RPH3A	BMPER	AC099508.2	FAXDC2	RNF224	DDX50P2	LINC02381	HOXB7
SPDYA	CAPN12	AC114956.1	FBXO43	RNF4	EPHA5	LSAMP-AS1	HOXC5
SPESP1	CEMIP	AC245297.1	FSD1L	RPS23P1	FBXO9	MAGI1	DBP
THCAT158	CISD1	ACTG1	FTX	RSPH9	FCF1	MAP3K8	AC012531.2
TSEN2	CLBA1	AL031599.1	GAS2	RSRP1	LGR6	MEG9	AC099489.1
AC007388.1	CR381670.1	AL117190.1	GIPC3	SCN8A	LINC01534	MIR4500HG	AC007906.2
AC011921.1	ELANE	AL121820.1	GUCY1B2	SCNN1D	LINC02048	MTHFD2L	AC026471.4
AC120114.1	EPHA5	AL139289.2	H1FX-AS1	SDK2	MAGI1	MZT1P2	CGN
AL121776.1	H2AFJ	AL157882.1	HAGH	SDK2	NNT-AS1	OTUD3	IQCH-AS1
AL133410.1	HAND2-AS1	AL450992.1	HCG27	SGCE	P2RX5-TAX1BP3	PATL2	NALCN
AL138752.2	HOXB7	AL592078.1	IFRD1	SGK3	PDZD4	PPWD1	SLC9C2
AL355303.1	IL1B	AL603839.3	ITGAD	SLC13A3	SLC6A8	RB1CC1	RF00019
AL512353.2	ITGB3BP	ALS2CL	KIAA1755	SLMAP	TCF12	RBMS3	HELLS
ASB4	KCNIP2	ANKRD36	KIF26A	SNAP25-AS1	TOMM20L	RHOXF1-AS1	AL353692.1
BACE2	LINC01376	ARHGAP22	KNDC1	SPATA17	AC007786.1	RNF20	C3orf20
C1orf54	MAP1A	ARMCX4	LAMA2	SPNS2	AC008267.3	RPS27L	HELLS
COL17A1	MED12L	BACH1	LCA5	SPRY4-AS1	AC009041.1	SERINC5	POLR1B
CR392039.3	MSS51	BCAR3	LEKR1	SUCLG2-AS1	AC055713.1	SLC16A1-AS1	SMOX
CYP4F11	MYO16	BTBD8	LINC00470	SUMO2	AC068707.2	SLC2A1	AC099489.1
CYP4F25P	RAB30	C5orf66	LINC00618	TAPT1-AS1	AC078881.1	SLC35F3	FRMPD2B
DNAH17	SAP30L-AS1	CAPRIN1	LINC01348	TBC1D25	AC078927.1	SPON2	AC013470.2
DRD4	SLC37A3	CCDC103	LIPE-AS1	TBC1D7	ADAMTSL3	SRFBP1	TSC22D1-AS1
FAM19A5	STXBP1	CCDC150	LRMDA	TLN2	AL137145.2	TSPO	LRRC6P1
ITGA1	TEX52	CCDC191	LRMDA	TMEM65	AL137247.1	TSSK3	SERINC3
LINC01305	TFCP2L1	CCDC7	MCMBP	TMTC1	AL590666.1	ZNF518B	AC108062.1
LINC01347	TNN	CD55	MIATNB	TPTE2P5	ANKRD20A21P	ZNF529	RF00003
LINC01572	TPI1P2	CD55	MRPL23	TRIB2	AP002992.1	ZNF570	SOCS3
MAST4	TPTE2P5	CD55	MRPL37	TRIM23	ATE1-AS1	BECN1	
MEG9	ATG5	CEP162	MSANTD4	TTC28	ATXN3	AP001767.3	
NFAT5	ATG!2	CES4A	MSANTD4	EPG5	BNC2	ARAP2	TREX2
PIGZ	WDR78	CHMP7	MSC-AS1	UBE2Q2P1	BZW1	CAPS2	ULK4P1
PLK3	Z84485.1	CMSS1	MUC13	UCP3	C2orf48	CBLB	AL355303.1
PTPN2	ZNF767P	CNKSR2	NAA15	WDR66	C9orf43	ELL3	TXNRD3
RAB30-AS1	ABCA12	CRYGS	NMUR1	WDR82	CAB39L	FBN2	
SLC25A41	AC005020.2	CSNK1D	NPSR1-AS1	WDR86-AS1	CACNA1B	GOLGA6L10	
SPACA6P-AS	AC006001.3	DENND3	PALLD	WNT2B	CCDC174	LINC00174	
SUCLG2-AS1	AC007000.3	DENND4A	PAX8-AS1	ZDHHC8P1	CLCN6	MAP3K13	
TLR1	AC007220.1	DGKH	PDE4D	ZNF239	COPS2	RAB27A	
UBE2Q2P1	AC007406.3	DHX15	PDE5A	ZNF483	CYB5B	RABGAP1L	
Z94721.1	AC008397.2	DNAH14	PLCG1-AS1	ZNF596	DLEU2	SGPP2	

Table 2. Continued

Up-regulated genes							
BRD9	POLR3A	AC027808.1	ZNF699	PKLR	TGS1	ZNRF2P2	CCDC91
TSPAN12	SCUBE2	AC114490.3	ADARB1	PRDM2	TMSB15B-AS1	HRASLS2	CD5L
CCNY	TBX18	AC114947.1	CEL	SCAF11	ZBTB20	TNF	CDHR3
CHMP6	TTC28	ADGRL2	COX10-AS1	SORBS1	ZBTB37	IFNA13	CDYL2
BAG1	WDR41	ANK1	ITGB1-DT	STK11	ZFAND4	AC007240.1	CEP152
EDIL3	ADGRB1	ARF1	LRP2BP	VARS2	ZKSCAN2	AC012651.1	CEP57L1
TTC33	ASH2L	ARNTL2-AS1	PARP10	WDR82	ZNF518A	AC016205.1	CGNL1
ATAD5	LINC00982	ATP2A1	PDZD4	ZNF391	ZNF800	AC027288.1	COBL
ULK4	LINC01232	CARD8	PHKG1	ZNF586	ZNF850	AC044860.1	CROCC
WDR60	RNU6-1310P	CC2D1B	TAB2	ZNF883	ZNF43	AC064871.1	DLEC1
BRINP1	SDK1	CCNC	TFPI	ZSWIM7	BNIP3P27	AC068533.3	DLEU2
SPON1	AC078927.1	CEMIP	AL365273.2	ABHD18	AC124319.2	AC091551.1	DNAH1
RAB30	AC110769.2	DPY19L2P2	AL512428.1	ABHD5	KBTBD11-OT1	AC098864.1	DUBR
AP000808.1	ANKRD44	ENO4	AP000808.1	AC007388.1	SORCS2	AC106795.3	EML5
PDE6G	C5orf66	FAM166A	C12orf60	AC011726.1	ZNHIT6	AC116609.2	ENSA
AC091551.1	FGF7P3	FLRT2	CASC2	AC013652.1	AC021180.1	AC132153.1	ENTPD1
AC245748.2	GTF2IP12	GPATCH2L	CCR7	AC114781.2	AC053527.1	ADAMTS1	EVI5
PKD1L2	LINC01237	GUCY2EP	EFCAB13	AIPL1	AC073254.1	ADAMTS4	EXOSC1
PRR5-ARHGAP8	MXD1	IGDCC4	EXOC3L1	AL590560.1	AC093734.1	ADAMTS7	FAM173B
RANBP17	PCAT1	KCNIP2	GLI3	AL592295.3	AC233280.2	AGBL5	FCN3
VOPP1	STX18-AS1	LINC01322	LARP1B	AP000640.2	AL035413.1	AKR1B1	FGF19
ZNF248	TBC1D7	LMBRD2	MMP20	BASP1	IRF2	AKR1C4	FMNL3
AC012441.1	YTHDF3	LRIG1	PABPC1	BCLAF3	IFNL1	AL023653.1	GHRLOS
GNAL	ZBTB20	MAJIN	SRMS	C1QTNF6	AL592429.2	AL121820.1	GREB1L
HERC2P5	AC007000.3	MEIS1	TMTC1	CDH4	AL592431.1	AL122010.1	GRM4
LINC01004	AC013714.1	MIR100HG	TNXB	CR392039.3	ARHGEF4	AL136038.4	GZF1
SLCO5A1	AL117336.3	MYLK2	TPRG1	SEC16B	C1orf35	AL136164.2	HCG27
BACH1	AL442647.1	NFIB	WDR66	DBNL	C2orf48	AL359915.2	HIST1H3J
AC245748.1	AP003900.1	NREP	SECTM1	GCKR	CAPS2	IFNA1	HMCN1
AP001462.1	FAM155A	POLK	IFIH1	HAGH	CCDC162P	IFIT1	HOXD10
CCR7	IFT22	PSMF1	P2RY6	HDAC9	CHMP6	LY6E	HPRT1
LINC00470	PKP2	PTDSS2	IL6	IL31RA	CHRM3	ALDOA	HSF2BP
ZNF549	RABIF	RBFOX3	IRF3	KLF3-AS1	CLDN10	ALG1L6P	ICA1L
AC083837.2	SEMA3D	SDCBP2	AP002373.1	LCA5	CYP2U1	ANKRD26	ICAM5
AL136164.2	TMEM266	SEC31B	CCDC32	LRP2	FAM189A1	ANKRD36	INTS6-AS1
CACNA1D	TTC39C	SLC22A11	CEMIP	LUCAT1	GHITM	ANKRD55	ISLR
MIR137HG	ZNF883	SLC35F3	CLEC4A	MEFV	HS6ST2	ANO4	ITGAD
RBM43	AC026785.3	SLCO4C1	EOMES	NPRL3	INTS6-AS1	AP4S1	ITGB3
SLC2A1	AC005943.1	SPRY3	FAM57A	NSL1	KCNT2	ATP6AP1L	KANTR
RAB3B	MGAT3	STARD9	FNDC5	PRKG1	LINC00824	ATXN3	KCNV2
ABCB7	NOSIP	TENM4	GIPC2	RGMA	LINC01359	BACH1	KIAA1109
AC097634.4	TRIM36	TEX52	GPLD1	RNF4	LINC02202	BEST3	KIF9
AC104447.1	TRIM5	TTYH1	GUCY1B2	ROPN1L	PSMB2	C17orf75	KRBOX4
CCDC153	AP001783.1	UNC5D	HRAT92	SDR16C5	RNF224	C1QTNF3	LHX4
CYP4F26P	HOXB-AS4	UNC79	KCNH1	SGK3	SLC4A2	CARD8	LINC00511
DPF2	SDCBP2-AS1	IFNA8	KDM4D	SMUG1	SNHG14	CARD9	LINC00910
ELFN2	SNHG14	IRF1	KRTAP5-AS1	SNX24	SNX8	CARD9	LIPE
ENPEP	LINC00641	ZFPM2-AS1	LRRC69	SPECC1P1	TEX19	CATSPER3	LRRC32
ING5	AC006001.3	ZNF131	MIR29B2CHG	SPEF2	TRDMT1	CCDC181	LRRC56
KLF15	AC009061.2	ZNF565	PKD1L2	TBX18	WNK2	CCDC91	LTC4S

Table 2. Continued

LY96	SMIM8	AC090539.1	INTS6-AS1	ZNF704	C1GALT1C1L	ANKRD1	PLSCR4
MAP1A	SRMS	AC108062.1	JMJD6	ZNF706	DAAM1	CCDC28B	GYG2
MAPK10	SRP14-AS1	AC112722.1	KIAA0825	ZNF718	GABBR1	DIO2	UBB
MCMBP	STARD9	AC136475.5	KIF1C	AC090061.1	ZNRF2P2	RNU6-8	HMGA2
MED12L	STK3	ADAMTS20	KLF13	AC244230.2	NCALD	IRF8	VANGL2
MEP1B	STK33	AF121898.1	KRBA1	BTN2A3P	SEMA7A	ADCY1	TNFSF15
MFSD2B	SUCLA2	AFG3L1P	LINC00240	CYP4F26P	EVI5L	LINC02081	E2F2
MIR137HG	TCF12	AL109936.6	LINC00858	DDC	LINC00630	SNRPFP4	DHRS11
MIR222HG	TET1	AL135937.1	LINC02381	GPR78	LARP1B	SYNGR4	CXCL10
MIR34AHG	TFCP2L1	AP000721.1	LPAL2	INSL6	PCAT19	SNCG	IGFBPL1
MIS18A-AS1	TMEM164	AP003049.2	MAP3K15	KNDC1	SERPINA3	FAM171A2	AC005544.1
MLANA	TMEM266	ARHGAP22	MGC32805	LINC01004	OR2I1P	MMS22L	AQP3
MRAP	TPTE2P5	ARR3	MIRLET7BHG	SLC27A4	RN7SL5P	SDS	MYLK-AS1
MRNIP	TRIOBP	ASPDH	MTBP	FTLP2	RPL7AP6	CYR61	CHSY3
MROH2A	TRIOBP	ATF6B	MYO15B	VIM	HBQ1	TMEM150C	ZNF138
MYO1F	TSG101	ATL1	NALCN	AC026785.3	ATAT1	DTX4	APOH
NOL6	TTC28	ATRNL1	NEMP1	DNM1P35	FABP6	PDGFB	C5
NPC1L1	TTC36	AZU1	NRG1	GGA2	AC074138.1	NAT8	ZNF280D
OSBPL10	UBE2F-SCLY	BMP7	NRG1	BANK1	AC110285.1	AUNIP	SPINK4
PCAT1	USP6	C3orf38	PELI2	ATL1	LINC01322	NAT8	ZNF92
PCBD2	VAV1	CCNT2-AS1	PPA1	STX18-AS1	ZNF658B	AMBP	F2RL2
PDE5A	VOPP1	CD55	PRR5-ARHGAP8	AC084262.2	PLIN1	HEATR5B	ADCY9
PELI2	WDR88	CFAP52	PRR5-ARHGAP8	ATL1	C2orf70	OLFM2	C3orf52
PIGQ	WSB1	CHAF1B	PRSS36	GGA2	AC068533.3	AC090673.1	NKX3-2
PIK3C2A	ZBTB20	CLDN14	PSMD6-AS2	AL157871.3	NINJ2	CDC25A	IRF8
PLOD2	ZC3H12D	COLEC11	PTPRN2	TRIM66	TFF1	CYP26B1	IFNB1
PMFBP1	ZFP37	COX7A2L	RBM26-AS1	PDE6G	OTULINL	C2CD2	CYP1B1
PPCS	ZNF131	CYP27C1	RIPOR3	BANK1	TNFRSF1B	IL12A	ZDHHC23
PPFIA4	ZNF3	DNAH14	RIPOR3	MYO1F	TSPAN2	CLDN2	GATA3
PPM1L	ZNF397	DPY19L2P2	SETD7	EXOC8	TFF1	ICK	BIN1
PPP1CA	ZNF718	DRG1	SETD7	PDGFRA	PARP8	ANKRD46	TESC
PPP2CB	ZNRF2P2	ELMO2	SNHG5	MYO1F	AL353743.1	DMRTA2	WTIP
PREP	AC007128.1	ENSA	SPACA6P-AS	DPYSL4	INTU	RPL7AP10	RTKN2
PSMA4	CCDC136	ENTPD8	STAG3L4	ALMS1P1	SYNGR4	TNK2	ERFE
RAB30	MED19	FAM155A	SYCP2L	SDHAF2	AC055764.1	FAM222A-AS1	NACA
RAPGEF4	PHYHIP	FAM21EP	TBC1D8	DGCR9	LINC01273	CLDN2	AC007608.1
RBM4	WDR18	FAM83E	TBL1X	ALDH1L1-AS1	OLFM2	F2	TESC
RGS20	AC004865.2	FGFR3	TIA1	DOCK7	IL11	MTTP	KRT80
RUFY4	AC009301.1	FKRP	TLR1	U2AF1L5	ISM1	REL	HYAL4
RUNDC3A	AC010754.1	FLVCR1-DT	TMEM139	EIF3CL	LTB	LINC01836	SLC35G1
SAP30L-AS1	AC012651.1	GNAL	TMEM52	U2AF1L5	NEK10	GYG2	PKD1L2
SCGB2B2	CXCL10	GPATCH2L	TRABD2B	AC138894.3	PPIAP31	ZNF273	FAM222A
SELENOS	RSAD2	GPR20	VPS54	ZNF268	SMOC1	CMTM8	PDCD1LG2
SETBP1	AC025164.1	GREB1	WBP2NL	CU633967.1	CKMT2-AS1	MPP2	LYPD3
SETD7	AC026803.2	GRIN2C	WDR86	SEMA7A	CD74	KRT80	ARID3B
SETD7	AC058822.1	GRTP1	ZNF136	BCL2L14	CD83	NEXN	AL031590.1
SHANK2	AC068305.2	HPS5	ZNF331	ZBED9	RASSF5	CXCL10	CISH
SLC25A53	AC068389.1	IDI2-AS1	ZNF586	CD74	PARD6G	RPL34P18	RIC3
SLC44A5	AC079447.1	IL31RA	ZNF616	C17orf75	AQP1	AKNA	SGK1
SLC49A3	AC080013.1	INTS4P2	ZNF620	CD22	SMOC1	U62317.1	NAV2

Table 2. Continued

PLIN1	ASS1	DGCR6L	IL32	RPL30	LBR	EHD1	UHRF1
ASMTL	CTU1	RPL18AP3	PKMYT1	ZFP36	CTSO	ASF1B	ARL5B
PTK7	AL591767.2	PNKD	RND1	KITLG	RPL31P58	NXN	RARRES3
CYR61	HSPA2	SLC19A2	RHOU	ZNF267	MCM6	PROSER2	TTLL4
FUT10	SMCO4	AC106820.2	IRF2BPL	ZNF367	DTL	MGMT	AP003721.1
TNF	ZBP1	KCNJ15	TCIM	ANKRD52	SNX4	RPF2	TSC22D2
RASAL2	ZBTB49	CCDC88C	TMEM160	FOS	AL133481.1	OOEP	SOCS5
NR4A3	PTHLH	PHLDB1	LBH	AC078929.1	SOWAHC	IGF2BP1	PNRC2
AC137936.2	ZC3HAV1L	MSX1	DDX39B	CD274	SIK1B	SERPINB9	MCM6
FAM135A	DANCR	FGFR4	MAMLD1	EXO1	RHOU	AC124784.1	FERMT2
ZBTB47	ZBTB34	RF00100	FGFR4	AC034105.3	DNPH1	CYTH1	CSRNP1
PKDCC	IGFBPL1	COL7A1	DNAH14	AKNA	COL6A2	CXCL11	AREG
CEP135	MIDN	B3GNT7	SHISAL1	ZFP36	FAM3C	RPL21P23	ARHGEF18
DNAJC6	IRF8	FOSB	AMER1	AC007686.3	LSM5	SDF2L1	AL109613.1
EIF4EBP2	GSDMB	AC016739.1	ELOA-AS1	CD274	IRGM	KCTD11	IFITM2
FBLN5	IRF7	FBLN5	AC009630.1	NUAK2	SNHG6	ELF4	TMEM184A
TGFB2-AS1	IFNL4	RNF216P1	HRASLS2	MCRIP1	SPRY4	TRIB1	ISG20
MICB	MAP3K14-AS1	ZBTB47	NR4A3	RPL34	AC068620.2	GINS1	IFIT5
KCNF1	NAPRT	WDR76	TNFRSF12A	KMT5C	CTU1	ZBTB5	MX1
ZNF283	ZNF235	GATA3	RBAK	ETS1	CLDN23	RNU6ATAC9P	
RNF38	ACSL5	VGLL3	ODC1	ZBTB5	SCAMP5	RAB5IF	HCP5
PARP8	CRY2	CX3CL1	MICALL2	MSX1	GNGT1	RPL21	SP140
AQP3	WT1	WEE1	TUSC2	AL163192.1	SERPINB9	LIAS	GTPBP2
KCNF1	ISG15	Z82188.2	LIME1	TMEM109	MED28	TRAPPC6A	GLI3
SDF2L1	C11orf86	RASSF8	GNG4	RPAP1	ZNF274	DUSP5	ANKS1B
ZNF428	DUSP1	IQCJ-SCHIP1-AS1	AC073130.2	COL1A1	SCARA3	COL5A1	XDH
EIF4EBP2	GEMIN2	VASH2	CLASP2	TCIM	ZNF274	IFNAR2	FAM106A
AC117383.1	GRAMD4	IGFBP3	SFRP1	DUSP16	RPSAP58	RPS29P2	IFIT2
FO393422.1	EFNA1	Z84485.1	AC016739.1	EDRF1-AS1	PROSER2-AS1	IGF2BP2	NEDD4
TNFRSF1B	C3orf52	AMBP	E2F1	GADD45B	AL365226.1	HGSNAT	KBTBD8
P2RY6	AC099560.2	RPL27A	AC091045.1	PRR5	TRAPPC6A	YPEL2	RGS22
ZNF117	ZNF92	SRD5A1	DICER1	TUFT1	ISOC1	TUFT1	TRIM69
SMAD7	SNHG8	KCNC4	RPL39	ATF7IP	SOCS2	CXCL8	FAM3C
ELOVL2-AS1	ODC1	RPS7P10	TGFB2	MCM3	BARD1	CDC6	PAK3
RND1	XKR8	AL355032.1	SCARA3	C21orf91	CCDC12	ATL1	SLC15A3
AL139294.1	PLPPR3	MORF4L1P3	BARX1	CCNE1	AC010618.3	MAFB	

Table T3

Negative Regulator	hsa-miR-30e Binding site	miRanda	DIANA	Target Scan	miRDB
TLR pathway		miRSVR Score	Pred.Score	Context++ Score	Target Score
TRIM 38	one site: 1157	-1.0306	---	-0.13	---
TANK	one site: 238	-1.0396	---	-0.29(highly conserved)	---
TRIM 35 [37]	one site: 281	-0.5210	0.756	-0.07	---
RIGI/MDA5 pathway					
ATG5	one site at:511	-1.2012	---	-0.44(highly conserved)	88
ATG12	two sites: 370, 388	-1.029 & -0.4650	Low score	-0.39	98
TRIM 13 [38]	two sites: 2740,3856	-0.1131 & -0.4454	---	---	64
TRIM 38	one site: 1157	-1.0306	---	-0.13	---
SOCS1	one site at:271	-1.2111	1.000	---	78
SOCS3	one site at:1411	-1.2147	0.998	---	85
BECN1	one site at:84	-1.3155	0.863	---	88
Inflammatory pathway/ Virus Reserves or Reactivation pathway					
EPG5 [39]	one site at:24	-0.4449	0.984	-0.25(highly conserved)	---
BECN 1	one site at:84	-1.3155	0.863	---	88
ATG5	one site at:511	-1.2012	---	-0.44(highly conserved)	88
DNA sensing pathway					
BECN1	one site at:84	-1.3155	0.863	---	88

Table T4

TRIM 38

•Gene ID:ENSG00000112343
•Gene Name: TRIM38
•RBP:AGO2
•Sample ID:GSE44404-GSM1084065
•Method: HITS-CLIP
•Chromosome:chr6
•Strand :+
•Binding site start:25974460
•Binding site end:25974480
•Binding signal:14
•P-value:0.00319213
•Genomic position: intron

TANK

•Gene ID:ENSG00000136560
•Gene Name: TANK
•RBP:AGO2
•Sample ID:GSE41437-GSM1020022
•Method: PAR-CLIP
•Chromosome:chr2
•Strand :+
•Binding site start:162092600
•Binding site end:162092620
•Binding signal:22
•P-value:8.88536e-07
•Genomic position:3'UTR

ATG 5

•Gene ID:ENSG00000057663
•Gene Name: ATG5
•RBP:AGO2
•Sample ID:GSE44404-GSM1084068
•Method: HITS-CLIP
•Chromosome:chr6
•Strand : -
•Binding site start:106632780
•Binding site end:106632800
•Binding signal:15
•P-value:0.00079613
•Genomic position:3'UTR

ATG 12

•Gene ID:ENSG00000145782
•Gene Name: ATG12
•RBP:AGO2
•Sample ID:GSE42701-GSM1048187
•Method: HITS-CLIP
•Chromosome:chr5
•Strand :-
•Binding site start:115167220
•Binding site end:115167240
•Binding signal:18
•P-value:0.00794433
•Genomic position:3'UTR

BECN1

•Gene ID:ENSG00000126581
•Gene Name: BECN1
•RBP:AGO2
•Sample ID:GSE28865-GSM714644
•Method: PAR-CLIP
•Chromosome:chr17
•Strand :-
•Binding site start:40962420
•Binding site end:40962440
•Binding signal:29
•P-value:2.98304e-08
•Genomic position:3'UTR

SOCS1

•Gene ID:ENSG00000185338
•Gene Name: SOCS1
•RBP:AGO2
•Sample ID:GSE28865-GSM714644
•Method: PAR-CLIP
•Chromosome:chr16
•Strand :-
•Binding site start:11348400
•Binding site end:11348420
•Binding signal:25
•P-value:2.5004e-07
•Genomic position:3'UTR

SOCS3

•Gene ID:ENSG00000184557
•Gene Name: SOCS3
•RBP:AGO2
•Sample ID:GSE42701-GSM1048188
•Method: HITS-CLIP
•Chromosome:chr17
•Strand :-
•Binding site start:76352920
•Binding site end:76352940
•Binding signal:62
•P-value:4.01318e-06
•Genomic position:3'UTR

TRIM13

•Gene ID:ENSG00000204977
•Gene Name: TRIM13
•RBP:AGO2
•Sample ID:GSE44404-GSM1084044
•Method: HITS-CLIP
•Chromosome:chr13
•Strand :+
•Binding site start:50591100
•Binding site end:50591120
•Binding signal:9
•P-value:0.00312875
•Genomic position: 3'UTR

EPG5

•Gene ID:ENSG00000152223
•Gene Name: EPG5
•RBP:AGO2
•Sample ID:GSE44404-GSM1084047
•Method: HITS-CLIP
•Chromosome:chr18
•Strand :-
•Binding site start:43432360
•Binding site end:43432380
•Binding signal:9
•P-value:0.000552801
•Genomic position:3'UTR

Table T5

S. No.	Age	Gender	Duration of disease (years)	Disease activity (SLEDAI)	Drugs	Serum complement level	Anti-nuclear antibody	Anti-dsDNA (IU)	Major oragn involved
1	23	Female	7	20	Pred, HCQS,	Low	Positive	212.3	Nephritis, gangrene
2	26	Female	5	24	Pred, HCQS	Low	Positive	>300	Nephritis
3	10	Female	0.3	6	Pred, HCQS	Low	Positive	>300	None
4	29	Female	7	2	Pred, HCQs,	Normal	Positive	>300	Interstitial lung disease
5	35	Female	0.5	13	Pred, HCQs, Thyroxin	low	Positive	>300	Nephritis, hemolytic anemia
6	25	Female	3	12	Pred, HCQS,	low	Positive	>300	Nephritis with renal failure
7	32	Female	4	8	Pred, HCQS,	Low	Positive	>300	Nephritis
8	27	Female	0.45	25	Pred, HCQs,	Low	Positive	>300	Nephritis
9	33	Female	8	0	Pred	not available	Positive	<10	Momoneuritis
10	20	Female	1	8	Pred, HCQS,	Low	Positive	88.6	Nephritis
11.	55	Female	7	12	Pred, HCQS,	Low	Positive	>300	Nephritis
12.	40	Female	0.5	6	Pred, MMF, Tac, HCQS	Low	Positive	130.2	Nephritis
13.	22	Female	6	4	none	Low	Positive	<10	None

Pred: Prednisolone, MMF: Mycophenolate mofetil, Tac: Tacrolimus, HCQS: Hydroxychloroquine

Table T6

	Baseline (n=7)	Post-treatment (n=7)	*p-value*
Median age (range)	32(23-60)	-	
Male	7	-	
AST (reference range: 10 - 40 U/L)	48.28(24.02-111.31)	41.57(25.28-91.2)	
ALT (reference range:7-56U/L)	27.27(19-47.6)	21.81(16.36-57.27)	
HbeAg	4 positive	4 positive	
HBV DNA Load log10 (IU/mL)	6.55(3.5-7.56)	3.2(1.28-3.94)	
hsa-miR-30e-5p (fold change/U6)	1.179(0.83-1.42)	0.199(0.046-1.34)	0.0313*

Data expressed as median (range); Baseline (before treatment); AST (aspartate transaminase); ALT (alanine transaminase); HBsAg (Hepatitis B surface Antigen); Anti-HBcIgM (IgM antibody to hepatitis B core antigen); HBeAg (Hepatitis B e-Antigen); hsa-miR-30e-5p (Human Micro(mi)-RNA-30e).

Real Time PCR primers

	5'-----sequence-----3'
18S_Fw	CTGCTTTCCTCAACACCACA
18S_Rv	ATCCCTGAAAAGTTCCAGCA
HBV RNA_Fw	GCACTTCGCTTCACCTCTGC
HBV RNA_Rv	CTCAAGGTCGGTCGTTGACA
HBVcccDNA_Fw	GGACTTGAATGTACGTTGGGG
HBVcccDNA_Rv	GGACTTGAATGTACGTTGGG
HBV DNA_Fw	ATGGAGAACACAACATCAGG
HBV DNA_RV	GAGGCATAGCAGCAGGATG
NDV_Fw	GGAGGATGTTGGCAGCATT
NDV_Rv	GTCAACATATACACCTCATC
SeV_Fw	CAGAGGAGCACAGTCTCAGTGTTC
SeV_Rv	TCTCTGAGAGTGCTGCTTATCTGTGT
HCMV_GLYB_Fw	AAGTACCCCTATCGCGTGTG
HCMV_GLYB_Rv	ATGATGCCCTCATCCAAGTC
IFIT1_Fw	TCAGGTCAAGGATAGTCTGGAG
IFIT1_Rv	AGGTTGTGTATTCCCACACTGTA
IFNa_Fw	TGCTTTACTGATGGTCCTGGT
IFNa_Rv	TCATGTCTGTCCATCAGACAG
IFNb_Fw	AGCTGCAGCAGTTCCAGAAG
IFNb_Rv	AGTCTCATTCCAGCCAGTGC
IFNλ1_Fw	CGCCTTGGAAGAGTCACTCA
IFNλ1_Rv	GAAGCCTCAGGTCCCAATTC
IL6_Fw	CTCAGCCCTGAGAAAGGAGA
IL6_Rv	CCAGGCAAGTCTCCTCATTG
OAS1_Fw	GAGCTCCAGGGCATACTGAG
OAS1_Rv	CCAAGCTCAAGAGCCTCATC
IP10_Fw	TGGCATTCAAGGAGGTACCTCTC
IP10_Rv	TGATCTCAACACGTGGACAAA
TLR-3_Fw	TTGCCTTGTATCTACTTTTGGGG
TLR-3_Rv	TCAACACTGTTATATTTGTGGGT
TLR-7_Fw	TCAAGCCTTAGATTGGCGATGTC
TLR-7_Rv	CCAGATTGATTTGGGAATTTGTG
TLR-9_Fw	AGTCCTCGACCTGGCAGGAA
TLR-9_Rv	GCGTTGGCGCTAAGGTTGA
miR_30e_5p_Prom_Fw	CGCGGTACCCTTAACTATACTAAATATGTTGGG
miR_30e_5p_Prom_Rv	CGCAAGCTTGTAGCAAAGACTGCCCAGAAAG
mIL6_Fw	CCTCTGGTCTTCTGGAGTACC
mIL6_Rv	ACTCCTTCTGTGACTCCAGC
mIP10_Fw	ACCATGAACCCAAGTGCTG
mIP10_Rv	GTGGCAATGATCTCAACACG
mTNFa_Fw	ATGAGCACAGAAAGCATGA
mTNFa_Rv	AGTAGACAGAAGAGCGTGGT
ATG5_Fw	ACTAGTGACCAGAAACACTTCGCTGC
ATG5_Rv	ACGCGTTTCCTCTAGGGCATTGTAGGC
ATG12_Fw	TTCCAACTTCTTGGTCTGGG
ATG12_Rv	AGAAGTGGGCAGTAGAGCGA
BECN1_Fw	TGTCTCTCGCAGATTCATCC
BECN1_Rv	ACGTTGAGCTGAGTGTCCAG
SOCS1_Fw	CACATGGTTCCAGGCAAGTA
SOCS1_Rv	CTACCTGAGCTCCTTCCCCT
SOCS3_Fw	TCCCCCCAGAAGAGAGCCTATTAC
SOCS3_Rv	TCCGACAGAGATGCTGAACCATCC
TANK_Fw	CCTCTTCGTCCTGTAGCATCA
TANK_Rv	GCATTGTTAGAGCCTGTGGA
TRIM38_Fw	GAAGACGTATGCCAGGGCTAC
TRIM38_Rv	GGAGATTCTTAAAGTCAGACCGG
m18S_Fw	GTAACCCGTTGAACCCCATT
m18S_Rv	CCATCCAATCGGTAGTAGCG
matg5_Fw	GACAAAGATGTGCTTCGAGATGTG
matg5_Rv	GTAGCTCAGATGCTCGCTCAG
matg12_ Fw	TGGCCTCGGAACAGTTGTTTA
matg12 _Rv	GGGCAAAGGACTGATTCACAT
msocs1_Fw	TCCGATTACCGGCGCATCACG
msocs1_Rv	CTCCAGCAGCTCGAAAAGGCA
msocs3_Fw	CACAGCAAGTTTCCCGCCGCC
msocs3_Rv	GTGCACCAGCTTGAGTACACA

Cloning Primers (5'----sequence-----3')

ATG5_UTR_Spe_Fw	ATAAACTAGTGACCAGAAACACTTCGCTGC
ATG5_UTR_MluI_Rv	ATAAACGCGTTTCCTCTAGGGCATTGTAGGC
ATG5_UTR_SDM_Fw	AATGACTTTGATAATGAACAGTGAG
ATG5_UTR_SDM_Rv	TGTAGTTAAGGAAAGATGGGTTTAC
ATG12_UTR_Spe_Fw	ATAAACTAGTCACGGAAGAGACAGCTCTGA
ATG12_UTR_HindIII_Rv	ATAAAAGCTTGGCACTCAATATGTGAATGACAG
BECN1_UTR_Fw_SpeI	ACTAGTGGGAGGTTTGCCTTAAAGGC
BECN1_UTR_Rv_MluI	ACGCGTGGCAGTTTTCAGACTGCAGC
BECN1_UTR_SDM_Fw	AATAAGAAAAAATCCACAAAAGC
BECN1_UTR_SDM_Rv	TGTATACCCGAATTTAATTTAAAACATG
SOCS1_UTR_HindIII_Fw	AAGCTTGATGGTAGCACACAACCAGGTG
SOCS1_UTR_SalI_Rv	GTCGACTAAAGCCAGACCCTCCC
SOCS1_UTR_SDM_Fw	TATGCTTTGCACAAACCAGGGG
SOCS1_UTR_SDM_Rv	AGTATAGGAGGTGCGAGTTCAG
SOCS3_UTR_SpeI_Fw	ACTAGTAAGGGCGCAAAGGGCAT
SOCS3_UTR_HindIII_Rv	AAGTTTAGCCTCAAGGGCCTGAG
SOCS3_UTR_SDM_Fw	TATGTCACTCTGTCTTTTATAAAGATTC
SOCS3_UTR_SDM_Rv	AGTAGAAACAAACAAAAAAATAGAGAAAAAAAC
TANK_UTR_Fw_SpeI	ACTAGTGACATTTGAAAACAGACATATCAAG
TANK_UTR_Rv_HindIII	AAGCTTGACACATTTGAAAACAGACATATCAAG
TANK_UTR_SDM_Fw	TATGTAATTCAAAATTATGTATGTGACTTAG
TANK_UTR_SDM_Rv	AGTAATTACAGTTTTATACAGAATTTTTTTTG
TRIM38_UTR_Spe_Fw	ACTAGTGATGGGGGATTCAGTTCTGG
TRIM38_UTR_HindIII_Rv	AAGCTTGTCTGGGTCAGCATACCGAG
TRIM38_UTR_SDM_Fw	TTAAACAAATCTGATATTTGTTGAAGTCCTAC
TRIM38_UTR_SDM_Rv	TCAGATTTGTTTAATTTTTTTTTTCCTTGAGGCAC